SYNTHESES AND CHARACTERIZATION OF BENZIMIDAZOLE CONTAINING POLYMERS: A COMPARITATIVE STUDY ON DONOR UNIT EFFECT AND INFLUENCE OF H-BONDING

A THESIS SUBMITTED TO
THE GRADUATE SCHOOL OF NATURAL AND APPLIED SCIENCES
OF
MIDDLE EAST TECHNICAL UNIVERSITY

BY

AYDA GÖYÇEK NURİOĞLU

IN PARTIAL FULFILLMENT OF THE REQUIREMENTS
FOR
THE DEGREE OF MASTER OF SCIENCE
IN
CHEMISTRY

JANUARY 2013

Approval of the thesis:

SYNTHESES AND CHARACTERIZATION OF BENZIMIDAZOLE CONTAINING POLYMERS: A COMPARITATIVE STUDY ON DONOR UNIT EFFECT AND INFLUENCE OF H-BONDING

submitted by **AYDA GÖYÇEK NURİOĞLU** in partial fulfillment of the requirements for the degree of **Master of Chemistry Department, Middle East Technical University** by,

Prof. Dr. Canan ÖZGEN _____
Dean, Graduate School of **Natural and Applied Sciences**

Prof. Dr. İlker ÖZKAN _____
Head of Department, **Chemistry**

Prof. Dr. Levent TOPPARE _____
Supervisor, **Chemistry Dept., METU**

Assoc. Prof. Dr. Ali ÇIRPAN _____
Co-advisor, **Chemistry Dept., METU**

Examining Committee Members:

Assoc. Prof. Dr. Yasemin Arslan UDUM _____
Adv. Tech. Dept., GAZI UNI

Prof. Dr. Levent TOPPARE _____
Chemistry Dept., METU

Assoc. Prof. Dr. Ali ÇIRPAN _____
Chemistry Dept., METU

Assist. Prof. Dr. Akın AKDAĞ _____
Chemistry Dept., METU

Dr. Yusuf NUR _____
Chemistry Dept., MUSTAFA KEMAL UNI

Date: 25.01.2013

I hereby declare that all information in this document has been obtained and presented in accordance with academic rules and ethical conduct. I also declare that, as required by these rules and conduct, I have fully cited and referenced all material and results that are not original to this work.

Name, Last name : AYDA GÖYÇEK NURİOĞLU

Signature :

ABSTRACT

SYNTHESES AND CHARACTERIZATION OF BENZIMIDAZOLE CONTAINING POLYMERS: A COMPARITATIVE STUDY ON DONOR UNIT EFFECT AND INFLUENCE OF H-BONDING

Nurioğlu, Ayda Göyçek
M.Sc., Department of Chemistry
Supervisor : Prof. Dr. Levent Toppare

January 2013, 71 pages

The first part of this work reports a comparative study on electrochromic properties of two Donor-Acceptor-Donor (DAD) type polymers, namely poly(2-heptyl-4,7-di(thiophen-2-yl)-1H-benzo[d]imidazole) (BImTh) and poly(4,7-bis(2,3-dihydrothieno[3,4-b][1,4]dioxin-5-yl)-2-heptyl-1H-benzo[d]imidazole) (BImEd). DAD type polymers are designed to bear the same acceptor unit, benzimidazole and two different donor units, thiophene and 3,4-ethylenedioxy thiophene (EDOT) to make a comparison based on the donor unit effect. The resulting polymers are both multichromic and have low band gap values (1.93 eV for PBImTh and 1.74 eV for PBImEd).

In the second part, 4,7-bis(2,3-dihydrothieno[3,4-b][1,4]dioxin-5-yl)-2-phenyl-1H-benzo[d]imidazole (BImBEd) is synthesized. In order to figure out the presence of an intramolecular hydrogen bonding between the amine bond of the imidazole ring and the oxygen of the EDOT molecule, different amounts of trifluoroacetic acid (TFA) and concentrated sodium hydroxide (NaOH) solutions were added during electrochemical polymerization. These treatments caused protonation of the imine and deprotonation of the amine bonds respectively. In order to prove the changes in the optical properties of the polymers due to different number of protonated and deprotonated imine and amine bonds, 1,4-bis(2,3-dihydrothieno[3,4-b][1,4]dioxin-5-yl)benzene (BEDOT-B) was also synthesized and treated with the same procedures. Results showed that it is possible to control the main chain conformation of even an insoluble polymer via acid and base treatments during in situ polymerization.

Keywords: Benzimidazole, Donor-Acceptor approach, electrochromism, hydrogen bonding.

ÖZ

BENZIMIDAZOL İÇEREN POLİMERLERİN SENTEZİ VE KARAKTERİZASYONU:
DONÖR ÜNİTESİNİN VE H-BAĞININ ETKİLERİ ÜZERİNE KARŞILAŞTIRMALI BİR ÇALIŞMA

Nurioğlu, Ayda Göyçek
Yüksek Lisans, Kimya Bölümü
Tez Yöneticisi : Prof. Dr. Levent Toppare

Ocak 2013, 71 sayfa

Bu çalışmanın ilk kısmı, iki Donör-Akseptör-Donör (DAD) tipi polimerin -poli(2-heptil-4,7-di(tiyofen-2-il)-1H-benzo[d]imidazol) (BImTh) ve poli(4,7-bis(2,3-dihidrotiyeno[3,4-b][1,4]dioksin-5-il)-2-heptil-1H-benzo[d]imidazol) (BImEd)- elektrokromik özelliklerinin karşılaştırılmasından oluşmaktadır. Donör ünitenin etkileri üzerine bir karşılaştırma yapmak amacıyla, sentezlenen DAD tipi polimerler aynı akseptör üniteyi –benzimidazol- ve iki farklı donör üniteyi –tiyofen ve 3,4-etilendioksi tiyofen (EDOT)- barındıracak şekilde dizayn edilmişlerdir. Elde edilen polimerlerin her ikisi de düşük enerji bant aralıklarına (PBImTh için 1.93 eV, PBImEd için 1.74 eV) ve multikromik özelliğe sahiptir.

Çalışmanın ikinci kısmında, 4,7-bis(2,3-dihidrotiyeno[3,4-b][1,4]diokzin-5-yl)-2-fenil-1H-benzo[d]imidazol (BImBEd) sentezlenmiştir. İmidazole halkasındaki amin grubu ile EDOT molekülündeki oksijen atomu arasındaki olası intramoleküler hidrojen bağını incelemek amacıyla, elektrokimyasal polimerleşme sırasında ortama farklı miktarlara trifloroasetik asit (TFA) ve derişik sodium hidroksit (NaOH) çözeltisi eklenmiştir. Bu uygulamalar sırasıyla imin bağının protonlanmasına ve amin bağından proton kopmasına sebep olmuştur. Polimerin optik özelliklerinde meydana gelen değişimlerin protonlanan amin bağları ile de-protonlanan imin bağlarının miktarına bağlı olduğunu kanıtlamak için 1,4-bis(2,3-dihidrotiyeno[3,4-b][1,4]diokzin-5-yl)benzen (BEDOT-B) de sentezlenip aynı uygulamalara maruz bırakılmıştır. Elde edilen sonuçlar, çözünebilir olmayan bir polimerin dahi zincir konformasyonunun polimerleşme sırasında yapılan asit ve baz uygulamalarıyla kontrol edilmesinin mümkün olduğunu göstermiştir.

Anahtar kelimeler: Benzimidazol, Donör-Akseptör yaklaşımı, elektrokromizm, hidrojen bağı.

To My Parents and İlkuş

ACKNOWLEDGMENTS

I would like to express my gratitude to my supervisor Prof. Dr. Levent Toppare not only for his guidance, support, encouragement, patience and for teaching us how to become a good scientist but also for listening and helping us in many ways.

I would like to thank to Assoc. Prof. Dr. Ali Çırpan for his valuable discussions and kind attitude.

I would like to thank to Merve Şendur and Hava Akpınar for teaching me patiently and always being supportive both as a fellow working and a very good friend.

I would like thank to all Toppare Research Group members for their cooperation and their kind friendship.

I am deeply grateful to İlkem for being more than a sister to me and making me believe in myself.

Many thanks to Tuğba, Seval, Melike, and Melike Oya for always being there for me, for their true friendship.

I should also thank to Öykü, Çağdaş, Enis and Okan for being like a family regardless of the distances.

Words fail to express my eternal gratitude to my family for believing in me and giving me endless support.

TABLE OF CONTENTS

ABSTRACT…….iv

ÖZ……...v

ACKNOWLEDGMENTS……..…vi

TABLE OF CONTENTS…….……vii

LIST OF FIGURES…….…….xii

LIST OF TABLES……...xvi

LIST OF ABBREVATIONS……..xvii

CHAPTERS

1. INRODUCTION…….……1

1.1. Conducting Polymers ……...……1

1.2. Electrochromism and Electrochromic Materials……..2

1.3. Band Theory……..5

1.4. Lowering the Band Gap ……9

1.4.1. Controlling Bond-Length Alternation (Peierls Distortion)……..11

1.4.2. Creating Highly Planar Systems……...12

1.4.3. Inducing Order by Interchain Effects……...12

1.4.4. Generating Resonance Effects Along the Polymer Backbone ……....12

1.4.5. The Donor Acceptor (DA) Approach……...13

1.5. Thiophene and EDOT (ethylenedioxy thiophene) as Donor Units……14

1.6. Benzimidazole as an Acceptor Unit……16

1.7. H-bonding ……..……17

1.8. Aim of This Work ……..…18

2. EXPERIMENTAL……19

2.1. Materials……19

2.2. Equipment……...19

2.3. Procedure……20

2.3.1. Synthesis……...20

2.3.1.1. Synthesis of 4,7-dibromobenzo[c][1,2,5]thiadiazole……..20

2.3.1.2. Synthesis of 3,6-dibromocyclohexa-3,5-diene-1,2-diamine……...…20

2.3.1.3. Synthesis of 4,7-dibromo-2-heptyl-1H-benzo[d]imidazole……....21

2.3.1.4. Synthesis of tributyl(thiophen-2-yl)stannane……21

2.3.1.5. Synthesis of tributyl(2,3-dihydrothieno[3,4-b][1,4]dioxin-5-yl)stannane……..22

2.3.1.6. Synthesis of 2-heptyl-4,7-di(thiophen-2-yl)-1H-benzo[d]imidazole (BImTh)……..22

2.3.1.7. Synthesis of 4,7-bis(2,3-dihydrothieno[3,4-b][1,4]dioxin-5-yl)-2-heptyl-1H-benzo[d]imidazole (BImEd)…….....23

2.4. Synthesis of Conducting Polymers via Electrochemical Polymerization…….....23

2.5. Characterization of Conducting Polymers……..24

2.5.1. Cyclic Voltammetry (CV)……24

2.5.2. Spectroelectrochemistry……26

2.5.3 Switching Studies……...27

3. RESULTS AND DISCUSSION……...29

3.1. Characterization of the monomers……...29

3.1.1. 2-heptyl-4,7-di(thiophen-2-yl)-1H-benzo[d]imidazole (BImTh)……29

3.1.2. 4,7-bis(2,3-dihydrothieno[3,4-b][1,4]dioxin-5-yl)-2-heptyl-1H benzo[d]imidazole……...31

3.2. Electrochemical and Electrochromic Properties of PBImTh and PBImEd……33

3.2.1. Electrochemistry of 2-heptyl-4,7-di(thiophen-2-yl)-1H-benzo[d]imidazole (PBImTh) and 4,7-bis(2,3-dihydrothieno[3,4-b][1,4]dioxin-5-yl)-2-heptyl-1H-benzo[d]imidazole (BImEd)……...33

3.2.2. Spectroelectrochemistry of poly(2-heptyl-4,7-di(thiophen-2-yl)-1H-benzo[d]imidazole) (PBImTh) and poly(4,7-bis(2,3-dihydrothieno[3,4-b][1,4]dioxin-5-yl)-2-heptyl-1H-benzo[d]imidazole) (PBImEd).....36

3.2.3. Kinetic Properties of poly(2-heptyl-4,7-di(thiophen-2-yl)-1H-benzo[d]imidazole) (PBImTh) and poly(4,7-bis(2,3-dihydrothieno[3,4-b][1,4]dioxin-5-yl)-2-heptyl-1H-benzo[d]imidazole) (PBImEd)…....38

4. EXPERIMENTAL……41

4.1. Materials……41

4.2. Equipment……...41

4.3. Procedure ……...41

4.3.1. Synthesis……...41

4.3.1.1. Synthesis of 4,7-dibromo-2-phenyl-1H-benzo[d]imidazole……...41

4.3.1.2. Synthesis of 4,7-bis(2,3-dihydrothieno[3,4-b][1,4]dioxin-5-yl)-2-phenyl-1H-benzo[d]imidazole (BImBEd)……...42

4.3.1.3. Synthesis of 1,4-bis(2,3-dihydrothieno[3,4-b][1,4]dioxin-5-yl)benzene (BEDOT-B)…...…42

4.4. Characterization of Conducting Polymers……..43

4.4.1. Fourier Transform Infrared Spectroscopy (FTIR)……43

4.4.2. Cyclic Voltammetry (CV)……44

4.4.3. Spectroelectrochemistry……45

4.4.4. Switching Studies……45

4.4.5. Colorimetry……..……46

5. RESULTS AND DISCUSSION…….……..49

5.1. Characterization of the monomers……..……49

5.1.1. 4,7-bis(2,3-dihydrothieno[3,4-b][1,4]dioxin-5-yl)-2-phenyl-1H-benzo[d]imidazole (BImBEd)…….……49

5.1.2. 1,4-bis(2,3-dihydrothieno[3,4-b][1,4]dioxin-5-yl)benzene (BEDOT-B)……..……..50

5.1.3. FT-IR analyses of 4,7-dibromo-2-phenyl-1H-benzo[d]imidazole, 4,7-bis(2,3-dihydrothieno[3,4-b][1,4]dioxin-5-yl)-2-phenyl-1H-benzo[d]imidazole (BImBEd) and 1,4-bis(2,3-dihydrothieno[3,4-b][1,4]dioxin-5-yl)benzene (BEDOT-B)……..……52

5.2. Electrochemical and Electrochromic Properties of 4,7-bis(2,3-dihydrothieno[3,4-b][1,4]dioxin-5-yl)-2-phenyl-1H-benzo[d]imidazole (BImBEd) and 1,4-bis(2,3-dihydrothieno[3,4-b][1,4]dioxin-5-yl)benzene (BEDOT-B)……52

5.2.1. Electrochemistry of 4,7-bis(2,3-dihydrothieno[3,4-b][1,4]dioxin-5-yl)-2-phenyl-1H-benzo[d]imidazole (BImBEd)……...52

5.2.2. X-ray photoelectron spectroscopy (XPS) studies for PBImBEd, PBImBEd02a and PBImBEd02b……56

5.2.3. Electrochemistry of 1,4-bis(2,3-dihydrothieno[3,4-b][1,4]dioxin-5-yl)benzene (BEDOT-B)….57

5.2.4. Spectroelectrochemistry of poly(4,7-bis(2,3-dihydrothieno[3,4-b][1,4]dioxin-5-yl)-2-phenyl-1H-benzo[d]imidazole) (PBImBEd) and poly(1,4-bis(2,3-dihydrothieno[3,4-b][1,4]dioxin-5-yl)benzene) (PBEDOT-B)……59

5.2.5. Kinetic Properties of poly(4,7-bis(2,3-dihydrothieno[3,4-b][1,4]dioxin-5-yl)-2-phenyl-1H-benzo[d]imidazole) (PBImBEd) and poly(1,4-bis(2,3-dihydrothieno[3,4-b][1,4]dioxin-5-yl)benzene) (PBEDOT-B)……64

6. CONCLUSION……69

REFERENCES……70

LIST OF FIGURES

FIGURES

Figure 1.1 Chemical structures and names of some common polymers……1

Figure 1.2 Representative structure of tungsten (VI) oxide (WO_3)……...2

Figure 1.3 Oxidation/reduction reactions of viologens……..3

Figure 1.4 Reactions occurring during partial oxidation and reduction of polymers……4

Figure 1.5 Charge carries in polypyrrole (PPy) and corresponding energy gaps……..5

Figure 1.6 Schematic band diagrams for an insulator, a semiconductor, a conductor……..6

Figure 1.7 Band structure of a conjugated polymer as a function of p-doping level…..7

Figure 1.8 Band generation of polyacetylene……8

Figure 1.9 Conductivity of some conjugated polymers……..9

Figure 1.10 Conductivity range of conducting polymers compared to those of other metarials……10

Figure 1.11 Common ways to lower the band gap……..11

Figure 1.12 Illustration of Peierls distortion……11

Figure 1.13 Effect of planarity on band gap of a conjugated polymer……12

Figure 1.14 Aromatic and quinoid structures of PITN……13

Figure 1.15 Band gap lowering due to DA approach……..13

Figure 1.16 Electrochemical oxidation mechanism of EDOT……15

Figure 1.17 Effect of EDOT on the band gap……..16

Figure 1.18 Structures of benzotriazole (BTz), benzothiadiazole (BTd), benzoselenadiazole (BSe), and benzimidazole (BIm)……16

Figure 1.19 Structures designed by Takagi et al. to investigate the effect of H-bonding and maximum wavelength values for absorption and emission……..17

Figure 2.1 Synthetic route for 4,7-dibromobenzo[c][1,2,5]thiadiazole…….....20

Figure 2.2 Synthetic route for 3,6-dibromocyclohexa-3,5-diene-1,2-diamine……20

Figure 2.3 Synthetic route for 4,7-dibromo-2-heptyl-1H-benzo[d]imidazole…….21

Figure 2.4 Synthetic route for tributyl(thiophen-2-yl)stannane……...21

Figure 2.5 Synthetic route for tributyl(2,3-dihydrothieno[3,4-b][1,4]dioxin-5-yl)stannane…….....22

Figure 2.6 Synthetic route for BImTh……..22

Figure 2.7 Synthetic route for BImEd…….23

Figure 2.8 Electrochemical polymerizations of BImTh and BImEd…….....23

Figure 2.9 Schematic representation of three electrode setup……..24

Figure 2.10 a) Triangular waveform of cyclic voltammetry. b) Current-potential relation of a reversible redox process……25

Figure 2.11 Dependance of current on scan rate……..26

Figure 2.12 Schematic representation of spectroelectrochemical instrumentation……..27

Figure 3.1 ^{1}H-NMR spectrum of BImTh……29

Figure 3.2 ^{13}C-NMR spectrum of BImTh……30

Figure 3.3 Mass spectrum of BImTh……...30

Figure 3.4 ^{1}H-NMR spectrum of BImEd……31

Figure 3.5 ^{13}C-NMR spectrum of BImEd……32

Figure 3.6 Mass spectrum of BImEd…….....32

Figure 3.7 Repeated potential scan of electrochemical polymerization of BImTh in equimolar 0.1 M $NaClO_4$ and $LiClO_4$, DCM:ACN (5:95, v:v) with 100 mV/s scan rate…….....33

Figure 3.8 Repeated potential scan of electrochemical polymerization of BImEd in equimolar 0.1 M $NaClO_4$ and $LiClO_4$, DCM:ACN (5:95, v:v) with 100 mV/s scan rate……34

Figure 3.9 First two cycles of repeated potential scan of electrochemical polymerization of BImEd in presence of base……35

Figure 3 :ate de of PB quimc $NaClO_4$ and $LiClO_4$, DCM:ACN (5:95,  100, 200, 300, 400 mV/s, b) oxidation and reduction……...35

Figure 3.11 Scan rate dependence of PBImEd in equimolar 0.1 M $NaClO_4$ and $LiClO_4$, DCM:ACN (5:95, v:v)a)  100, 200, 300, 400 mV/s, b) oxidation and reduction……...36

Figure 3.12 Normalized absorption spectra of PBImTh film on an ITO coated glass slide in monomer-free equimolar 0.1 M $NaClO_4$ and $LiClO_4$, ACN solution upon doping between 0.5 V and 1.2 V with 0.1 V increments……37

Figure 3.13 Normalized absorption spectra of PBImEd film on an ITO coated glass slide in monomer-free equimolar 0.1 M $NaClO_4$ and $LiClO_4$, ACN solution upon doping between 0.4 V and 1.3 V with 0.1 V increments……38

Figure 3.14 Percent transmittance change of PBImTh deposited on ITO electrode switching between 0.3 V and 1.2 V monitored at 440 and 1114 nm in monomer free equimolar 0.1 M $NaClO_4$ and $LiClO_4$, ACN solution……..39

Figure 3.15 Percent transmittance change of PBImEd deposited on ITO electrode switching between 0.3 V and 1.3 V monitored at 533 and 1120 nm in monomer free equimolar 0.1 M $NaClO_4$ and $LiClO_4$, ACN solution……..39

Figure 4.1 Synthetic route for 4,7-dibromo-2-phenyl-1H-benzo[d]imidazole…….....41

Figure 4.2 Synthetic route for BImBEd…….....42

Figure 4.3 Synthetic route for BEDOT-B……42

Figure 4.4 Electrochemical polymerization of BImBEd in neutral, acidic and basic conditions……44

Figure 4.5 Electrochemical polymerization of BEDOT-B in neutral and acidic conditions……...45

Figure 4.6 Representative applied potential and percent transmittance change……...46

Figure 4.7 CIELAB color space…….....46

Figure 5.1 ^{1}H-NMR spectrum of BImBEd……...49

Figure 5.2 ^{13}C-NMR spectrum of BImBEd……50

Figure 5.3 ^{1}H-NMR spectrum of BEDOT-B…….....51

Figure 5.4 ^{13}C-NMR spectrum of BEDOT-B……..51

Figure 5.5 FT-IR spectrum of BEDOT-B (up), 4,7-dibromo-2-phenyl-1H-benzo[d]imidazole (middle) and BImBEd (down) scanned in the amine stretching region in $CHCl_3$ solution……52

Figure 5.6 Repeated potential scan of electrochemical polymerizations of **(a)** BImBEd, **(b)** BImBEd01a, **(c)** BImBEd02a, **(d)** BImBEd03a, **(e)** BImBEd04a, **(f)** BImBEd01b, **(g)** BImBEd02b, **(h)** BImBEd03b and **(i)** BImBEd04b in 0.1 M $TBAPF_6$, DCM:ACN (5:95, v:v) with 100 mV/s scan rate……..54

Figure 5.7 Structures of BImBEd derivatives with acid and base addition…….56

Figure 5.8 N1s XPS data for (A) PBImBEd, (B) PBImBEd02b, and (C) PBImBEd02a……57

Figure 5.9 Repeated potential scan of electrochemical polymerizations of **(a)** BEDOT-B, **(b)** BEDOT-B01a, **(c)** BEDOT-B02a, **(d)** BEDOT-B03a, **(e)** BEDOT-B04a in 0.1 M $TBAPF_6$, DCM:ACN (5:95, v:v) with 100 mV/s scan rate……58

Figure 5.10 Electrochemical polymerization mechanism of BEDOT-B…….……59

Figure 5.11 Reduced (black lines) and oxidized (red lines) absorption spectra of (a) PBImBEd, (b)PBImBEd01a, (c) PBImBEd02a, (d) PBImBEd03a, (e) PBImBEd04a, (f) PBImBEd01b, (g)PBImBEd02b, (h) PBImBEd03b and (i) PBImBEd04b……..60

Figure 5.12 Reduced (black lines) and oxidized (red lines) absorption spectra of (a) PBEDOT-B, (b) PBEDOT-B01a, (c) PBEDOT-B02a, (d) PBEDOT-B03a, (e) PBEDOT-B04a……61

Figure 5.13 Normalized vis spectra of PBImBEd, PBImBEd01a, PBImBEd02a, PBImBEd03a, PBImBEd04a (left) and PBImBEd, PBImBEd01b, PBImBEd02b, PBImBEd03b, PBImBEd04b (right) in their reduced states……62

Figure 5.14 Normalized vis spectra of PBEDOT-B, PBEDOT-B01a, PBEDOT-B02a, PBEDOT-B 03a, PBEDOT-B04a in their reduced states…….62

Figure 5.15 Colors of the polymer films in their reduced (left) and oxidized (right) states for a) PBEDOT-B, b) PBImBEd, c) PBImBEd01a, d) PBImBEd02a, e) PBImBEd03a, f) PBImBEd04a, g) PBImBEd01b, h) PBImBEd02b, i) PBImBEd03b and j) PBImBEd04b……..63

Figure 5.16 Percent transmittance differences for PBImBEd, PBImBEd01a, PBImBEd02a, PBImBEd03a, PBImBEd04a, PBImBEd01b, PBImBEd02b, PBImBEd03b and PBImBEd04b at maximum absorption wavelengths in a) visible region, b) NIR region…….....65

Figure 5.17 Percent transmittance differences for BEDOT-B, BEDOT-B01a, BEDOT-B02a, BEDOT03a and BEDOT-B04a at their maximum absorption wavelengths in a) visible region, b) NIR region…….66

LIST OF TABLES

TABLES

Table 5.1 Results of the electrochemical properties of polymers with changing the amounts of acid/base during successive polymerizations of BImBEd……55

Table 5.2 Results of the electrochemical properties of polymers with changing the amounts of acid during successive polymerizations of BEDOT-B……58

Table 5.3 Optical band gap values of the polymers with changing the amounts of acid/base during successive polymerizations of BImBEd……63

Table 5.4 List of L, a, b values of all the polymer films……..64

Table 5.5 Optical contrast values of the polymers at their maximum absorption wavelengths in vis and NIR region……67

LIST OF ABBREVATIONS

PA	Polyacetylene
PPP	Polyparaphenylene
PT	Polythiophene
OLED	Organic Light Emitting Diode
OSC	Organic Solar Cell
OFET	Organic Field Effect Transistor
PPy	Polypyrrole
Eg	Band gap
DA	Donor Acceptor
PITN	Polyisothianaphthene
Th	Thiophene
EDOT	Ethylenedioxy thiophene
BTz	Benzotriazole
BTd	Benzothiadiazole
BSe	Benzoselenadiazole
BIm	Benzimidazole
RGB	Red Green Blue

CHAPTER I

INTRODUCTION

1.1. Conducting Polymers

All carbon based polymers were known to be insulators untill 1977 when Alan J. Heeger, Alan G. MacDiarmid and Hideki Shirakawa accidentally discovered that conjugated polymers can gain high conductivity upon doping. They were awarded with Nobel Prize in chemistry "for the discovery and development of electrically conductive polymers" in the year 2000 [1, 2]. The doping process can be done by insertion or removal of electrons from the polymer backbone, corresponding to the reduction or the oxidation, respectively. Shirakawa et. al. doped polyacetylene (PA) with iodine: As iodine is a strong electron acceptor, it disturbed the electron localization of PA and enabled the polymer to conduct electricity billion folds more than undoped PA. This breakthrough caused intense research of the other conjugated polymers, such as polyparaphenylene (PPP) and polythiophene (PT) (Figure 1.1) [3, 4].

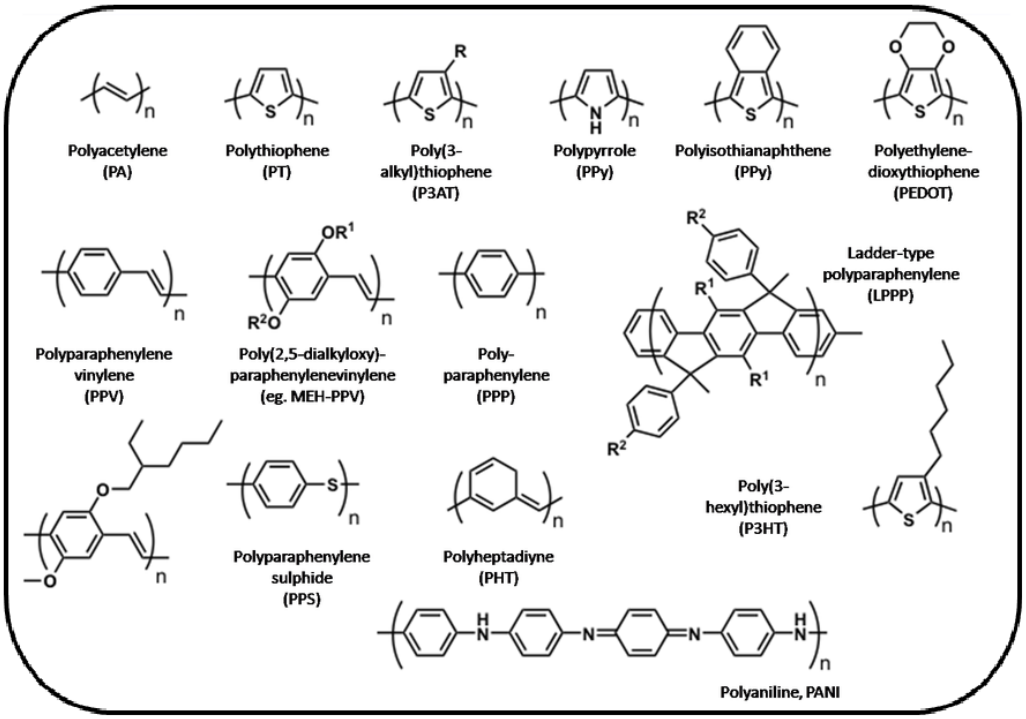


Figure 1.1 Chemical structures and names of some common polymers. Adapted from http://photonicswiki.org/images/1/1b/Conjugated_polymer_common.png.

The promising results of these studies ended up with the term "synthetic metals" as the conducting polymers acquires the electrical, electronic, magnetic and optical properties of a metal, and mechanical properties and processability of an organic polymer. These conducting polymers have numerous applications such as electrochromic devices [5], organic light emitting diodes (OLEDs) [6], organic solar cells (OSCs) [7], organic field effect transistors (OFETs) [8], enzyme immobilization [9].

1.2. Electrochromism and Electrochromic Materials

Chromism is defined as the reversible change in optical properties of a material, such as absorbance and reflectance, caused by an external force. Common types of chromism are photochromism, thermochromism, ionochromism, solvatochromism and electrochromism [10]. In case of electrochromism, the external force is an applied potential. That is to say, electrochromism can be defined as the reversible optical change of a material stimulated by an electric current. The change in the color of a material can be between transparent and color states, or between different colors. The material is denominated to be multichromic if it possesses more than two colors [11].

Electrochromic property was first discovered in inorganic materials and has been studied since 1968 [12]. Most common of the inorganic electrochromic materials is the tungsten (VI) oxide (WO_3) in which octahedral WO_6 molecules which share corners and forms a cubic structure as seen in Figure 1.2. This cubic structure contains empty spaces that are capable of including guest ions to the structure. Contribution of electrons and cations (M^+ such as Li^+ or H^+) to these empty spaces are accepted to be responsible for the electrochromic property of WO_3 [13]. Insertion of metallic cations and corresponding electrons to the structure through reduction causes the tungsten sites with +6 oxidation state to have +5 oxidation state and change color from very pale yellow to blue. Oxidation of the molecule reverses the color back to pale yellow, which makes the process reversible. The reduction reaction can be summarized as;

$$\underset{\text{(very pale yellow)}}{WO_3 + x(M^+ + e^-)} \rightarrow \underset{\text{(blue)}}{M_x W^{VI}_{(1-x)} W^{V}_{x} O_3}$$

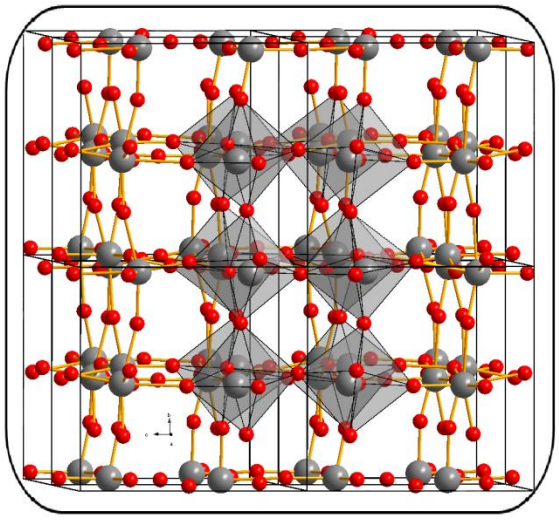


Figure 1.2 Representative structure of tungsten (VI) oxide (WO_3).

Dyes and conducting polymers are the other important branches of electrochromic materials. Viologens (bipyridinium derivatives of 4,4'-bipyridyl) are the most common examples for the electrochromic dye molecules as their color alter reversibly for multiple times upon oxidation/reduction reactions [14]. The color changes are provided by the three different redox states of the viologens (Figure 1.3). The dication structure of the viologen is colorless whereas the radical cation formed by reduction of the dication is intensely colored. The color of the radical cation is caused by the charge transfer between the +1 and zero valent nitrogens and can be adjusted by changing the nitrogen substituents.

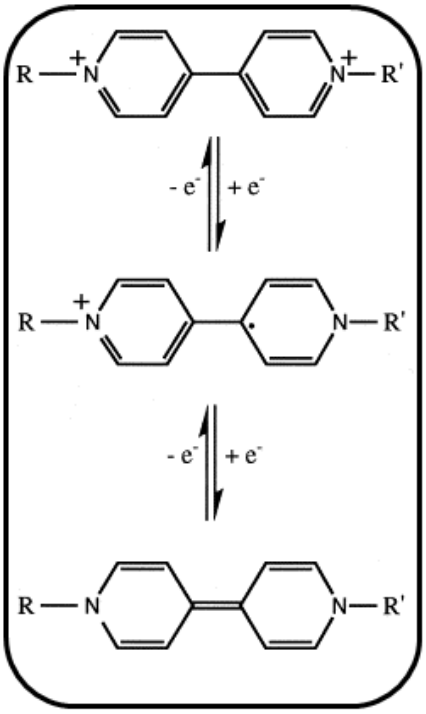


Figure 1.3 Oxidation/reduction reactions of viologens. Adapted from R. J. Mortimer, Electrochimica Acta, 44 (1999) 2971.

The last important class of electrochromic materials is conducting polymers. Conducting polymers have several advantages [15] such as;

- low cost during process,
- improved mechanical properties,
- high coloration efficiency,
- short switching time,
- band gap tuning through structure modification.

The change in the optical properties of conducting films is acquired by the partial oxidation or reduction of the polymer chains as shown in Figure 1.4. The color that the polymer possesses depends on the wavelength it absorbs light, thus the energy gap. The energy gap refers to onset energy of the π-π^* transition in the neutral state of a conducting polymer.

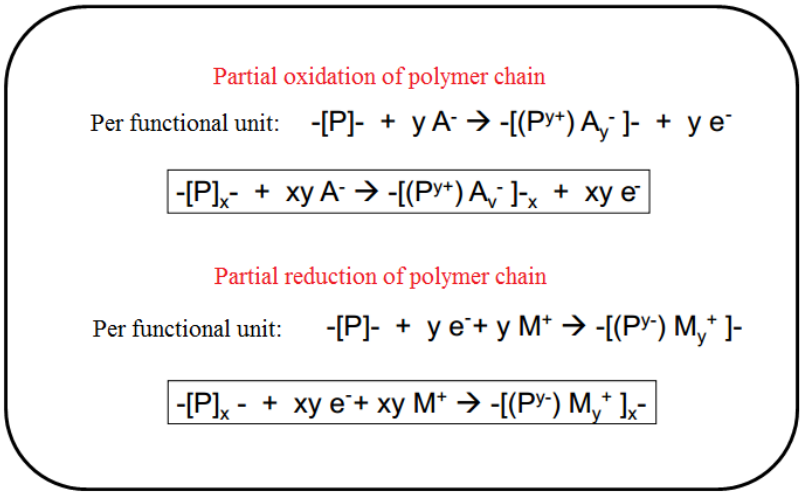


Figure 1.4 Reactions occurring during partial oxidation and reduction of polymers.

The energy gap corresponds to a transition between the valence band to the conduction band of the polymer in the neutral state. However, the energy gap decreases upon oxidation with the formation of polarons as an electron is removed from the valence band. This results in a higher energy state containing an unpaired electron. Simultaneously, the corresponding antibonding energy level in the conduction band is lowered. As a result, two new intragap states and for possible transitions are formed. This phenomenon is schematically described in Figure 1.5 by using polypyrrole (PPy) as an example. In the same vain, reduction of a polymer chain causes new intragap states by inserting an electron to the conduction band. The newly formed intragap states have lower energy gap thus absorbs light at higher wavelength and this shift in absorption results in change of color [16].

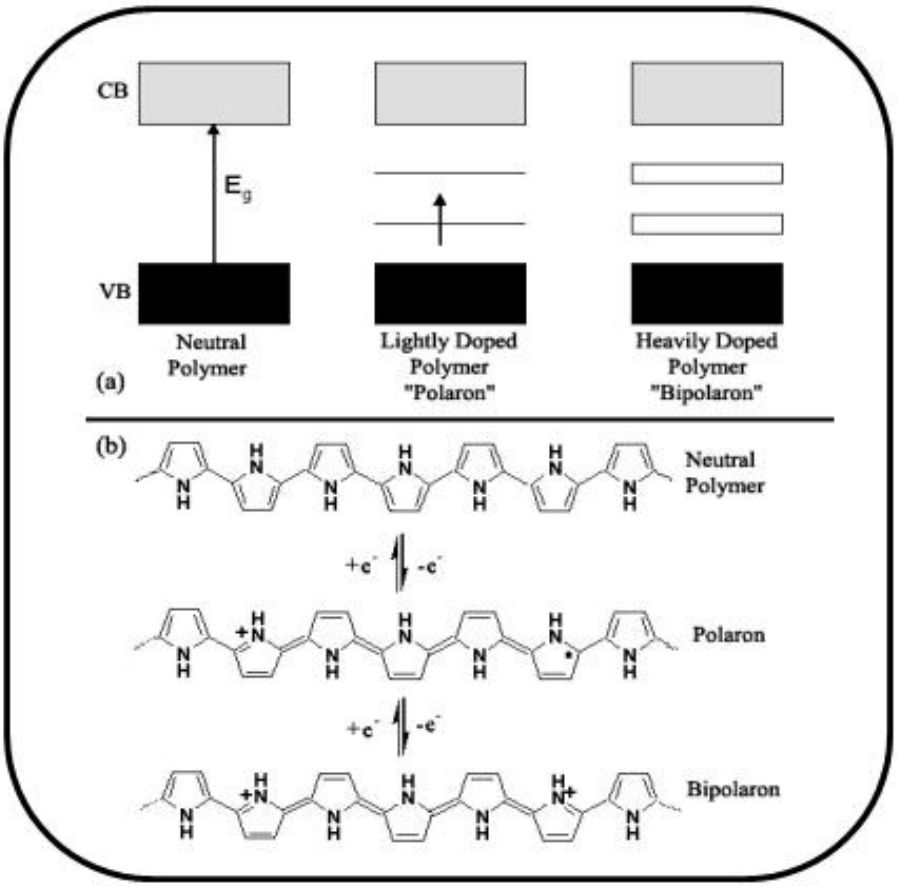


Figure 1.5 Charge carries in polypyrrole (PPy) and corresponding energy gaps.

As an outcome of the advantages mentioned before together with the easy color tuning, electrochromic conducting polymers can be used in various applications such as;

- information display and data storage [17],
- rear-view mirrors and visors in the automotive industry [18],
- smart windows in architecture [19].

1.3. Band Theory

Electronic structure of the insulators, semiconductors, and conductors (metals) are described by the band theory.

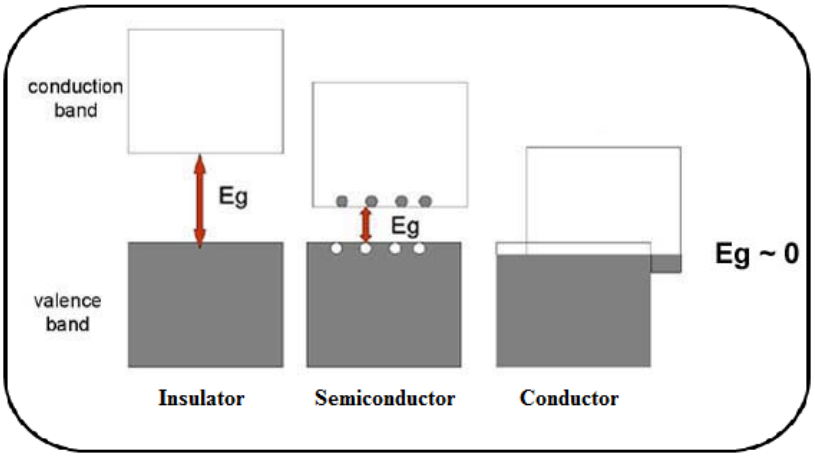


Figure 1.6 Schematic band diagrams for an insulator, a semiconductor, a conductor. Adapted from http://education.mrsec.wisc.edu/Edetc/background/LED/band.htm.

The electrical conductivity is provided by the current flow caused by the excitation of the electron from the lowermost valence band to the uppermost unoccupied conduction band. In case of metals, these bands are intertwined and there exists a band which is partly empty and partly occupied which enables the free movement of electrons. This provides high conductivity to metals regardless of temperature. In case of semiconductors and insulators, the valence and conduction bands are separated by a band gap (E_g) (Figure 1.6). This band gap is larger for insulators, thus the excitation does not occur and the material does not conduct electricity. The semiconductors have smaller band gap than the insulators which enables excitation of the electrons from valence band either thermally or photochemically. The electron transfer can occur by means of carrier generation and the charge carriers can be holes or electrons [20]. This brings semiconductors in conductivity but strongly dependent on the temperature. Band structure of a conjugated polymer in the presence of holes as charge carriers (p-doping) is shown in Figure 1.7.

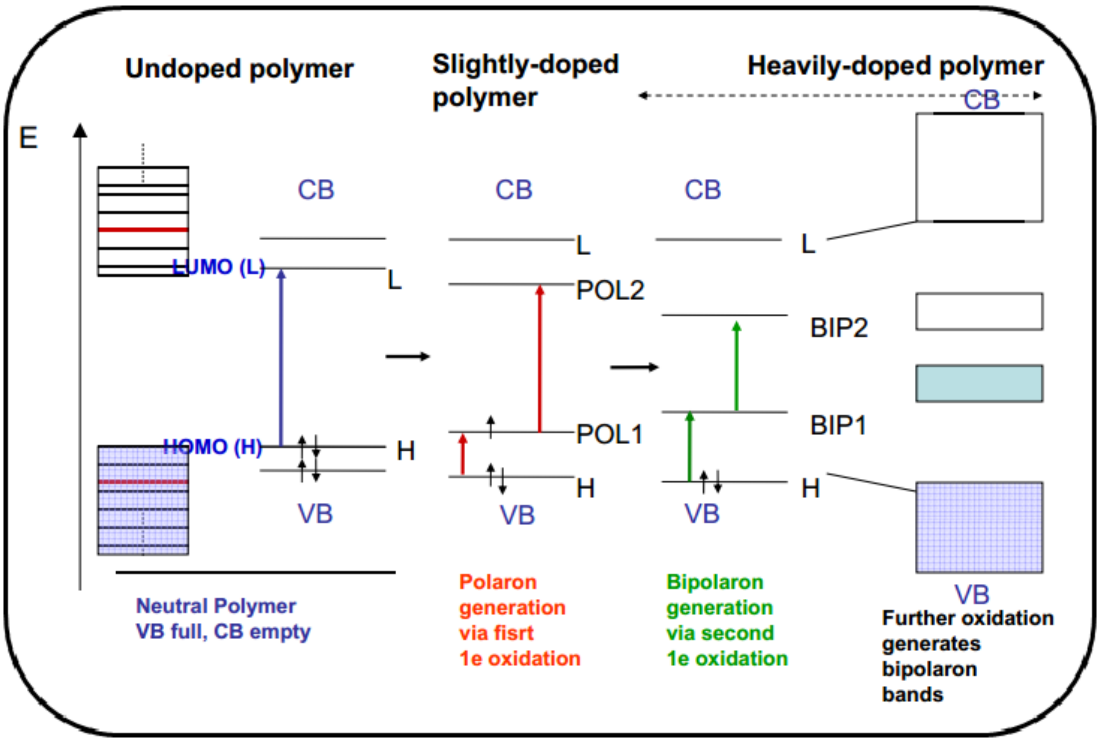


Figure 1.7 Band structure of a conjugated polymer as a function of p-doping level. Adapted from http://www.public.asu.edu/~ntao1/Teaching/EEE598/Erica%20ppt%20[Compatibility%20Mode].pdf.

Polyacetylene offers an easy way to study the band theory of conducting polymers as it has a simple structure composed of sp^2 hybridized carbon atoms with alternating single and double bonds. Also all the bond lengths are equal because of the extensive delocalization. The band structure varies as in Figure 1.8 with the change in conjugation length. The electronic levels lose their discrete characteristic and display continuum band structures as the conjugation length increase. Repeating units' π orbitals can overlap throughout the chain [21].

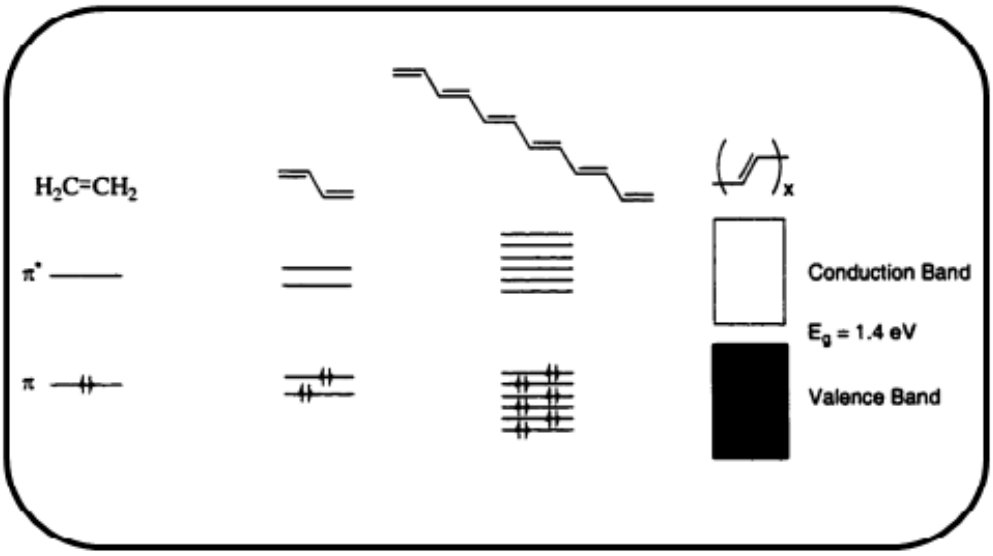


Figure 1.8 Band generation of polyacetylene. Adapted from A. Balan, Synthesis of Benzotriazole Bearing Donor Acceptor Type Electroactive Monomers Towards High Optical Contrast and Fast Switching Electrochromic Materials, MSc. Thesis, METU, 2009.

Doping the polyacetylene with high conjugation length reveals quite high conductivity up to 10^5 S/cm with the formation of solitons [22]. However, the resulting polymer is air unstable, thus hard to work with. This complication generated necessity of studies on other conjugated polymers which are more stable and applicable conducting polymers. The poly(heterocycles) are discovered to be quite conductive in the early 1980's. Conductivity values of some conducting polymers are shown in Figure 1.9. These polymers can be doped chemically or electrochemically to be used as conducting polymers. Congruent with the soliton formation in PA, radical cation formation corresponding to the polaronic states are occurring in case of these conducting polymers. Furher doping of the polymers removes the unpaired electron and/or combines the polarons and causes dication formation corresponding to the bipolaronic states (Figure 1.5).

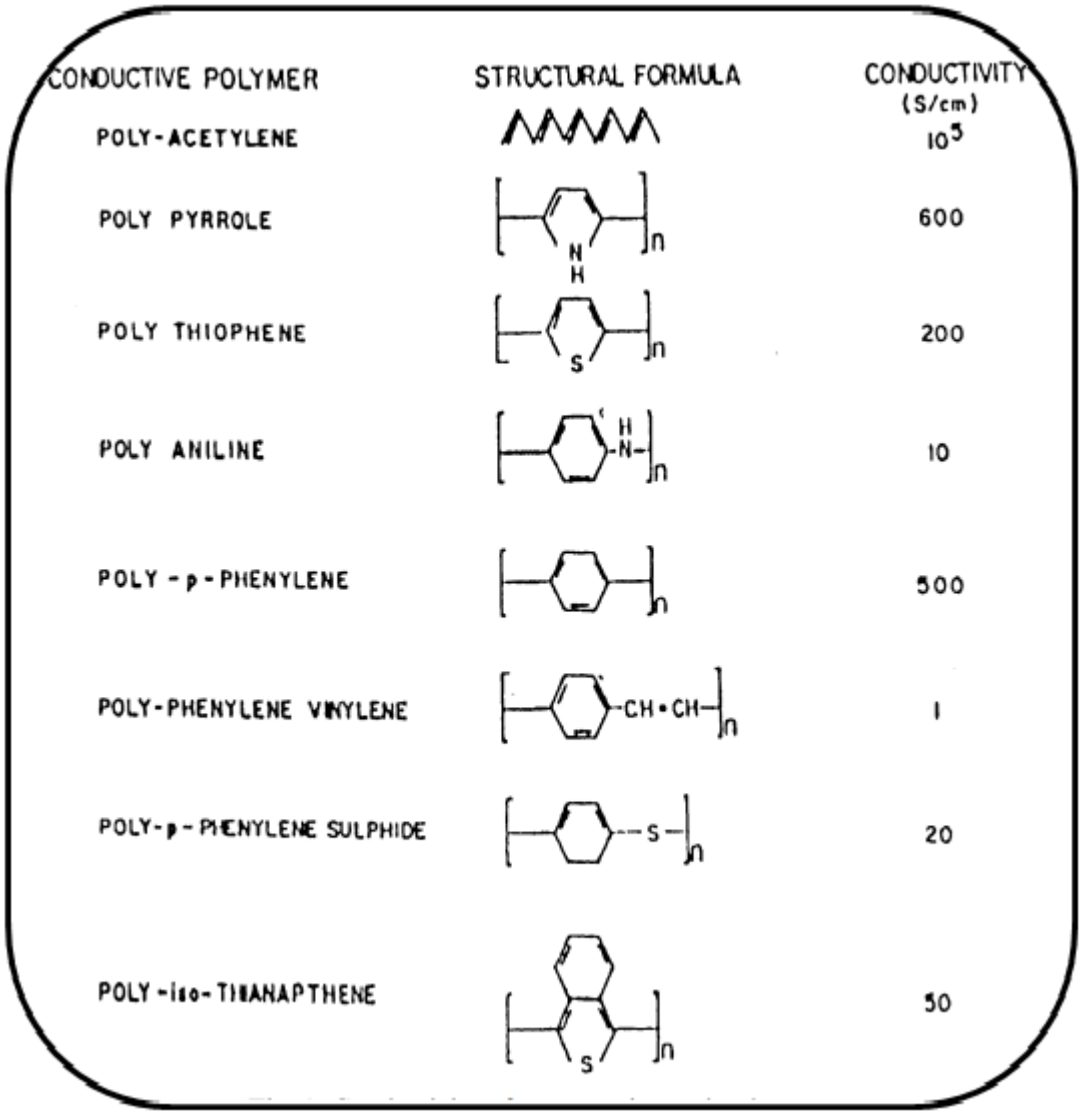


Figure 1.9 Conductivity of some conjugated polymers. Adapted from D. Kumar, R. C. Sharma, Eur. Polym. J., 34 (1998) 1053.

1.4. Lowering the Band Gap

For the aim of maximizing the neutral conductivity of conjugated polymers, lowering the band gap is a vital goal. The conducting polymers have a wide range of conductivity (Figure 1.10) [24]. Most of the conjugated polymers synthesized for the purpose have band gaps greater than 2 eV which is in the range of mid- to high band gap polymers. To be considered as a low band gap polymer, the band gap value should be below 1.5 eV.

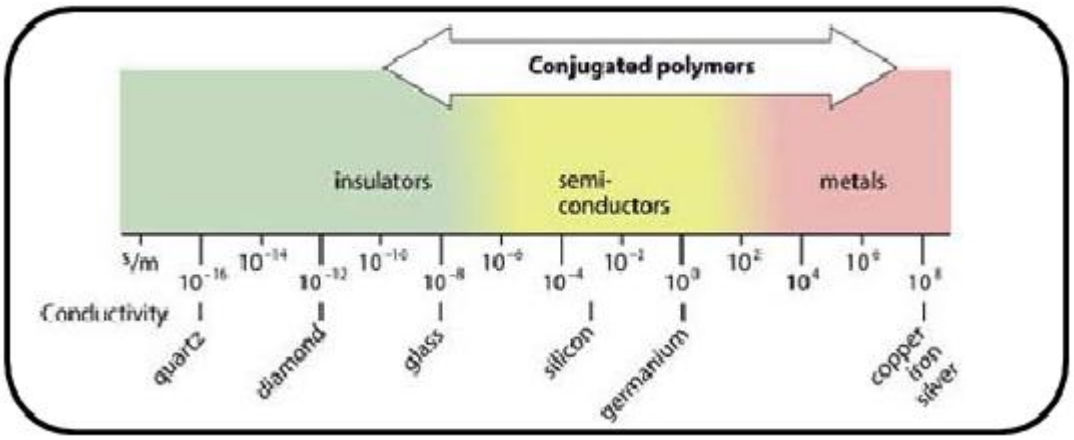


Figure 1.10 Conductivity range of conducting polymers compared to those of other metarials. Adapted from http://www.surfacefinishing.com/doc.mvc/Conductive-Polymers-a-Surprising-Discovery-0001.

The conductivity, the color of the material, the ease of doping, and the stability in the doped states strongly depend on the band gap value of the polymer. Lowering the band gap derives a moral certainty of polymers to be transparent in the doped state. This outcome results in the polymers to be used in numerous applications such as smart windows where existence of a transparent state is substantial.

Lowering the band gap of a conducting polymer according to the application purpose become more of an issue as the application area diversifies. There are various ways to alter the band gap such as (Figure 1.11) [23];

- controlling bond-length alternation (Peierls distortion),
- creating highly planar systems,
- inducing order by interchain effects,
- generating resonance effects along the polymer backbone,
- using the Donor Acceptor (DA) approach.

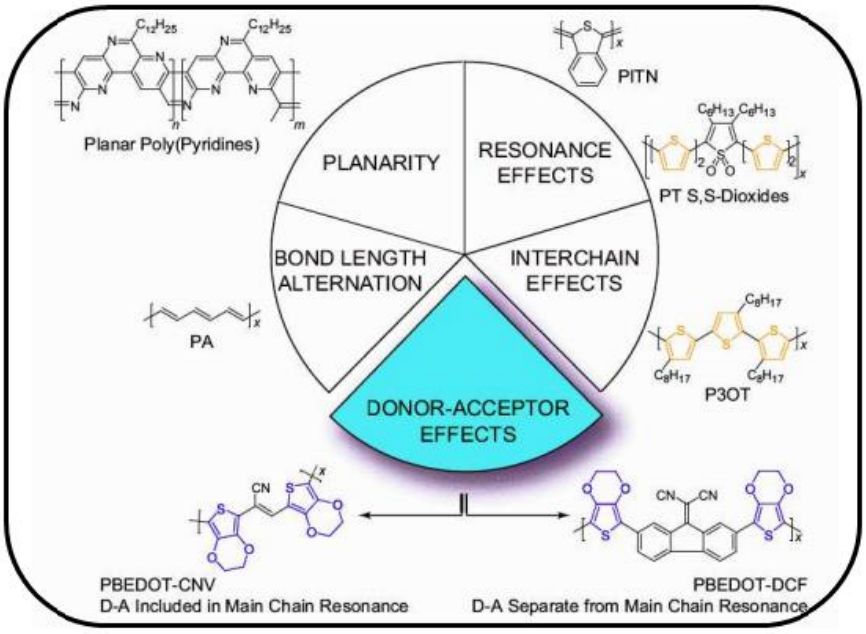


Figure 1.11 Common ways to lower the band gap. Adapted from A. Balan, Synthesis of Benzotriazole Bearing Donor Acceptor Type Electroactive Monomers Towards High Optical Contrast and Fast Switching Electrochromic Materials, MSc. Thesis, METU, 2009.

1.4.1. Controlling Bond-Length Alternation (Peierls Distortion)

Peierls distortion is distortion of a uniform one dimensional chain with a partially occupied band to give bond alternation to lower its energy [24]. This leads to dimerization or oligomerization in one of the two ways illustrated in Figure 1.12.

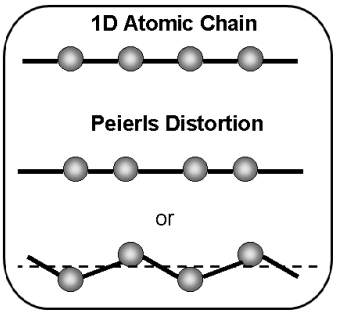


Figure 1.12 Illustration of Peierls distortion. Adapted from http://nanowiz.tripod.com/lowdim/peierls.htm

Bond-length alternation of the conjugated polymers is achieved using the length variation of single and double bonds along the polymer backbone.

1.4.2. Creating Highly Planar Systems

Band gap of a conjugated polymer increases with increasing torsional angle between which is a problem to be overcame with highly planar systems [25]. Different ways of creating planar conjugated polymers are studied in the literature such as ladder-like polyarylenes and polyquinoxalines. However these systems resulted in higher band gaps than expected due to the bond length alternation.

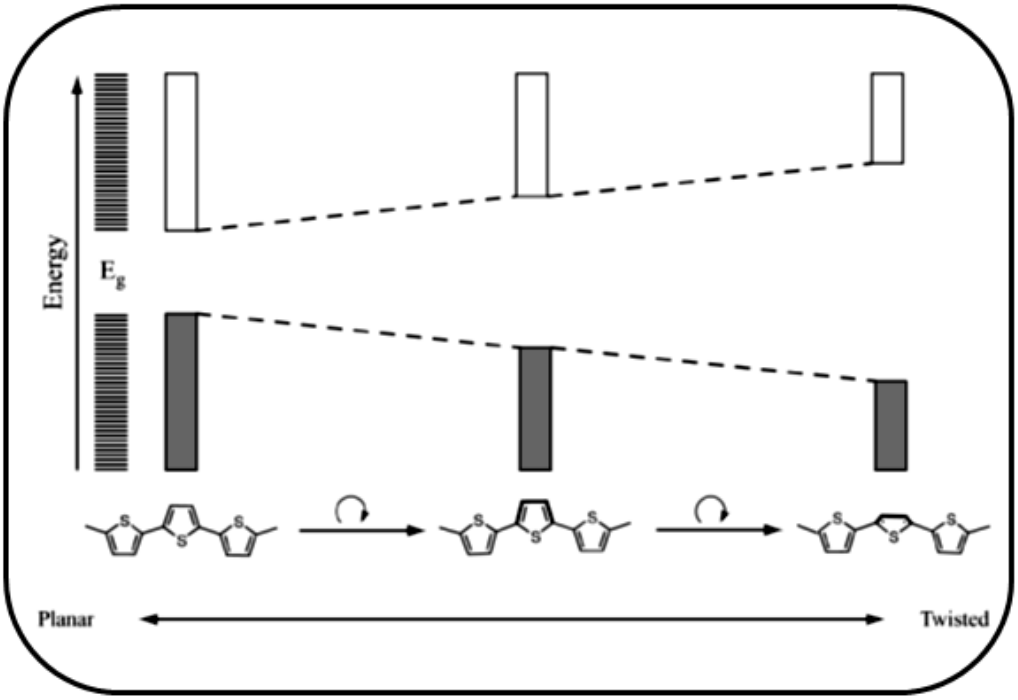


Figure 1.13 Effect of planarity on band gap of a conjugated polymer

1.4.3. Inducing Order by Interchain Effects

The interchain effects come into play when the polymer chains or individual molecules assemble into a material. As the conducting polymer chains have finite molecular weight, the conductivity is supplied by interchain hopping which is dependent on the interchain π-π stacking [26]. The interchain interactions may provide better stacking between the chains or cause electron transitions from π-band of one chain to the π-band of another chain. However the interchain interactions are significantly weaker than the intra-chain π-electron interactions [27].

1.4.4. Generating Resonance Effects Along the Polymer Backbone

Conducting polymers have two different resonance structures as aromatic and quinoid due to their non-degenerate ground states. The aromatic form has higher band gap than the quinoid form [28]. In this vain, creating quinoidal state on the polymer backbone is a way of lowering the band gap.

Polyisothianaphthene (PITN) as an appropriate example for this purpose. Aromatic and quinoid resonance structures of PITN are given in Figure 1.14. PITN composes of benzene and thiophene having 1.56 eV and 1.26 eV aromatization energies, respectively. This makes PITN to be more stable in the quinoid form and lowers the band gap compared to polythiophenes.

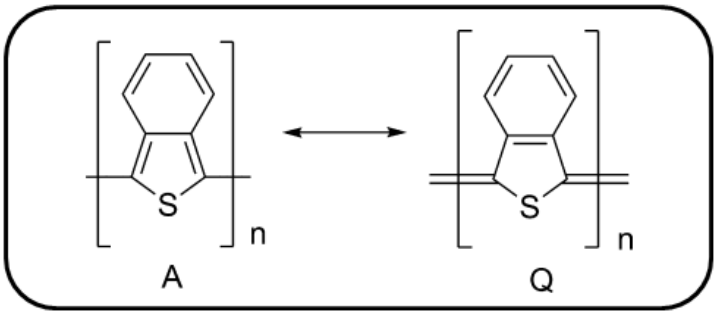


Figure 1.14 Aromatic and quinoid structures of PITN.

1.4.5. The Donor Acceptor (DA) Approach

The DA approach has attracted attention during the last decade as it provides a controlled way of tuning the band gap [29, 30]. Lower band gap is obtained by coupling an electron rich donor unit and an electron deficient acceptor unit. This coupling combines the high HOMO of the donor and low LUMO of the acceptor to generate a new lower band gap (Figure 1.15).

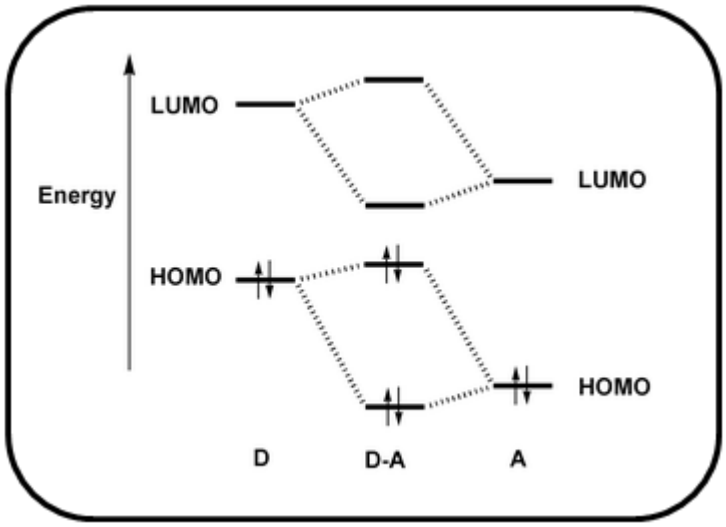


Figure 1.15 Band gap lowering due to DA approach. Adapted from H. A. M. van Mullekom, The Chemistry of High and Low Band Gap π-Conjugated Polymers. Ph. D. Thesis, Technishe Universiteit Eindhoven, 2000.

DA approach is important not only for lowering the band gap but also for providing the possibility of combining properties of two different moieties. This combination generally generates two distinct absorptions due to different π-π^* transitions. The absorption with the higher energy corresponds to the transition from the valence band of the donor unit to its antibonding state, whereas the one with the lower energy corresponds to the transition from the same band to the substituent localized conduction band [31]. If both absorption bands occur in the visible region, one covering the blue region and the other one

covering the red region with the same intensity, it is possible that the polymer reveals green color [32]. For the resulting polymer to carry these necessities, the donor and acceptor units can be varied to obtain a match between the moieties.

1.5. Thiophene and EDOT (ethylenedioxy thiophene) as Donor Units

Thiophene (Th) is an electron rich unit which is widely used in DA type polymers. Another important characteristic of Th is the empty 3- and 4-positions which make the molecule suitable for derivations. Alkyl chains can be substituted from the empty positions to make the corresponding polymer more soluble. Moreover, Heywang and Jonas substituted ethylenedioxy group into Th in 1992 and obtained a more stable polymer [33]. The resulting polymer, poly(ethylenedioxy thiophene) (PEDOT) revealed high optical contrast and fast switching times which made it an advantageous choice for electrochromic applications. PEDOT possesses transmissive sky blue color in the doped state, which is also beneficial for the use in device applications.

The oxygen atoms added to the Th structure resulted in a higher electron density. As both Th and EDOT have similar electrochemical polymerization mechanisms (Figure 1.16), the more electronegative EDOT lowers the oxidation potential of the DA type monomer it is participated in more than Th.

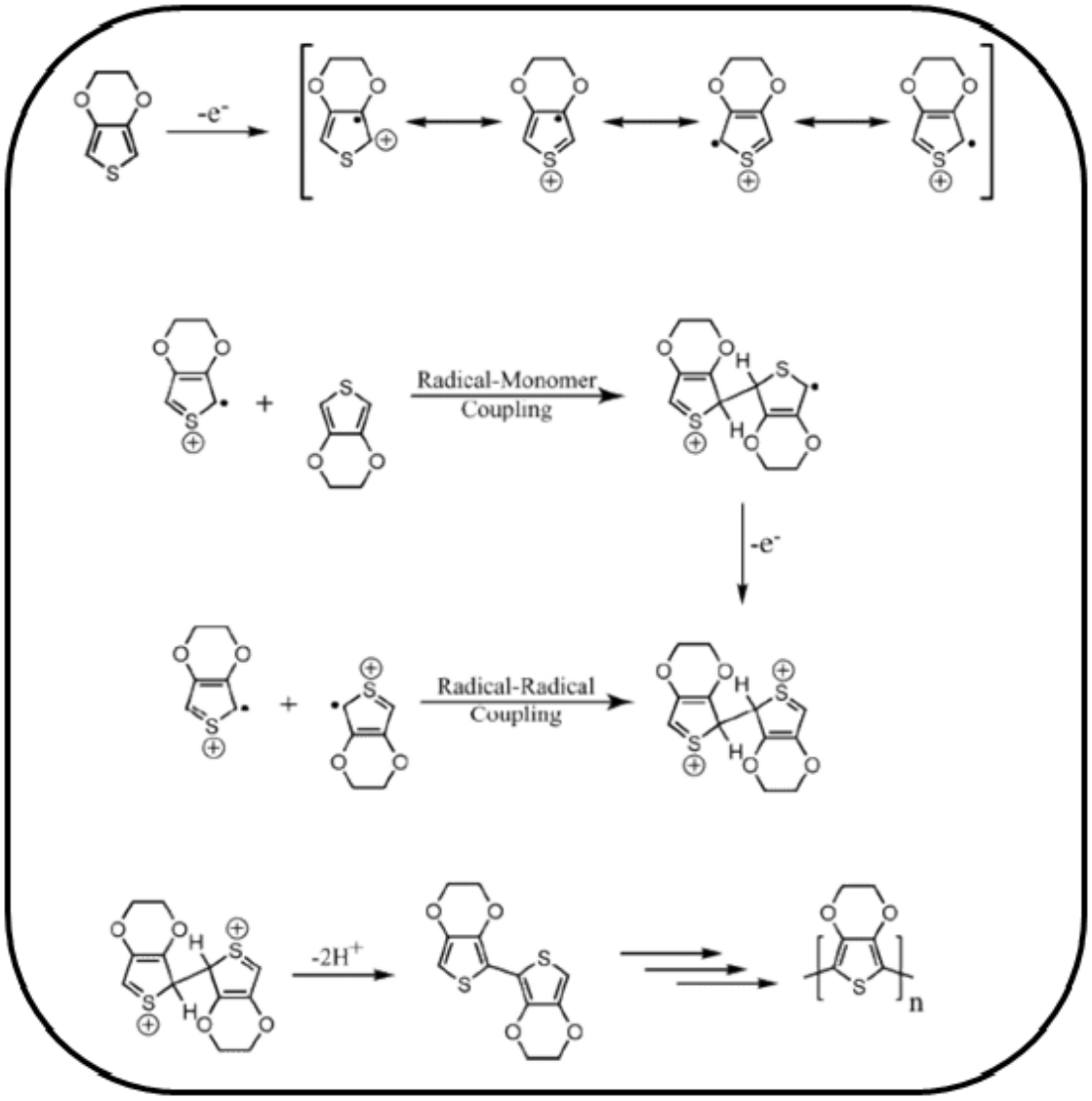


Figure 1.16 Electrochemical oxidation mechanism of EDOT. Adapted from H. Z. Akpınar, Synthesis of Benzimidazole Containing Donor Acceptor Electrochromic Polymers, MSc. Thesis, METU, 2011.

Including EDOT unit in the polymer backbone is expected to lower the band gap more than including Th. Thomas et. al. showed this with a study in 2004 [34], by coupling cyanovinylene (used as acceptor unit) with thiophene from both sides, thiophene and EDOT from each sides, and EDOT from both sides. The resulting polymers have 1.6 eV, 1.2 eV, and 1.1 eV, respectively as shown in Figure 1.17. These results indicate that the bend gap lowers with increasing number of EDOT units in the polymer backbone.

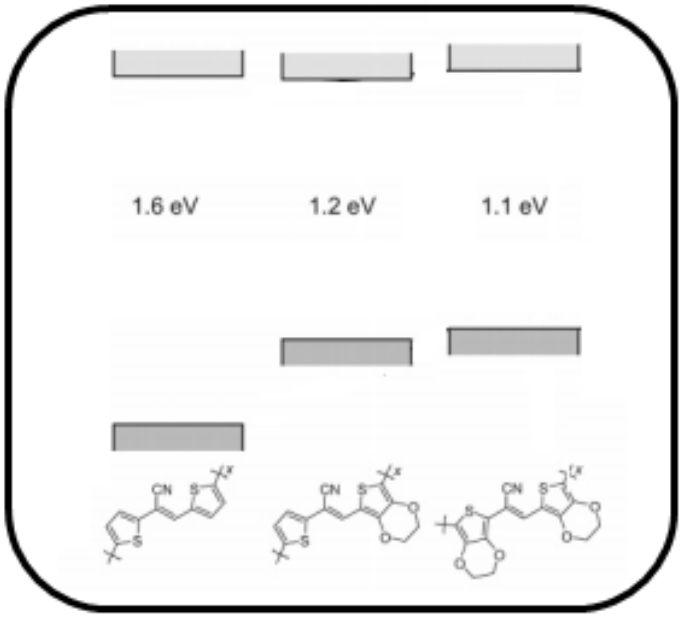


Figure 1.17 Effect of EDOT on the band gap. Adapted from C. A. Thomas, K. Zong, K. A. Abboud, P. J. Steel, J. R. Reynolds,, J. Am. Chem. Soc., 126 (2004) 16440.

1.6. Benzimidazole as an Acceptor Unit

Benzazole derivatives are commonly used as acceptor units in the literature. Benzotriazole (BTz), benzothiadiazole (BTd), benzoselenadiazole (BSe), and benzimidazole (BIm) are the most widely studied examples of benzazole derivatives (Figure 1.18).

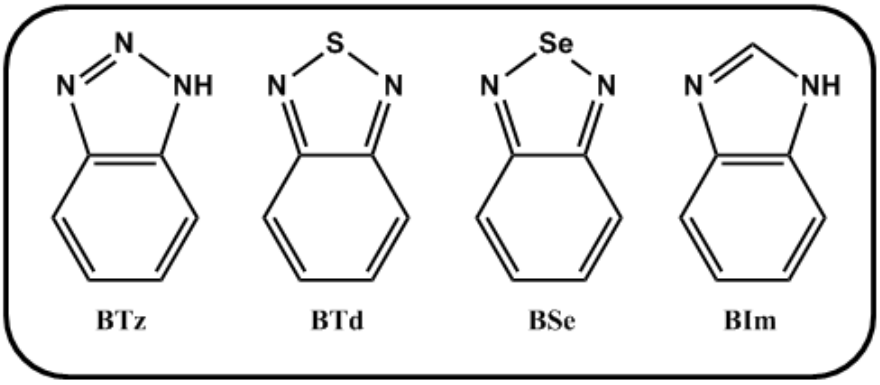


Figure 1.18 Structures of benzotriazole (BTz), benzothiadiazole (BTd), benzoselenadiazole (BSe), and benzimidazole (BIm).

DAD type conducting polymers bearing benzazole derivatives as acceptor unit and Th or EDOT as donor unit resulted in fine-tune optoelectronic properties. The first green to transmissive polymer was obtained

from BSe [35], also the first and only (up to now) polymer to possess all RGB (red- green- blue) colors and transmissive state was obtained using BTz [29].

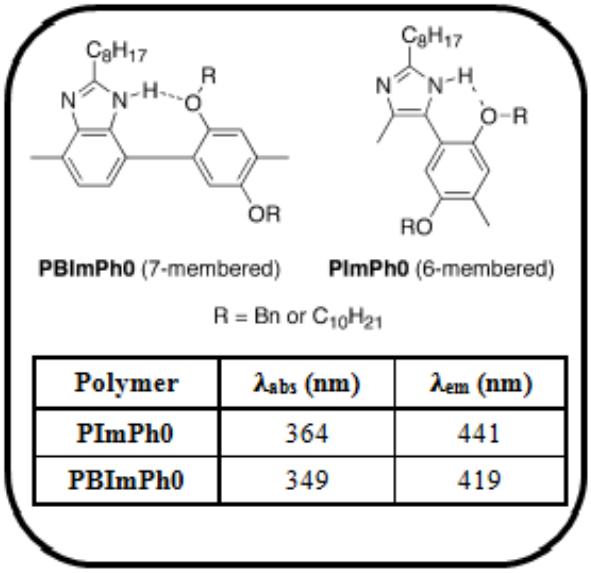
BIm was first electrochemically polymerized in 2000 by Shaheen Taj et. al. and it was proved that BIm and substituted benzimidazoles produce electroactive and conducting polymers [36].

The conjugated π-bonds in their structure and the electron deficient imine bond make the benzazoles important acceptor units. In addition to these, benzimidazoles contain an amine bond which is available for structural modification. Moreover, the acidic hydrogen of the amine bond can interact with the neighboring atoms and also provides vulnerability towards pH to the structure. Polybenzimidazoles also has photoluminescence property and great thermal stability. These attractive properties make the BIm containing polymers useful in various applications in aerospace field, biological applications and photovoltaics.

1.7. H-bonding

Recent studies showed that H-bonding can be used as a way of tuning the properties of conducting polymers [37, 38]. Although the effects of H-bonding seem to be secondary, the change on the optoelectronic properties caused by this kind of an interaction is considerable.

The H-bonding can cause different variations in the structure of a molecule. That is to say, the effect can be completely reverse in case of generation of a 6- membered and a 7-membered ring. Takagi et al. investigated this effect in 2008 by constructing two different molecules containing same structures as shown in Figure 1.19 [39]. They concluded that formation of 6-membered ring increases planarity thus directly decreased the band gap, whereas formation of 7-membered ring drastically decreases the planarity.



Polymer	λ_{abs} (nm)	λ_{em} (nm)
PImPh0	364	441
PBImPh0	349	419

Figure 1.19 Structures designed by Takagi et al. to investigate the effect of H-bonding and maximum wavelength values for absorption and emission. Adapted from K. Takagi, K. Sugihara, J. Ohta, Y. Yuki, S. Matsuoka, M. Suzuki, Polym. J., 40 (2008) 614.

Moreover, a partial charge accumulated on the sub-chain of the polymer in the presence of H-bonding effects the redox process and optoelectronic properties of the polymers [40].

1.8. Aim of This Work

In the first part of this study, the syntheses and characterization of electrochromic properties of benzimidazole (BIm) containing DAD type polymers were performed. Two different donor moieties, thiophene and EDOT were coupled with the same acceptor unit in order to highlight the effect of the donor moiety.

In the second part, the influence of hydrogen bonding on the conducting polymers was highlighted by using BIm as the acceptor and EDOT as the donor units. Control experiments were also performed to deduce reasonable conclusions.

CHAPTER 2

EXPERIMENTAL

2.1. Materials

Hydrobromic acid (Merck), bromine (Across), benzothiadiazole (Aldrich), sodium borohydride (Aldrich), hydrogen peroxide (Aldrich), octanal (Aldrich), ammonium cerium(IV)nitrate ($NH_4Ce(NO_2)_6$) (Aldrich), thiophene (Aldrich), n-butyl lithium (Aldrich), tributyltin chloride (Aldrich), ethylenedioxythiophene (EDOT) (Aldrich), bis(triphenylphosphine)palladium(II) dichloride ($Pd(PPh_3)_2Cl_2$) (Aldrich) were used as received. Tetrahydrofuran (THF) (Across) was dried over Na and benzophenone (Aldrich). Dicholoromethane (DCM) (Merck), chloroform ($CHCl_3$) (Merck), ethyl alcohol (EtOH) (Merck), anhydrous acetonitrile (ACN) (Across), ethyl acetate (Merck) and hexane (Merck) were used without further purification. Sodium bisulfide (Aldrich), sodium chloride (Aldrich), magnesium sulfate (Aldrich), ammonium chloride (Aldrich), Lithium perchlorate (Aldrich), Sodium perchlorate (Aldrich) were used as received.

2.2. Equipment

The NMR spectra of all intermediates and the final monomer were recorded on a Bruker-Instrument-NMR Spectrometer [DPX-400] using $CDCl_3$ as the solvent. Chemical shifts were given in ppm relative to tetramethylsilane as the internal standard. TOF Bruker Mass Spectrometer with an electron impact ionization source was used for the mass analyses. Cyclic voltammograms were recorded with a Voltalab 50 potentiostat. Indium tin oxide (ITO) coated glass, platinum wire and Ag wire were used as the working, counter and pseudo reference electrodes, respectively in a three-electrode cell during electrochemical polymerizations. Spectroelectrochemistry studies were performed using the same three-electrode cell in combination with a Solartron 1285 potentiostat/galvanostat with a Varian Cary 5000 spectrophotometer at a scan rate of 2000 nm/min. All of the measurements were conducted under nitrogen atmosphere at room temperature.

2.3. Procedure

2.3.1. Synthesis

2.3.1.1. Synthesis of 4,7-dibromobenzo[c][1,2,5]thiadiazole

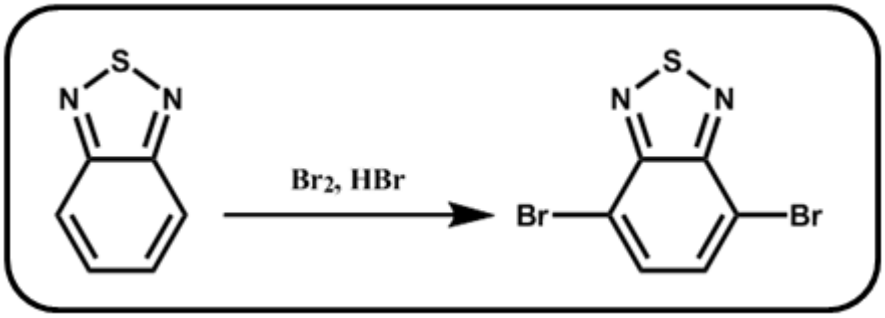


Figure 2.1 Synthetic route for 4,7-dibromobenzo[c][1,2,5]thiadiazole.

A mixture containing hydrobromic acid (16 mL) and bromine (2 mL) was added in small portions to a mixture containing hydrobromic acid (36 mL) and benzothiadiazole (2.0 g, 0.015 mol) with continuous stirring at 150°C. The reaction mixture was left overnight for reflux. Then the mixture was kept in ice bath, to produce the orange crystals, in about 3 to 4 hours. The orange crystals were filtrated, and then dissolved in dichloromethane. This organic phase was extracted by two portions of sodium bisulfide solution, and then with saturated sodium chloride solution. After the washing process, the mixture was dried over $MgSO_4$ and the solvent DCM was evaporated by rotary evaporator. The yellowish solid was vacuumed and then collected after drying in oven overnight. [41].

2.3.1.2. Synthesis of 3,6-dibromocyclohexa-3,5-diene-1,2-diamine

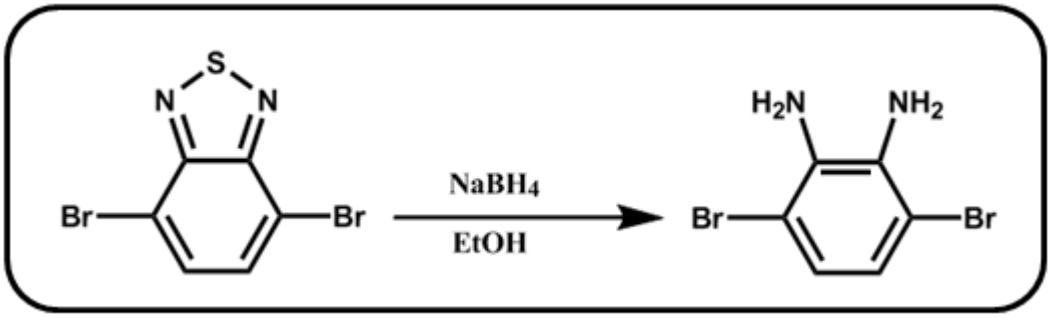


Figure 2.2 Synthetic route for 3,6-dibromocyclohexa-3,5-diene-1,2-diamine.

4,7-Dibromobenzo[c][1,2,5]thiadiazole (5.1 g) was dissolved in ethyl alcohol (170 mL) at 0°C. Sodium borohydride (12.2 g) was added to the prepared solution for 4 hours under argon atmosphere. After the addition of sodium borohydride was completed, the solution was stirred 12 hours at room temperature and the solvent ethanol was evaporated by rotary evaporator and the product was obtained with 67% yield [42].

2.3.1.3. Synthesis of 4,7-dibromo-2-heptyl-1H-benzo[d]imidazole

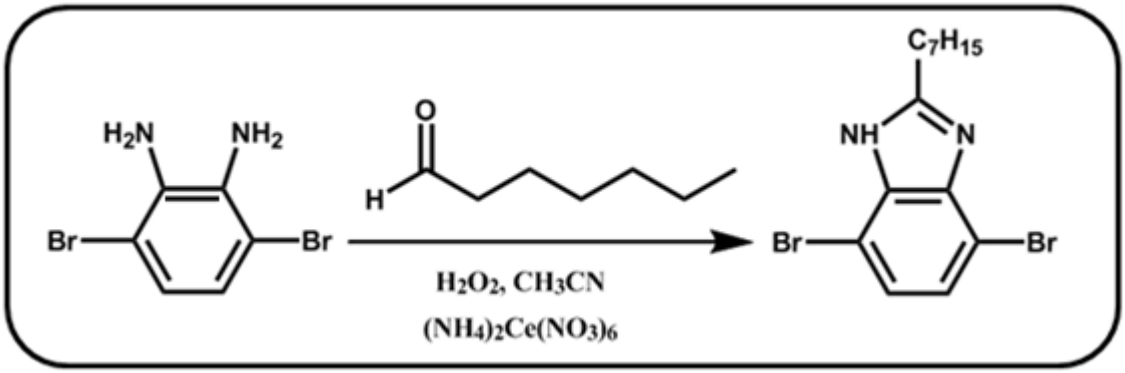


Figure 2.3 Synthetic route for 4,7-dibromo-2-heptyl-1H-benzo[d]imidazole.

1.88 mmol 3,6-dibromobenzene-1,2-diamine (500 mg) were dissolved in 24 mL acetonitrile in a flask with magnetic stirrer. 1.6 mL H_2O_2 was added directly to the solution. 3.76 mmol octanal was added dropwise and catalytic amount of $NH_4Ce(NO_2)_6$ was added at room temperature. The solution was refluxed overnight at 100^0C. After cooling the solution, extraction with ethyl acetate (3x75 mL) was performed. For further purification, coloumn chromatography with chloroform as solvent was used. 429.5 mg 4,7-dibromo-2-heptyl-1H-benzo[d]imidazole was synthesized successfully with 61.06 % yield [42].

2.3.1.4. Synthesis of tributyl(thiophen-2-yl)stannane

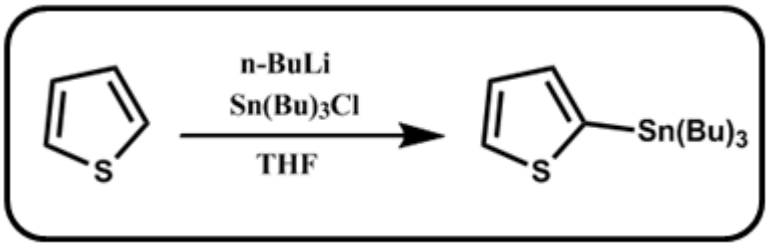


Figure 2.4 Synthetic route for tributyl(thiophen-2-yl)stannane.

Stannylation of thiophene was performed according to a procedure described in the literature [43]. At -78°C, in argon atmosphere, to a solution of thiophene (11.9 mmol, 0.96 ml) and THF (20 ml), n- butyl

lithium (13 mmol, 2.5 M in hexane) was added slowly. Solution was stirred at -78°C for 1.5 hours. Then, tributyltin chloride (13 mmol, 3.5 ml) was added very slowly keeping the temperature at – 78°C. After addition was completed, reaction was stirred for 4 hours at -78°C. Then, the reaction was left for overnight at room temperature. THF was evaporated and reaction mixture was washed with DCM and NH_4Cl, and then dried over $MgSO_4$. The product was obtained as a yellowish brown viscous liquid.

2.3.1.5. Synthesis of tributyl(2,3-dihydrothieno[3,4-b][1,4]dioxin-5-yl)stannane

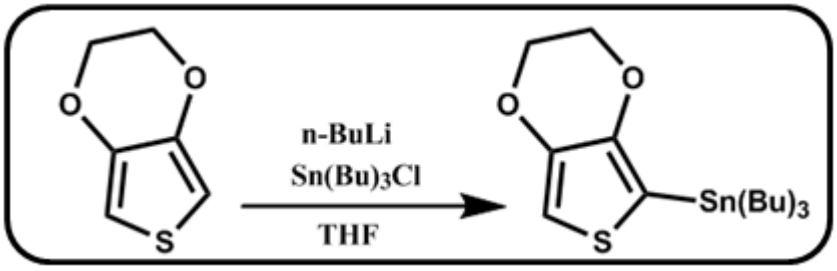


Figure 2.5 Synthetic route for tributyl(2,3-dihydrothieno[3,4-b][1,4]dioxin-5-yl)stannane.

This compound was prepared with the same procedure described for the synthesis of tributyl(2,3-dihydrothieno[3,4-b][1,4]dioxin-5-yl)stannane. EDOT (4g, 28.1 mmol) was dissolved in 80 mL THF. n-Buthyllithium (17.6 mL, 28.1 mmol) and tributyltin chloride (9.2 g, 28.1 mmol) were added at -78°C slowly in given order. Then the reaction mixture was kept under stirring at -78°C for 4 hours and overnight at room temperature. The mixture was washed with DCM and NH_4Cl after THF was removed. DCM was evaporated and the product was obtained as a brown viscous liquid.

2.3.1.6. Synthesis of 2-heptyl-4,7-di(thiophen-2-yl)-1H-benzo[d]imidazole (BImTh)

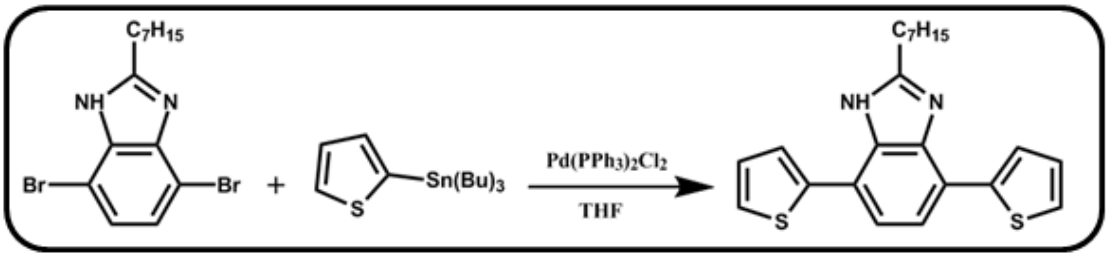


Figure 2.6 Synthetic route for BImTh.

4,7-Dibromo-2-heptyl-1H-benzo[d]imidazole (200 mg, 0.54 mmol) and tributyl(thiophen-2-yl)stanne (278.03 mg, 2.14 mmol) were dissolved in dry tetrahydrofuran (THF) (60 mL) and set for refluxing under argon atmosphere. The catalyst, $Pd(PPh_3)_2Cl_2$ (90 mg, 1.27 mmol) was added and then the mixture was stirred at 100°C under argon atmosphere for 16 hours with TLC control. At the end of 16 hours, the mixture was cooled and the solvent THF removed from the mixture by rotary evaporator. Then the residue

was subjected to column chromatography (chloroform as the solvent) to afford a yellow solid. 108.0 mg of 2-heptyl-4,7-di(thiopen-2-yl)-1H-benzo[d]imidazole was synthesized successfully with 51.85% yield [43].

2.3.1.7. Synthesis of 4,7-bis(2,3-dihydrothieno[3,4-b][1,4]dioxin-5-yl)-2-heptyl-1H-benzo[d]imidazole (BImEd)

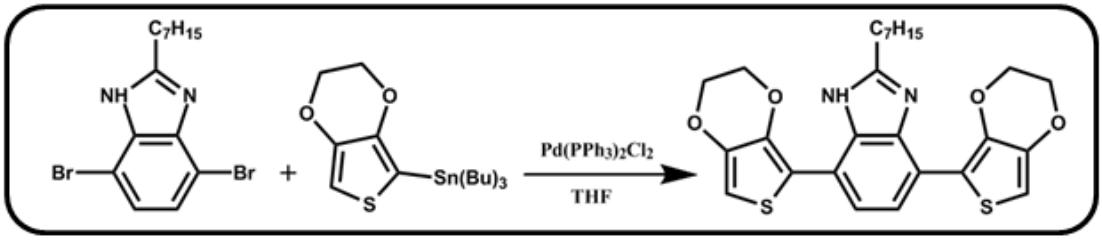


Figure 2.7 Synthetic route for BImEd.

BImEd was prepared with the same procedure described for the synthesis of BImTh using 4,7-dibromo-2-heptyl-1H-benzo[d]imidazole (200 mg, 0.54 mmol), tributyl(2,3-dihydrothieno[3,4-b][1,4]dioxin-5-yl)stannane (914 mg, 2.14 mmol) and $Pd(PPh_3)_2Cl_2$ (60 mg, 0.054 mmol). The monomer was obtained as a yellow solid after purification over silica gel by using chloroform as solvent with a yield of 38%.

2.4. Synthesis of Conducting Polymers via Electrochemical Polymerization

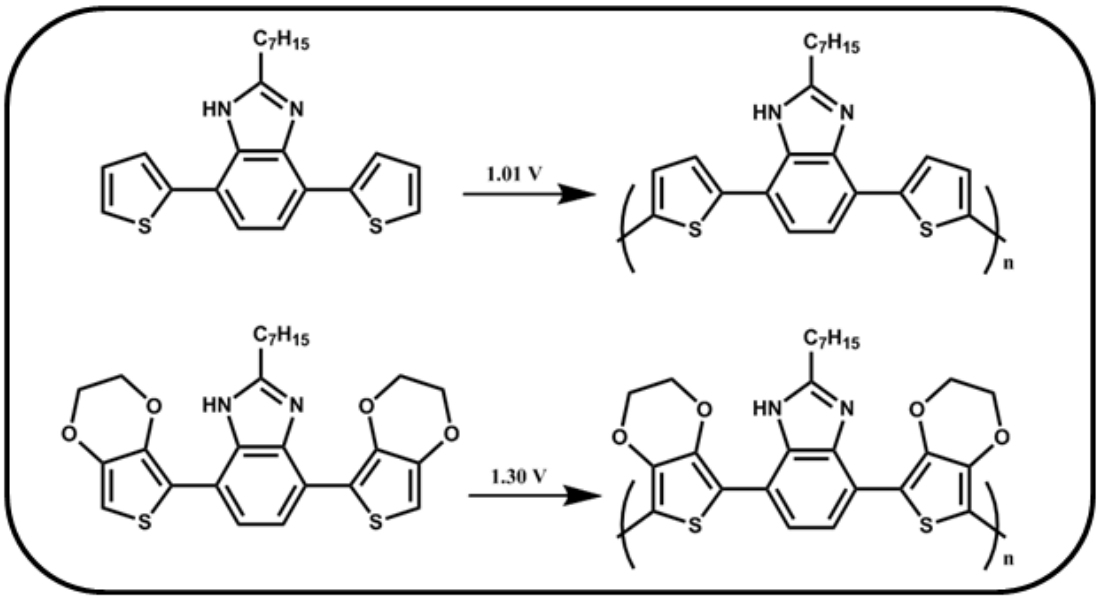


Figure 2.8 Electrochemical polymerizations of BImTh and BImEd.

The electrochemical polymerizations of both BImTh and BImEd (1 x 10^{-2} M) were performed using equimolar 0.1 M $NaClO_4$ and $LiClO_4$ as the supporting electrolyte in a DCM and ACN (5/95, v/v) mixture. ITO coated glass slides, Pt wire and Ag wire were used as the working, counter and reference electrodes, respectively. The polymers were coated on working electrode with repeated scan intervals between 0 and 1300 mV versus Ag wire pseudo-reference electrode at a 100 mV/s scan rate. Before further characterization, in order to remove the unreacted monomer and excess electrolyte, polymer films were washed with ACN.

2.5. Characterization of Conducting Polymers

2.5.1. Cyclic Voltammetry (CV)

For the analyses of electroactivity of monomers and determination of redox potentials of polymers, cyclic voltammetry (CV) studies were performed. For these analyses a three electrode setup was used with ITO coated glass slides, Ag wire and Pt wire. In this setup, electron supplying and potential referencing missions have been divided between the counter and reference electrodes, respectively (Figure 2.9) in order to eliminate the difficulty of one electrode to be kept at constant potential and pass current at the same time.

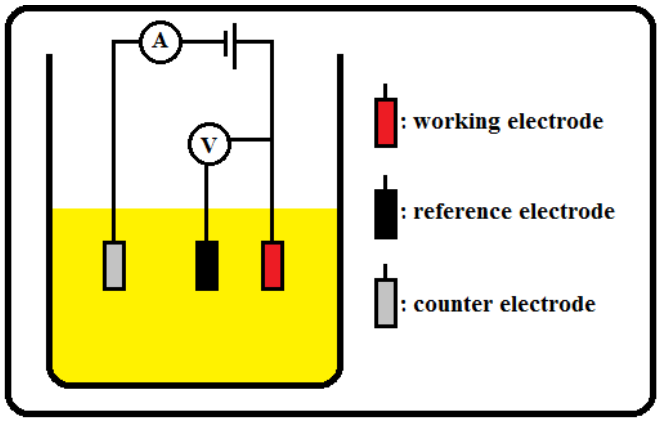


Figure 2.9 Schematic representation of three electrode setup

Cyclic voltammetry is a reversible linear sweep voltammetry (LSV) measurement in which the potential is scanned using a triangular waveform (Figure 2.10a). The current change resulting from this potential sweep is measured using a potentiostat and the expected current-potential relation of a reversible redox process for one potential cycle is shown in Figure 2.10b.

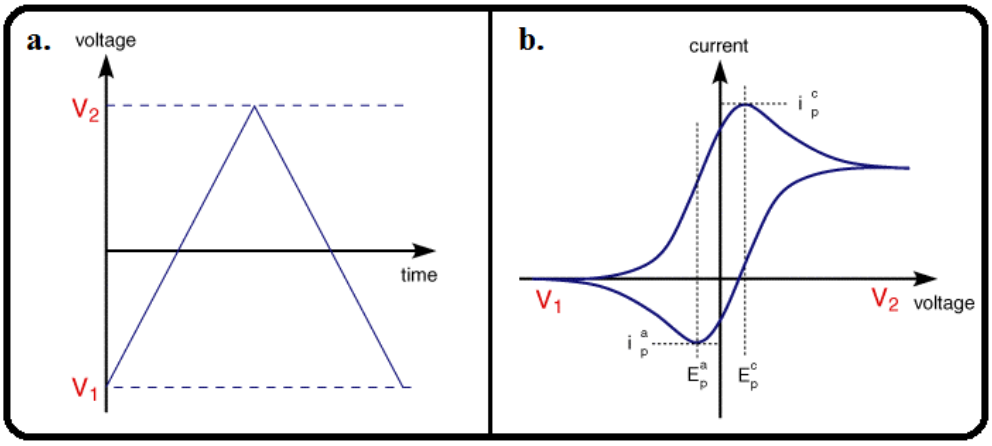


Figure 2.10 a) Triangular waveform of cyclic voltammetry. b) Current-potential relation of a reversible redox process. Adapted from http://www.ceb.cam.ac.uk/pages/linear-sweep-and-cyclic-voltametry-the-principles.html.

The current peaks occur in the CV due to the continuous change in concentration of electroactive material in the diffusion layer close to the electrode surface, indicating the diffusion controlled mechanism. Peak height (i_p) is directly proportional to the concentration according to the Randles-Sevcik equation:

$$i_p = 0.4463\, nFAC(nFvD/RT)^{1/2}$$ (or if the system is at room temperature; $i_p = (269{,}000)n^{3/2}AD^{1/2}Cv^{1/2}$)

In this equation;

i_p: peak hight (A)
n: number of electrons transferred in half reaction of the redox couple
F: Fradays constant (96485 C/mol)
A: electrode area (cm^2)
C: concentration (mol/cm^3)
v: scan rate (V/s)
D: diffusion coefficient (cm^2/s)
R: gas constant (8.314 J/K mol)
T: absolute temperature (K)

For the use of this equation as is, both the reactants and products should be soluble in the system and the surface processes such as adsorption should be neglected. However, electrochemical studies of a polymer are performed in a monomer free system where the polymer is immobilized at the surface of working electrode. At these conditions, Randles-Sevcik equation is not valid and substituted with the following equation:

$$i_p = n^2 F^2 \Gamma \nu / 4RT$$

(**Γ** stands for the total amount of electroactive material.)

The equation states that the current peak height should be directly proportional to the scan rate. This linear relation between the current and scan rate (Figure 2.11) enables to determine whether the electrochemical process is diffusion controlled.

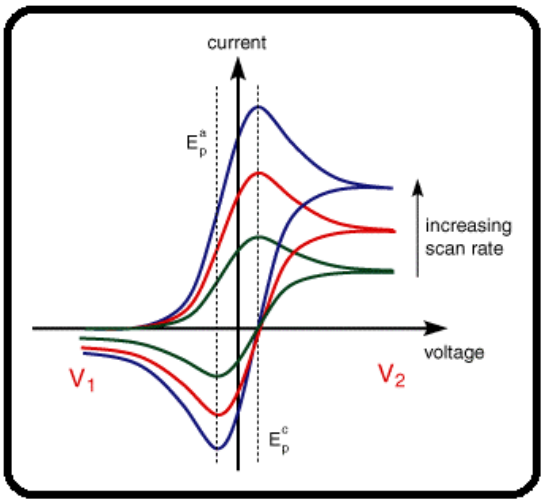


Figure 2.11 Dependance of current on scan rate. Adapted from http://www.ceb.cam.ac.uk/pages/linear-sweep-and-cyclic-voltametry-the-principles.html

2.5.2. Spectroelectrochemistry

Spectroelectrochemistry is a useful tool that combines spectroscopic and electrochemical techniques and operates synchronous. Spectra of the polymer films are recorded while increasing the applied potential stepwise with this instrumentation (Figure 2.12). As the potential is applied, the polymer gets oxidized which changes the electronic transitions thus the absorbance. Recording the spectra during stepwise oxidation provides information of polaron and bipolaron band evolution and all the colors that the polymers possess upon doping. Spectroelectrochemistry studies also reveal some important information such as band gap (E_g).

Spectral changes were recorded using a UV-vis- NIR spectrophotometer in order to investigate the electronic transitions upon doping. Polymer films coated electrochemically on the ITO coated glass slides were placed in monomer free, 0.1 M $NaClO_4$ and $LiClO_4$ (equimolar), ACN solution and the potentials were swept from 0.5 V to 1.2 V for PBImTh, from 0.3 V to 1.3 V for BImEd with 0.1 V increments.

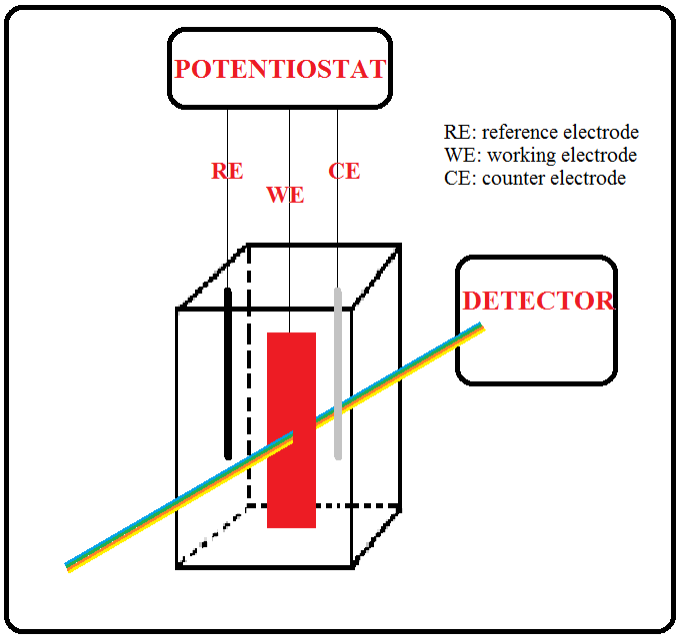


Figure 2.12 Schematic representation of spectroelectrochemical instrumentation

2.5.3 Switching Studies

Optical contrast and switching time of the electrochromic materials are important parameters to be investigated. In order to determine the percent transmittance changes and switching times, electrochromic switching experiments are performed at the maximum absorption wavelengths of the polymers by altering the potential repeatedly between the most reduced and oxidized states.

PBImTh and PBImEd films deposited on ITO coated glass slides were subjected to square wave potential between most reduced and fully oxidized states with 5 second time intervals in a monomer free 0.1 M $NaClO_4$ and $LiClO_4$ (equimolar), ACN solution.

CHAPTER 3

RESULTS AND DISCUSSION

3.1. Characterization of the monomers

^{1}H-NMR, ^{13}C-NMR spectra of the monomers were investigated in $CDCl_3$ and chemical shifts (δ) were given relative to tetramethylsilane as the internal standard. Mass analyses were also performed for the characterization of BImTh and BImEd.

3.1.1. 2-heptyl-4,7-di(thiophen-2-yl)-1H-benzo[d]imidazole (BImTh)

^{1}H (400 MHz, $CDCl_3$, δ): 7.69 (s, 2H), 7.44 (s, 2H), 7.33 (d, 1H), 7.32 (d, 1H), 7.12 (m, 2H), 2.87 (t, 2H), 1.84–1.76 (m, 2H), 1.40–1.21 (m, 8H), 0.86 (t, 3H).

^{13}C NMR (100 MHz, $CDCl_3$, δ): 155.4, 140.7, 127.9, 125.5, 125.4, 125.1, 121.0, 31.7, 29.5, 29.4, 29.0, 28.3, 22.6, 14.1.

MS (m/z): 380.6592 [M^+]

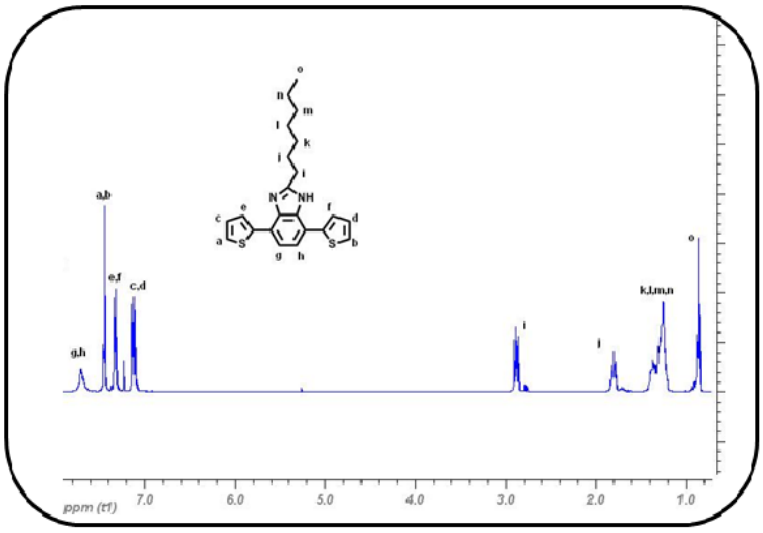


Figure 3.1 ^{1}H-NMR spectrum of BImTh

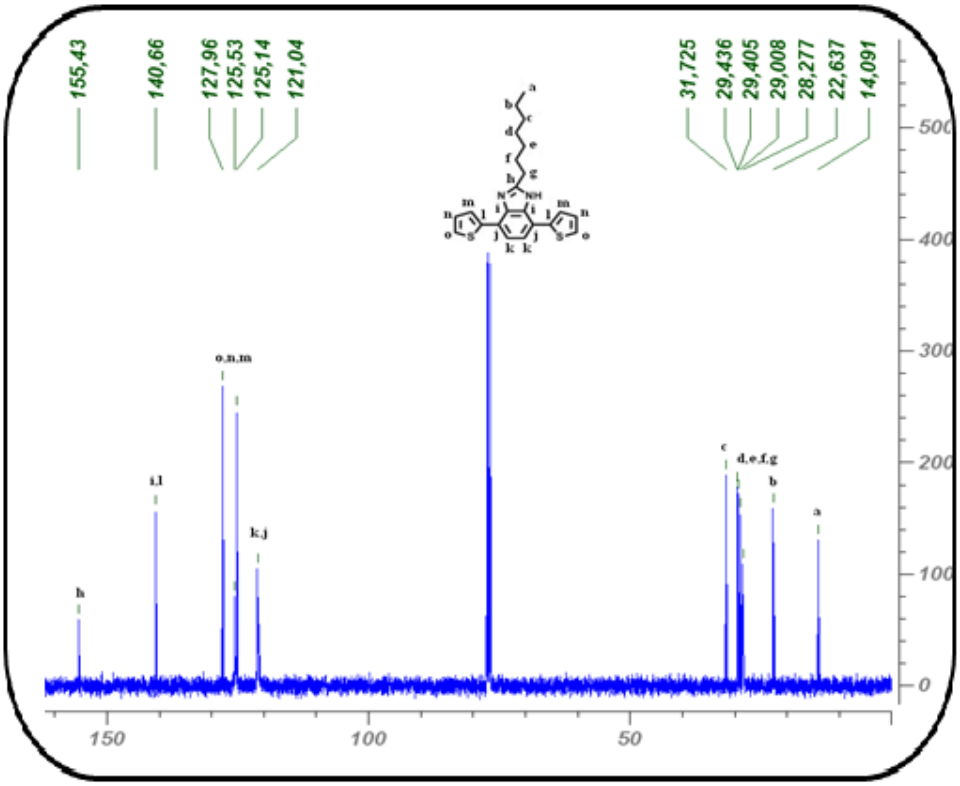


Figure 3.2 ^{13}C-NMR spectrum of BImTh

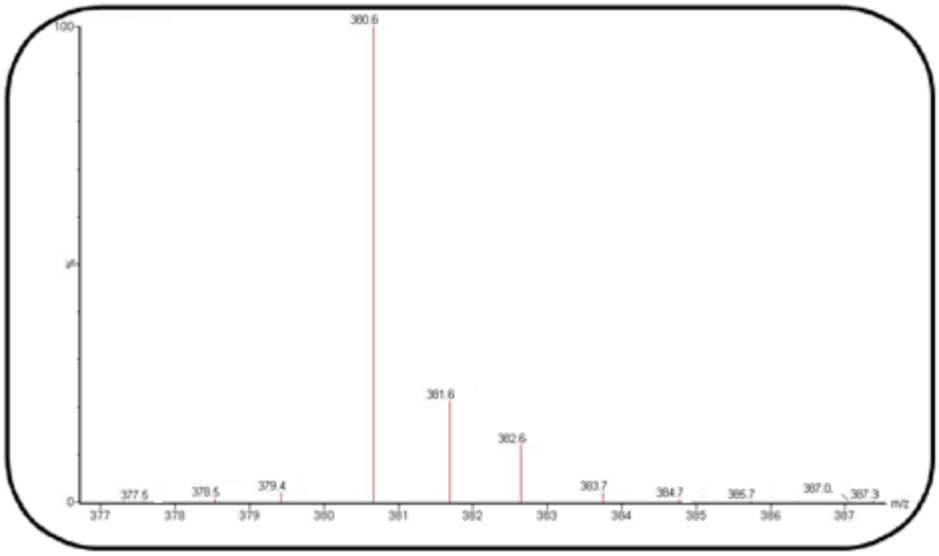


Figure 3.3 Mass spectrum of BImTh

3.1.2. 4,7-bis(2,3-dihydrothieno[3,4-b][1,4]dioxin-5-yl)-2-heptyl-1H benzo[d]imidazole

^{1}H (400 MHz, $CDCl_3$, δ): 7.85 (s, 2H), 6.36 (s, 2H), 4.28 (s, broad, 4H), 4.22 (s, broad, 4H), 2.90 (t, 2H), 1.79 (p, 2H), 1.42–1.18 (m, 8H), 0.82–0.78 (m,3H).

^{13}C NMR (100 MHz, $CDCl_3$, δ): 152.4, 151.9, 139.6, 132.9, 125.1, 125.0, 110.4, 97.3, 62.9, 62.2, 29.6, 27.5, 27.3, 27.2, 26.9, 25.9, 20.5.

MS (m/z): 496.4 [M^+]

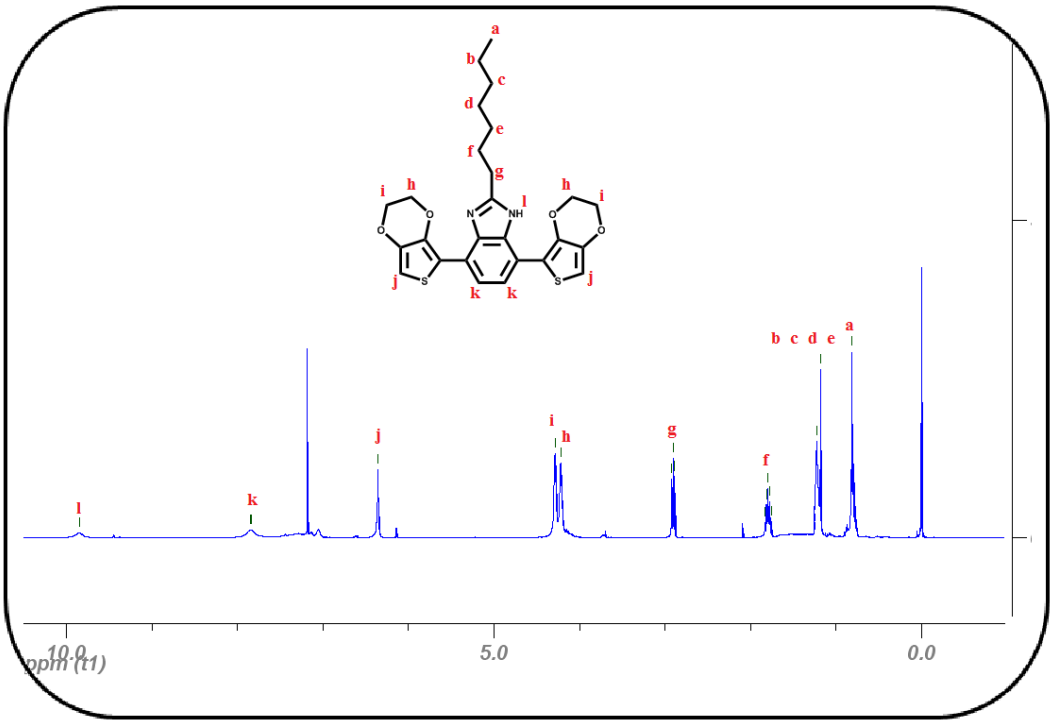


Figure 3.4 ^{1}H-NMR spectrum of BImEd

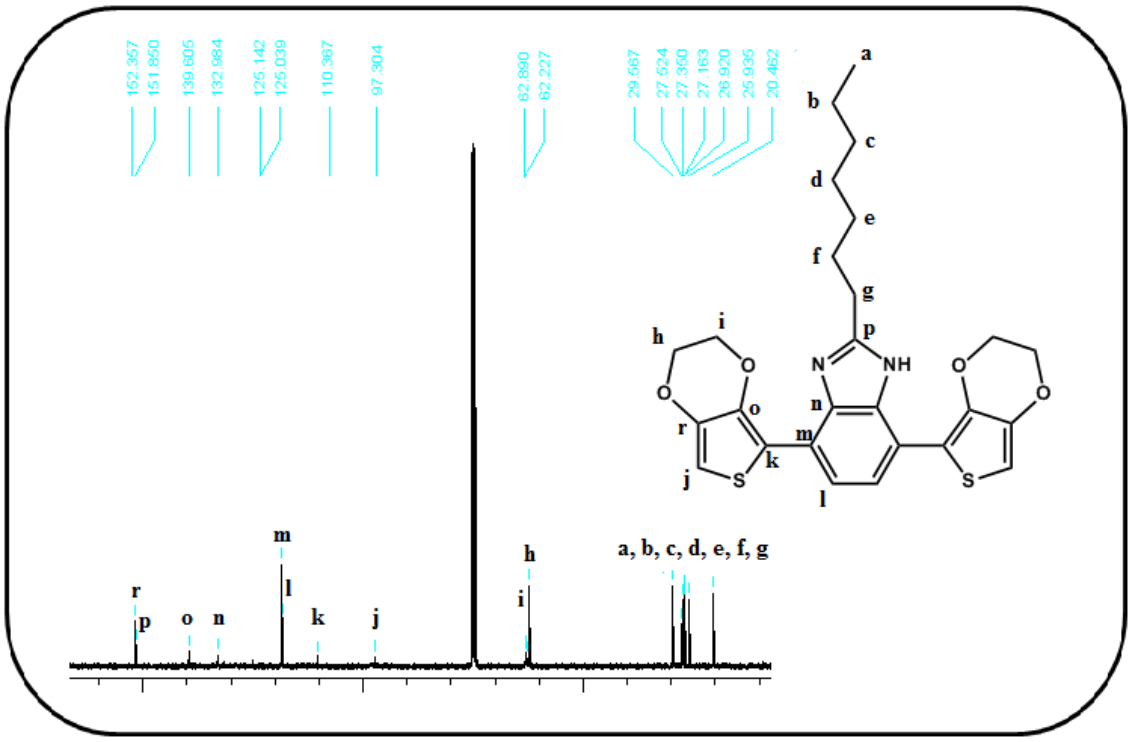


Figure 3.5 ^{13}C-NMR spectrum of BImEd

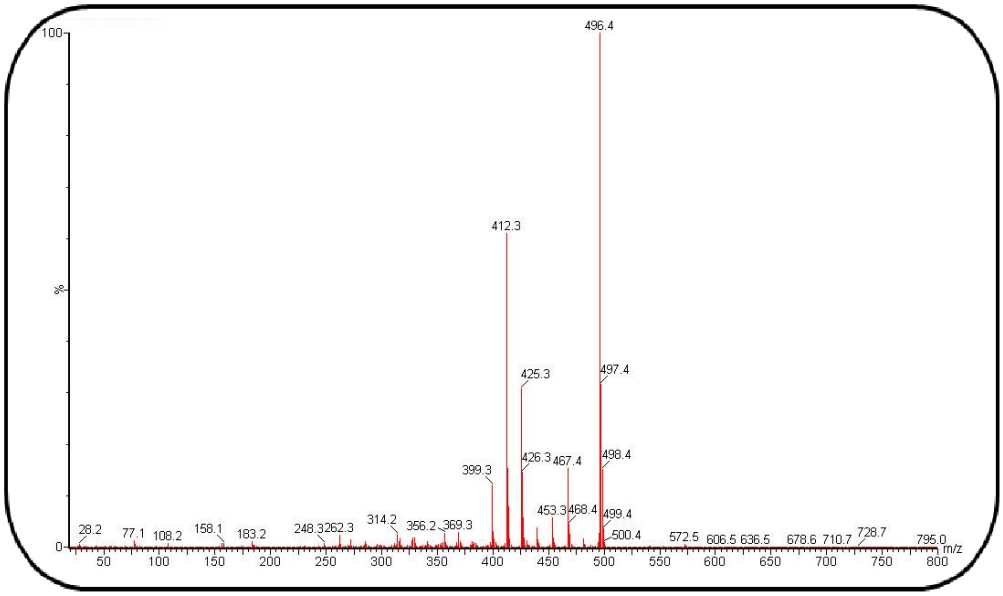


Figure 3.6 Mass spectrum of BImEd

3.2. Electrochemical and Electrochromic Properties of PBImTh and PBImEd

3.2.1. Electrochemistry of 2-heptyl-4,7-di(thiophen-2-yl)-1H-benzo[d]imidazole (PBImTh) and 4,7-bis(2,3-dihydrothieno[3,4-b][1,4]dioxin-5-yl)-2-heptyl-1H-benzo[d]imidazole (BImEd)

Electrochemical polymerizations of monomers BImTh and BImEd (1 x 10^{-2} M) were performed in equimolar 0.1 M $NaClO_4$ and $LiClO_4$ containing DCM:ACN (5:95, v:v) solution. DCM was used to increase the dielectric constant of the solution and dissolve the monomers. BImTh was polymerized by sweeping the potential between 0.0 V and 1.3 V versus Ag wire pseudo reference electrode for 10 cycles with 100 mV/s scan rate where potential was altered between 0.0 V and 1.35 V for the polymerization of BImEd. Cyclic voltammogram of BImTh and BImEd are shown in Figure 3.7 and Figure 3.8, respectively. The monomer oxidation potentials appeared at 1.01 V for BImTh and 1.30 V for BImEd in the first cycles of cyclic voltammogram and reversible redox peak couples of polymers were centered at 0.68 and 0.52 V for PBImTh, 0.76 and 0.68 V for PBImEd versus Ag wire pseudo-reference electrode.

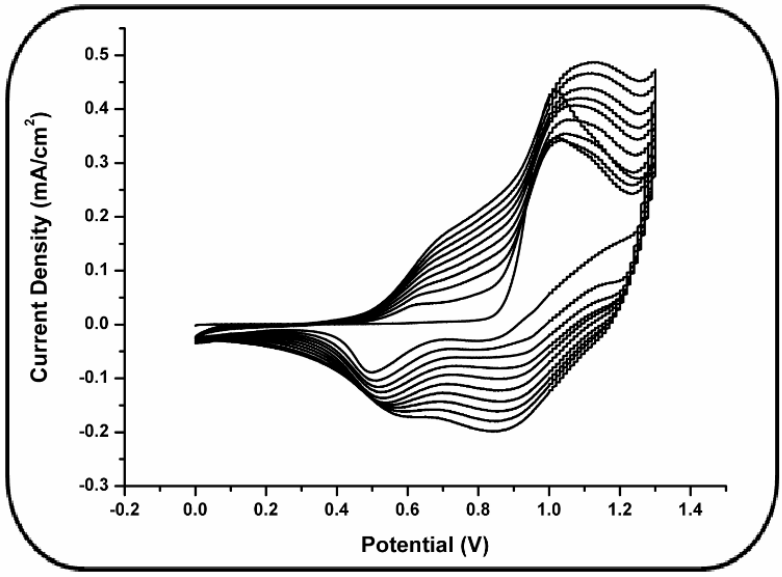


Figure 3.7 Repeated potential scan of electrochemical polymerization of BImTh in equimolar 0.1 M $NaClO_4$ and $LiClO_4$, DCM:ACN (5:95, v:v) with 100 mV/s scan rate

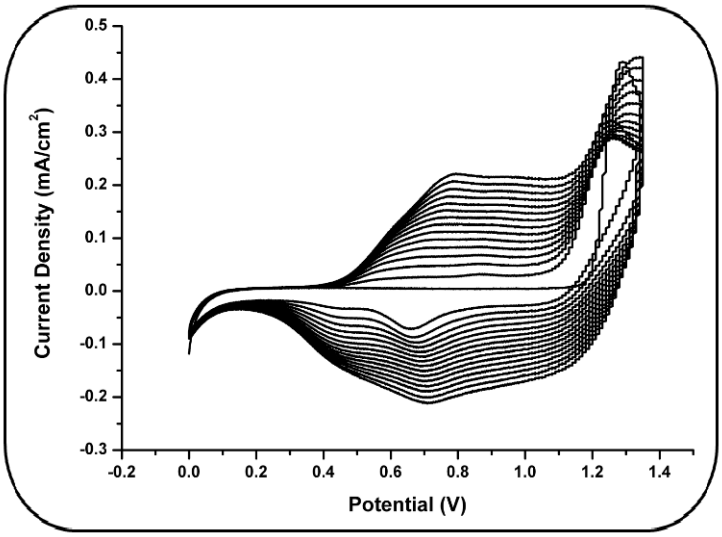


Figure 3.8 Repeated potential scan of electrochemical polymerization of BImEd in equimolar 0.1 M $NaClO_4$ and $LiClO_4$, DCM:ACN (5:95, v:v) with 100 mV/s scan rate

EDOT bearing monomer (BImEd) was expected to get oxidized at a lower potential than the thiophene containing derivative (BImTh) as EDOT is more electron rich than thiophene. However, the results reveal a 0.30 V lower monomer oxidation potential for BImTh than that of BImEd. This unexpected result is most probably caused by the interaction between the hydrogen of the secondary amine of BIm unit and the oxygen of EDOT [44]. In order to prove this reasoning, electrochemical polymerization of BImEd was performed in the presence of base (0.05 mL of 0.01 M NaOH solution was added to the electrolyte). As the base quenches the polymerization process, only first two cycles are shown in Figure 3.9. In the first run of the polymerization, the monomer oxidation potential was reduced by more than 0.1 V even with the addition of a small amount of base. Also the redox potentials of the polymer were reduced nearly 0.25 V, as seen in the second run of CV. These shifts of the potentials prove that the unexpected results were caused by the H-bonding between the acceptor and the donor units of BImEd. However, as the base also acts as a quencher, it is not possible to deduce more detailed arguments by only one CV. The influence of H-bonding on conducting polymers is discussed more detailed in the second part of my thesis.

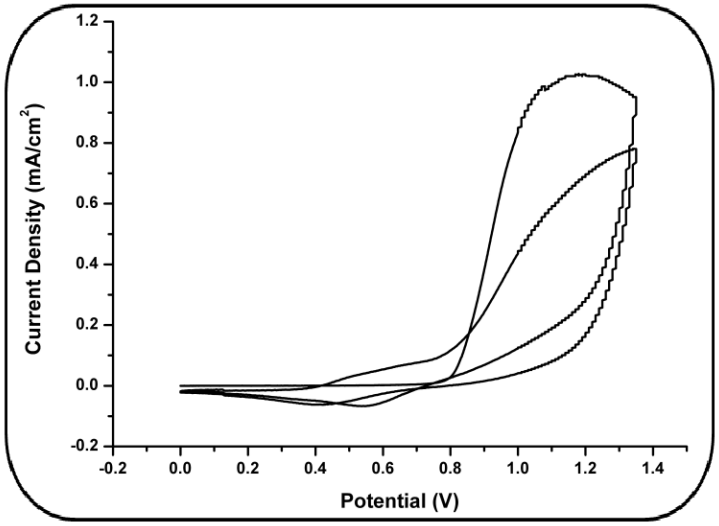


Figure 3.9 First two cycles of repeated potential scan of electrochemical polymerization of BImEd in presence of base

To prove that the conducting polymers are forming film on the ITO surface and the resulting polymers are electroactive, the scan rate was increased stepwise during the repeated cycling. As seen in Figure 3.10 (for PBImTh) and Figure 3.11 (for PBImEd), the current density is increasing with the increasing scan rate which shows the conducting polymers were successfully coated on the working electrode and the electrochemical processes are quasi-reversible and non-diffusion controlled even at high scan rates [45].

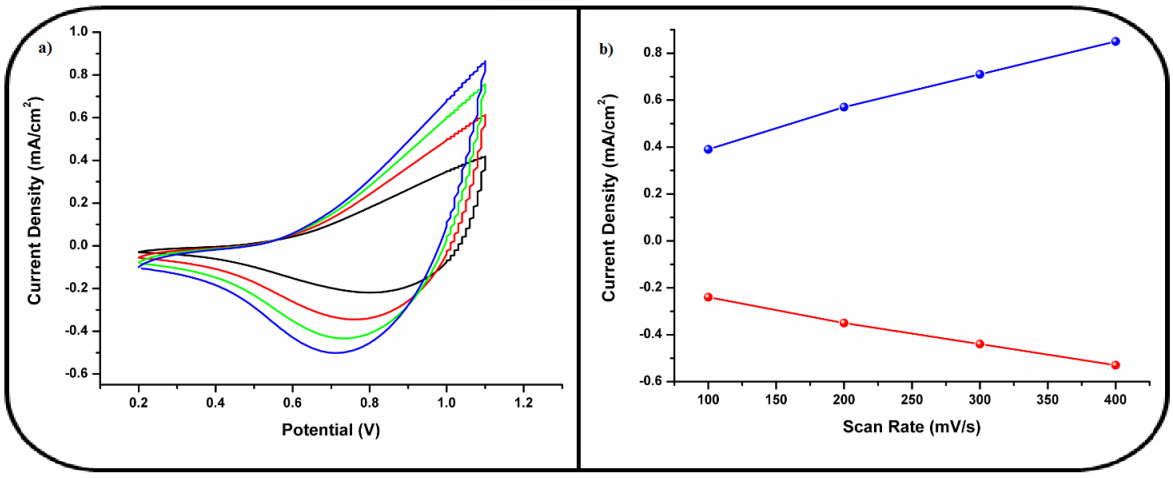


Figure 3.10 Scan rate dependence of PBImTh in equimolar 0.1 M $NaClO_4$ and $LiClO_4$, DCM:ACN (5:95, v:v) a) 100, 200, 300, 400 mV/s, b) oxidation and reduction

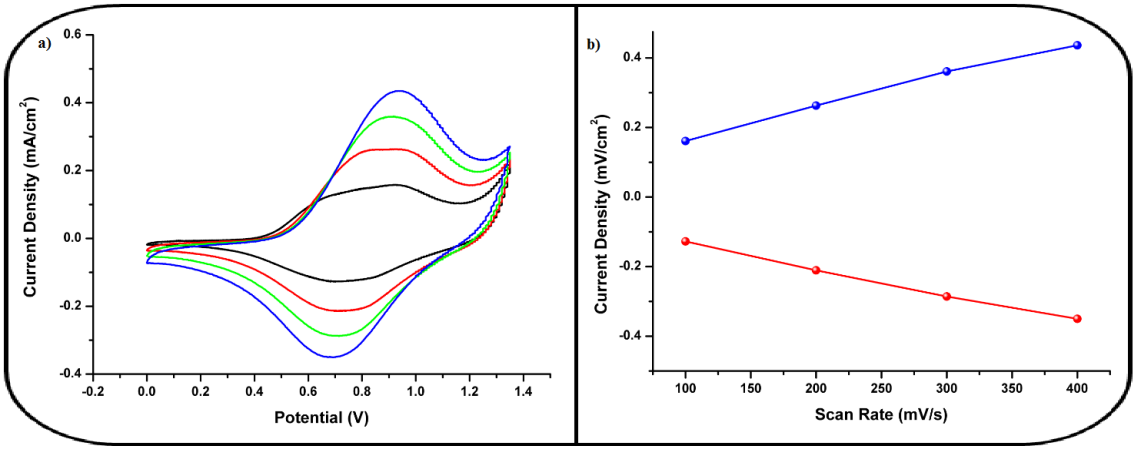


Figure 3.11 Scan rate dependence of PBImEd in equimolar 0.1 M $NaClO_4$ and $LiClO_4$, DCM:ACN (5:95, v:v)a) 100, 200, 300, 400 mV/s, b) oxidation and reduction

3.2.2. Spectroelectrochemistry of poly(2-heptyl-4,7-di(thiophen-2-yl)-1H-benzo[d]imidazole) (PBImTh) and poly(4,7-bis(2,3-dihydrothieno[3,4-b][1,4]dioxin-5-yl)-2-heptyl-1H-benzo[d]imidazole) (PBImEd)

Spectral changes of the polymers upon applied potential were investigated using UV-vis-NIR spectrophotometer in monomer free, 0.1 M $NaClO_4$ and $LiClO_4$ (equimolar) ACN solution. The potentials were swept from 0.5 V to 1.2 V for PBImTh (Figure 3.12), from 0.3 V to 1.3 V for PBImEd (Figure 3.13) with 0.1 V increments.

In the spectra of PBImTh, the peak at 440 nm corresponds to the π-π^* transition of the undoped polymer and is consistent with the orange color. As the polymer is doped, intensity of the aforementioned absorbance decreases and new absorption bands corresponding to polaronic and bipolaronic states evolve at 671 nm and 1114 nm, respectively. The polymer reveals green color at 1.1 V applied potential as the absorptions at red and blue regions become equal. Absorption at the visible region becomes nearly equally distributed at 1.2 V applied potential, so the polymer film possess greenish gray color at the fully oxidized state.

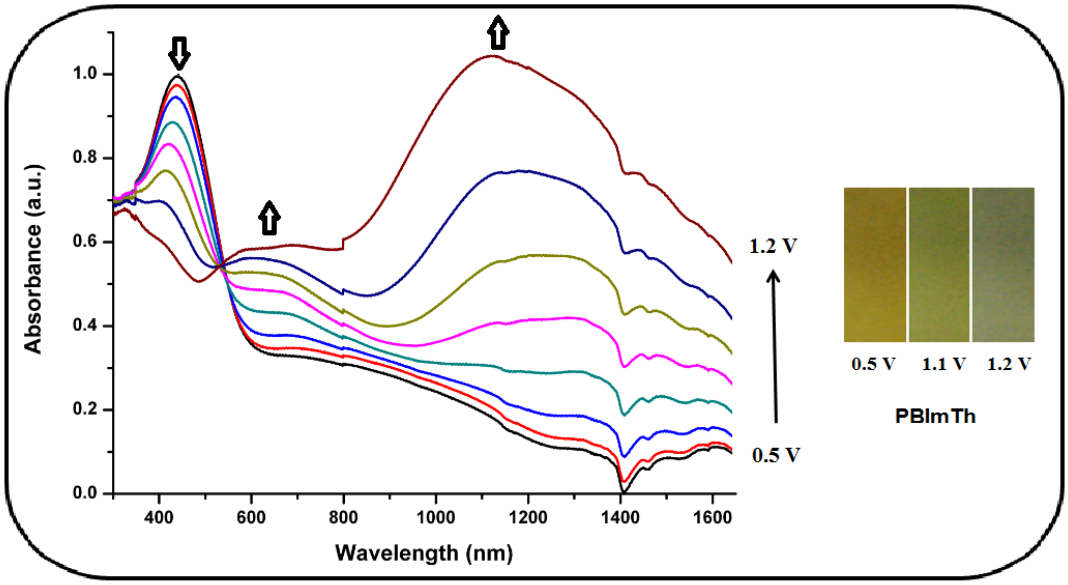


Figure 3.12 Normalized absorption spectra of PBImTh film on an ITO coated glass slide in monomer-free equimolar 0.1 M $NaClO_4$ and $LiClO_4$, ACN solution upon doping between 0.5 V and 1.2 V with 0.1 V increments

In the spectra of PBImEd, two different transitions can be seen for the neutral polymer film due to its donor-acceptor nature. The peak corresponding to higher energy is attributed to the transition from the valence band of the donor moiety to its antibonding counterpart. The peak at 533 nm which corresponds to lower energy is attributed to the transition from EDOT-based valence band to the substituent –localized conduction band. The intensity as well as the energy of both transitions is related to the interactions and the match between the DA couple [46, 47]. As seen from the absorption spectra, the peak intensity at the lower-energy is significantly higher which indicates a strong interaction between EDOT and BIm units as predicted. Absorption bands corresponding to polaronic and bipolaronic states are centered at 720 nm and 1120 nm, respectively. PBImEd is also multichromic revealing purple color in its neutral state; gray at 1.1 V applied potential and blue in its fully oxidized state.

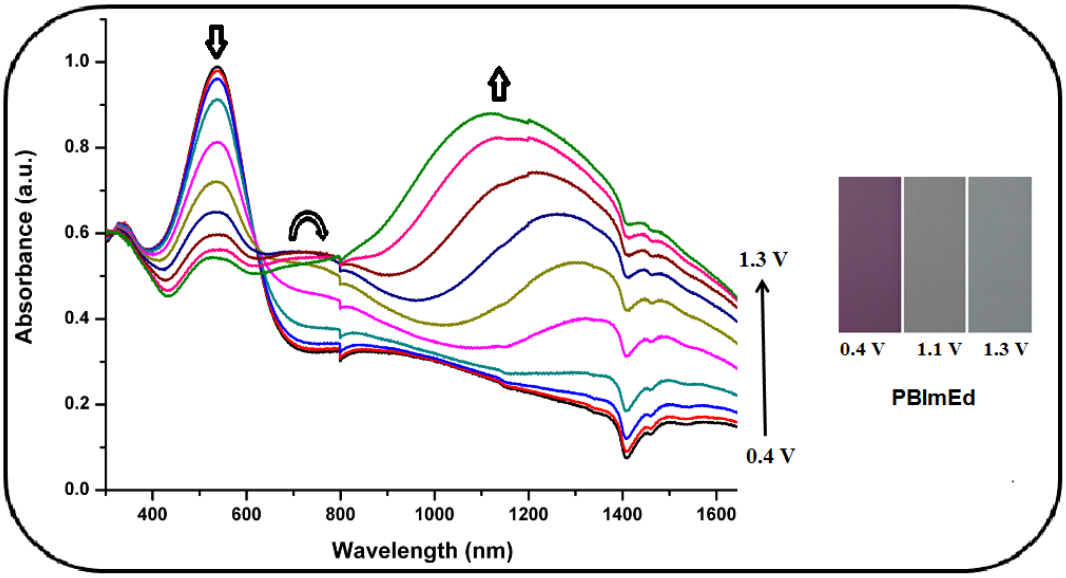


Figure 3.13 Normalized absorption spectra of PBImEd film on an ITO coated glass slide in monomer-free equimolar 0.1 M $NaClO_4$ and $LiClO_4$, ACN solution upon doping between 0.4 V and 1.3 V with 0.1 V increments

Band gap values of both polymers were calculated from the onset of their π-π^* transitions. The band gap values of the polymers depend both on the individual characteristics of donor and acceptor units, such as HOMO and LUMO levels; and the match of these units. The energy gap was calculated as 1.93 eV for PBImTh and 1.74 eV for PBImEd. As EDOT is more electron rich than thiophene and also there exists a strong interaction between EDOT and BIm units, it is consistent that the energy gap is lower for PBImEd than that of PBImTh.

3.2.3. Kinetic Properties of poly(2-heptyl-4,7-di(thiophen-2-yl)-1H-benzo[d]imidazole) (PBImTh) and poly(4,7-bis(2,3-dihydrothieno[3,4-b][1,4]dioxin-5-yl)-2-heptyl-1H-benzo[d]imidazole) (PBImEd)

Kinetic properties of the polymer films were investigated using UV-vis-NIR spectrophotometer in a monomer free, 0.1 M $NaClO_4$ and $LiClO_4$ (equimolar) ACN solution. Optical contrasts and the switching times of the polymers between their neutral and oxidized states were determined at their maximum absorption wavelengths, in this context. Polymer films were switched between their reduced and fully oxidized states with 5 second stepping intervals and the switching times are calculated from the first cycle.

Optical contrast values for PBImTh are determined as 25.7 % and 33.0 % at 440 nm and 1114 nm, respectively (Figure 3.14). PBImTh revealed 2.98 s switching time in the vis region and 2.33 s switching time in the NIR region. PBImEd revealed 40.3 % optical contrast and 0.25 s switching time at 533 nm, 52.5 % optical contrast and 0.28 s switching time at 1120 nm (Figure 3.15).

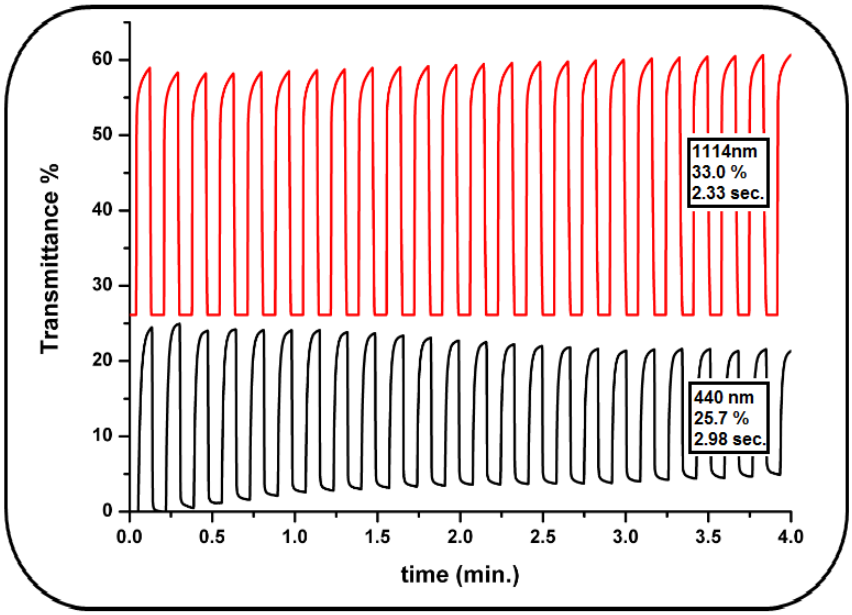


Figure 3.14 Percent transmittance change of PBImTh deposited on ITO electrode switching between 0.3 V and 1.2 V monitored at 440 and 1114 nm in monomer free equimolar 0.1 M $NaClO_4$ and $LiClO_4$, ACN solution

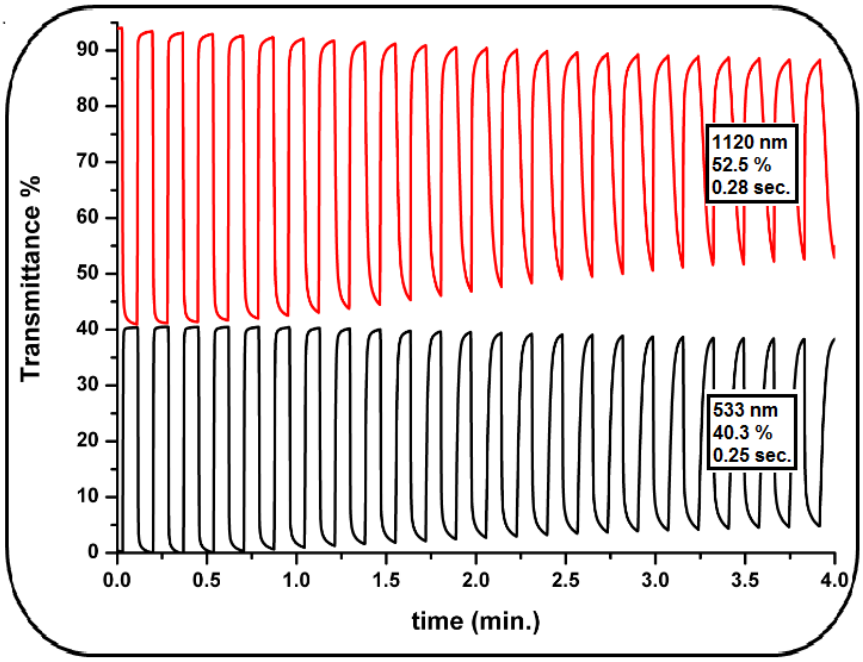


Figure 3.15 Percent transmittance change of PBImEd deposited on ITO electrode switching between 0.3 V and 1.3 V monitored at 533 and 1120 nm in monomer free equimolar 0.1 M $NaClO_4$ and $LiClO_4$, ACN solution

PBImEd have significantly higher optical contrast values than PBImTh which can be explained by the charge they are capable of loading. Starting from the Beer-Lambert law, the following equations can be derived stating that the optical contrast is directly proportional with the charge loaded on the material [48]:

$T = \exp(-A)$

$\Delta T\% = 100\,(T_c - T_d) = 100\,[\exp(-A_c) - \exp(-A_d)]$

$A = \eta\, q$

$\Delta T\% = 100\,[\exp(-\eta_c\, q) - \exp(-\eta_d\, q)]$

where;

c: clear state

d: dark state

η: coloration efficiency (cm^2/C)

q: charge (C)

As charge is in the level of mC, q stands between 0 and 1 which makes percent transmittance difference directly proportional with the loaded charge. It is clearly seen in CV of BImTh (Figure 3.7) and BImEd (Figure 3.8) that the area under the polymer oxidation, which corresponds to the charge loaded, of PBImEd is larger than that of PBImTh. That may be the most considerable reason for the higher optical contrast of PBImEd.

CHAPTER 4

EXPERIMENTAL

4.1. Materials

Apart from the materials mentioned in chapter 2.1, benzaldehyde (Merck), 1,4-dibromobenzene (Aldrich) and *p*-toluenesulfonic acid (PTSA) (Aldrich) were used as received. Trifluoroacetic acid (TFA) (Aldrich) and sodium hydroxide (NaOH) (Aldrich) were also used without any further purification.

4.2. Equipment

Except for the equipments described in chapter 2.2, Minolta CS-100 spectrophotometer was used for colorimetry measurements. Infrared (IR) spectra were recorded in solution form by using $CHCl_3$ as solvent with Varian 1000 FT-IR spectrophotometer. XPS studies were performed using X-ray photoelectron spectroscopy (XPS) (PHI 5000 Versa Probe (F ULVACPHI, Inc., Japan/USA) with monochromatized Al Kα radiation (1486.6 eV) 10 as an X-ray anode at 24.9 W.

4.3. Procedure

4.3.1. Synthesis

4.3.1.1. Synthesis of 4,7-dibromo-2-phenyl-1H-benzo[d]imidazole

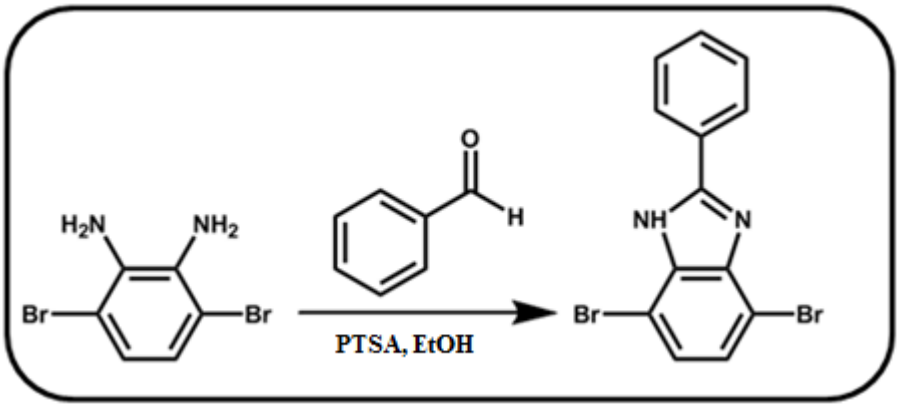


Figure 4.1 Synthetic route for 4,7-dibromo-2-phenyl-1H-benzo[d]imidazole

4,7-Dibromo-2-phenyl-1H-benzo[d]imidazole was synthesized according to a previously published procedure [49]. 3,6-Dibromobenzene-1,2-diamine (500 mg, 1.88 mmol) (synthesized as described in chapter 2.3.1.2), benzaldehyde (798 mg, 7.52 mmol) and PTSA (catalytic amount) were dissolved in 25 ml EtOH. The mixture was refluxed overnight at 100 ^{o}C. Solvent was evaporated and the crude product was purified over silica gel by using chloroform: hexane (7:1) as solvent. The product was obtained as a white solid with 67% yield.

4.3.1.2. Synthesis of 4,7-bis(2,3-dihydrothieno[3,4-b][1,4]dioxin-5-yl)-2-phenyl-1H-benzo[d]imidazole (BImBEd)

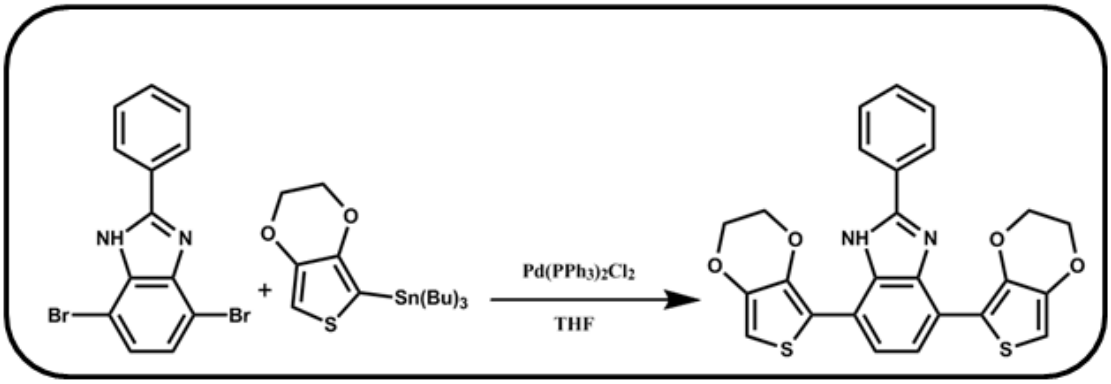


Figure 4.2 Synthetic route for BImBEd

Stille coupling reaction (as described in chapter 2.3.1.6) was performed for the synthesis of BImBEd using 4,7-dibromo-2-phenyl-1H-benzo[d]imidazole (0.56 mmol, 200 mg), tributyl(2,3-dihydrothieno[3,4-b][1,4]dioxin-7-yl)stannane (2.28 mmol, 980 mg) (synthesized as described in chapter 2.3.1.5) and $Pd(PPh_3)_2Cl_2$ (60 mg, 0.054 mmol). BImBEd was obtained as a yellow solid after purification over silica gel by using ethyl acetate: hexane (1:2) mixture as solvent with a yield of 58.7%.

4.3.1.3. Synthesis of 1,4-bis(2,3-dihydrothieno[3,4-b][1,4]dioxin-5-yl)benzene (BEDOT-B)

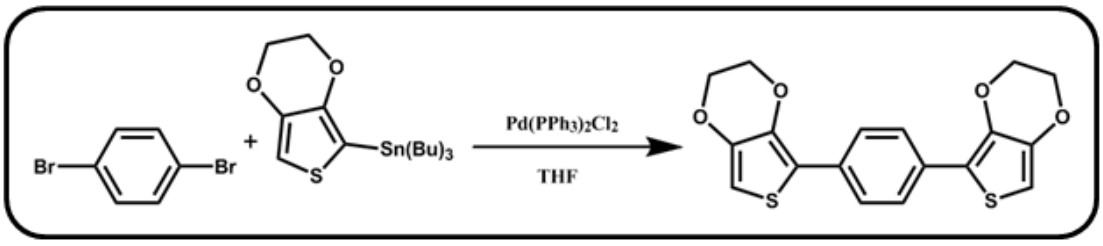


Figure 4.3 Synthetic route for BEDOT-B

BEDOT-B [50] was synthesized via Stille coupling using 1,4-dibromo benzene (0.42 mmol, 100 mg), tributyl(2,3-dihydrothieno[3,4-b][1,4]dioxin-7-yl)stannane (2.71 mmol, 735 mg) and $Pd(PPh_3)_2Cl_2$ (45 mg, 0.041 mmol). The monomer was obtained as yellow solid with a yield of % 52.4.

4.4. Characterization of Conducting Polymers

4.4.1. Fourier Transform Infrared Spectroscopy (FTIR)

FTIR is a convenient technique to prove the existence of some interactions and bonds by using the specific stretching values. FTIR studies were performed in the amine stretching region (between 3550 cm^{-1} and 3250 cm^{-1}), in order to prove the presence of an H-bonding between the oxygen of the EDOT and the amine of the imidazole ring.

The FTIR studies were performed for 4,7-dibromo-2-phenyl-1H-benzo[d]imidazole, BImBEd and BEDOT-B molecules in $CHCl_3$.

4.4.2. Cyclic Voltammetry (CV)

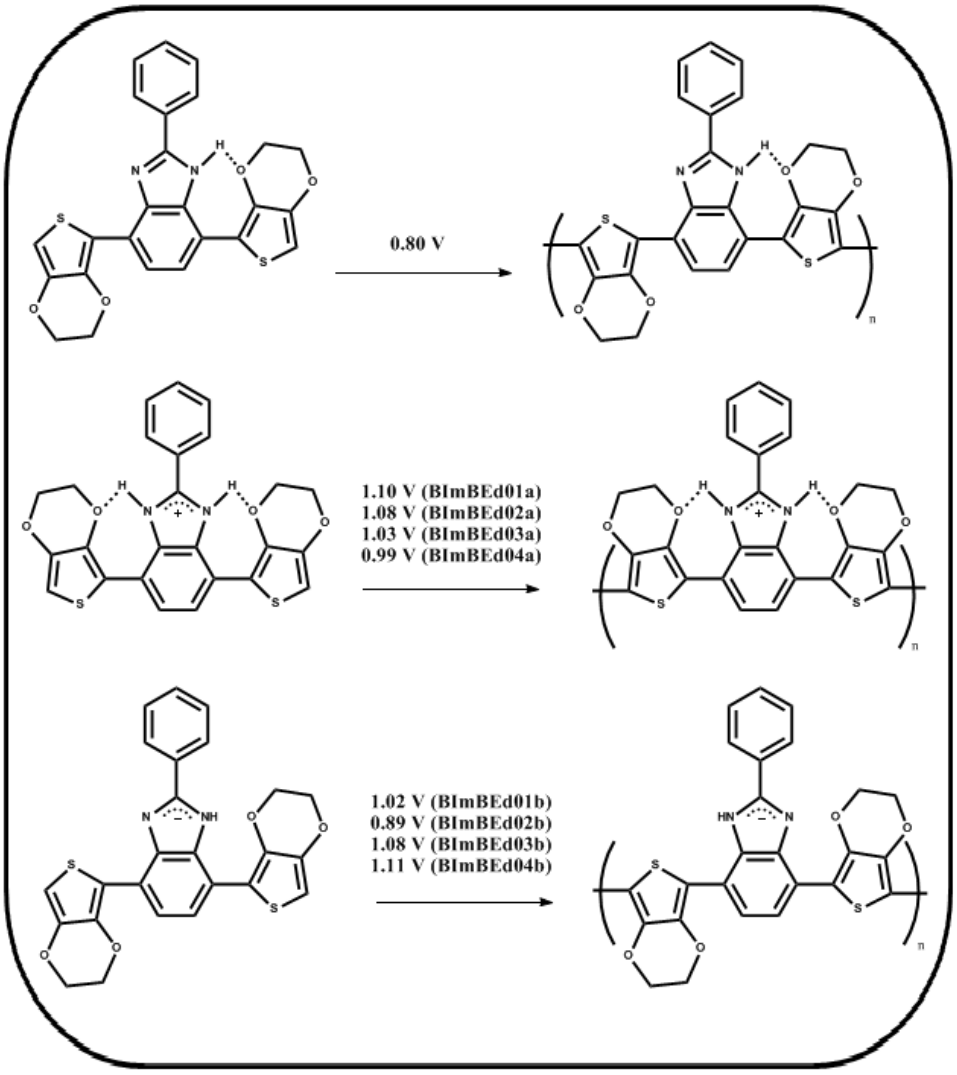


Figure 4.4 Electrochemical polymerization of BImBEd in neutral, acidic and basic conditions

The electrochemical polymerization of BImBEd (1 x 10^{-2} M) was performed in 2.0 mL 0.1 M $TBAPF_6$ containing 5:95 (v:v) DCM:ACN solution by using ITO coated glass slide, Pt wire and Ag wire as the working, counter and reference electrodes, respectively. Electrochemical polymerizations were achieved sweeping the potential between 0.0 V and 1.25 V by 10 repeated cycles at a 100 mV/s scan rate. The resulting polymer was named as PBImBEd.

Besides polymerization in DCM:ACN solution, electrochemical polymerizations of the same monomer (BImBEd) with addition of different amounts of acid (trifluoroacetic acid) and base were also performed scanning between the same potentials with the same number of cycles. Resulting polymers obtained with

the addition of 0.1 mL, 0.2 mL, 0.3 mL and 0.4 mL acid to the 2.0 mL of polymerization solution were named as PBImBEd01a, PBImBEd02a, PBImBEd03a and PBImBEd04a respectively. Resulting polymers obtained with the addition of 0.1 mL, 0.2 mL, 0.3 mL and 0.4 mL base to the 2.0 mL of polymerization solution were named as PBImBEd01b, PBImBEd02b, PBImBEd03b and PBImBEd04b, respectively.

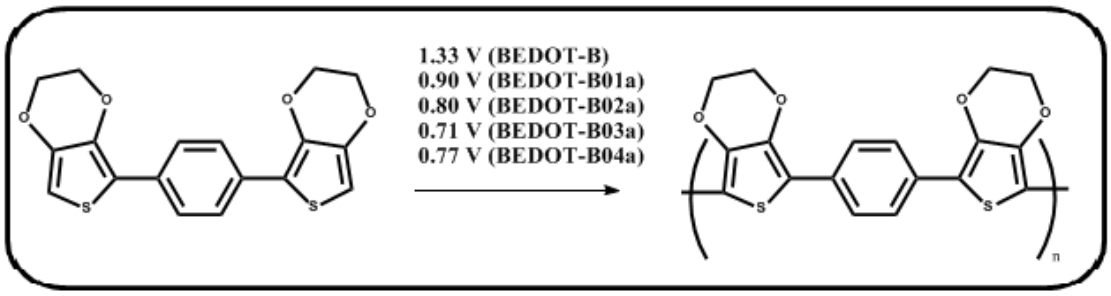


Figure 4.5 Electrochemical polymerization of BEDOT-B in neutral and acidic conditions

Polymerization of BEDOT-B (1 x 10^{-2} M) was performed electrochemically using the same conditions and setup and the resulting polymer was named as PBEDOT-B. Addition of acid (TFA) and base (NaOH) was also performed for the electrochemical polymerization of BEDOT-B. Resulting polymers with the addition of 0.1 mL, 0.2 mL, 0.3 mL and 0.4 mL acid to the 2.0 mL of polymerization solution were named as PBEDOT-B01a, PBEDOT-B02a, PBEDOT-B03a, and PBEDOT-B04a, respectively. The same amounts of base (NaOH) were also added to the polymerization media but no polymer films were obtained.

Polymer films were washed with ACN before further characterization, in order to remove the unreacted monomer and excess electrolyte.

The cyclic voltammogram obtained during the electrochemical polymerizations were used to elicit the monomer oxidation and polymer redox potentials and the effect of acid and base addition to the polymerization media.

4.4.3. Spectroelectrochemistry

Spectroelectrochemistry studies, which combine spectroscopic and electrochemical techniques, were performed in 2.0 mL 0.1 M $TBAPF_6$ containing 5:95 (v:v) DCM:ACN solution by recording the absorption spectra of the neutral and fully oxidized polymer films electrochemically deposited on ITO coated glass electrodes. Electronic transitions, maximum wavelengths ($\boldsymbol{\lambda}_{max}$), and band gap ($E_g$) values are determined and discussed using the data obtained from the spectra.

4.4.4. Switching Studies

Percent transmittance changes and switching times for the resulting polymers were determined at their maximum absorption wavelengths by altering the potential repeatedly between the most reduced and oxidized states (Figure 4.6).

Polymer films deposited on ITO coated glass slides were subjected to square wave potential between most reduced and fully oxidized states with 5 second time intervals in a monomer free 0.1 M $TBAPF_6$ containing ACN solution.

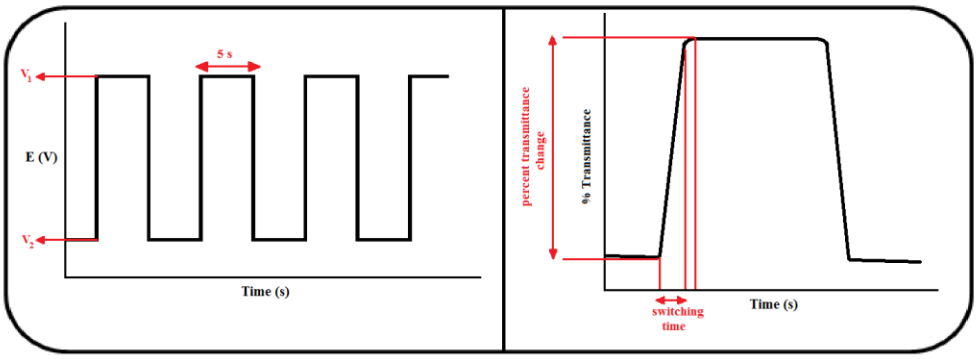


Figure 4.6 Representative applied potential and percent transmittance change

4.4.5. Colorimetry

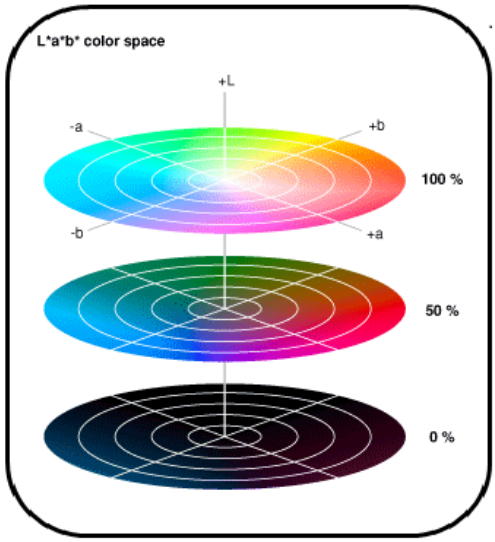


Figure 4.7 CIELAB color space. Adapted from [https://developer.apple.com/library/mac/#documentation/Cocoa/Conceptual/DrawColor/Concepts/AboutColorSpaces.html]

Colors of the polymers were indicated scientifically by hue, saturation and brightness values. Hue stands for the dominant wavelength which is referred to color generally. Saturation represents the intensity of the color and brightness defines the transmittance of light or the luminance of a sample.

Colors of the polymers in this study were recorded with L*a*b* CIE color space (Figure 4.7) which is one of the systems established by The Commission Internationale de l'Eclairge. L* from 0 to 100 means from black to white, negative values for a* indicate green while positive values state magenta, negative values for b* indicate blue whereas positive values define yellow color.

CHAPTER 5

RESULTS AND DISCUSSION

5.1. Characterization of the monomers

5.1.1. 4,7-bis(2,3-dihydrothieno[3,4-b][1,4]dioxin-5-yl)-2-phenyl-1H-benzo[d]imidazole (BImBEd)

^{1}H (400 MHz, $CDCl_3$, δ): 10.61 (s, 1H), 8.09 (d, 2H), 8.05 (d, 1H), 7.50 (m, 3H), 7.42 (d, 1H), 6.52 (s, 1H), 6.44 (s, 1H), 4.48 (d, 2H), 4.38 (d, 4H), 4.29 (d, 2H).

^{13}C NMR (100 MHz, $CDCl_3$, δ): 150.4, 142.0, 141.5, 141.1, 139.5, 135.9, 131.5, 130.2, 129.9, 129.0, 128.2, 126.4, 125.3, 123.9, 121.3, 120.7, 116.7, 114.6, 114.5, 100.9, 99.2, 65.6, 64.9, 64.5, 64.4.

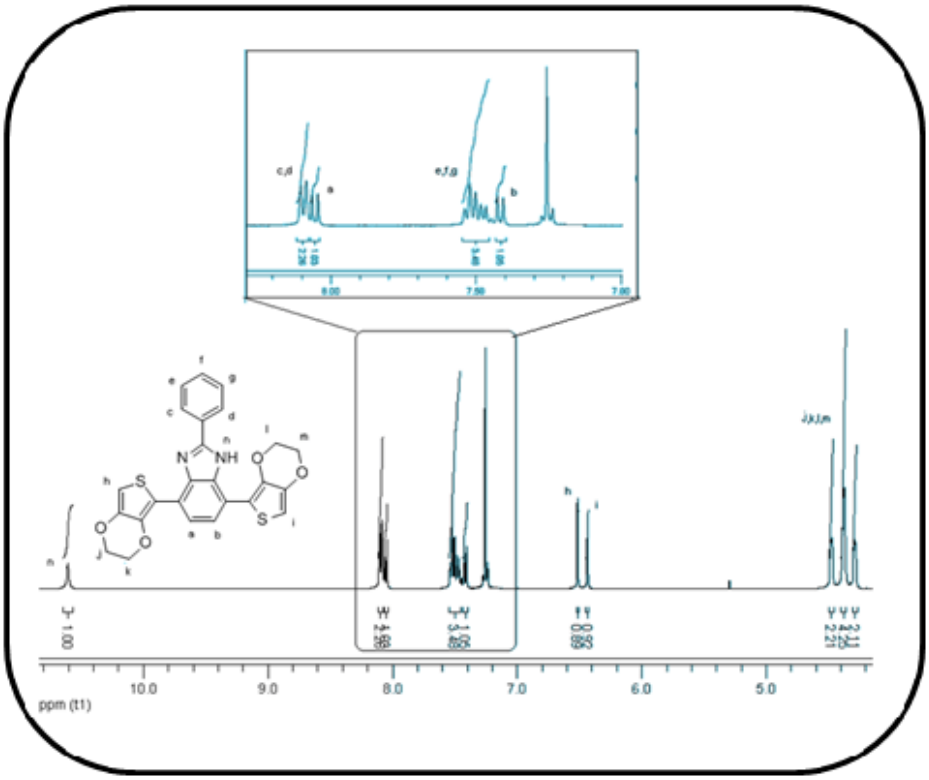


Figure 5.1 ^{1}H-NMR spectrum of BImBEd

The ^{1}H-NMR spectrum of BImBEd revealed asymmetric character as there are two doublets centered at 8.05 ppm and 7.42 ppm for the benzene. For the molecule to be asymmetric, the tautomerization of the imidazole ring should be hindered somehow. In this case, the H-bonding between the hydrogen of amine and the oxygen of EDOT is the most probable reason for hindering the tautomerization thus the asymmetric nature of the molecule. The same asymmetric nature is also seen in the ^{13}C-NMR, as 25 different peaks exists for every carbon atom.

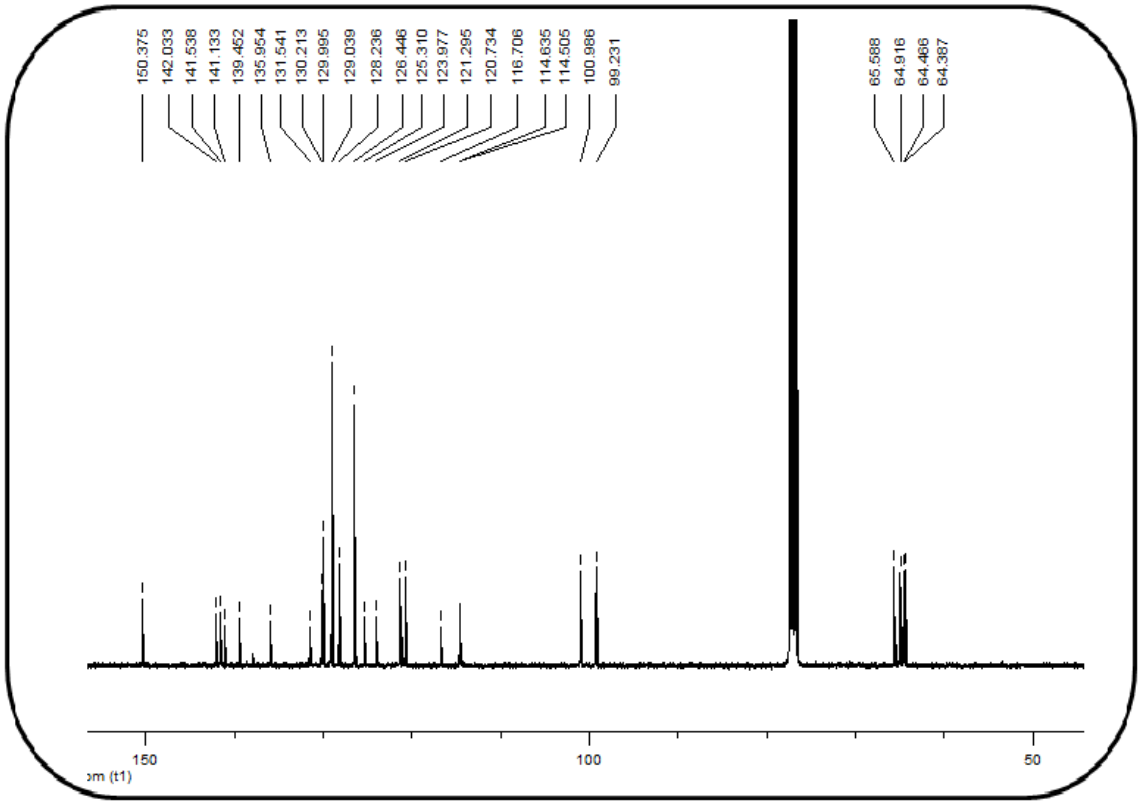


Figure 5.2 ^{13}C-NMR spectrum of BImBEd

5.1.2. 1,4-bis(2,3-dihydrothieno[3,4-b][1,4]dioxin-5-yl)benzene (BEDOT-B)

^{1}H (400 MHz, $CDCl_3$, δ): 7.63 (s, 4H), 6.22 (s, 2H), 4.25 (t, 4H), 4.19 (t, 4H).

^{13}C NMR (100 MHz, $CDCl_3$, δ): 149.8, 149.2, 136.3, 124.2, 115.5, 95.6, 62.9, 62.6.

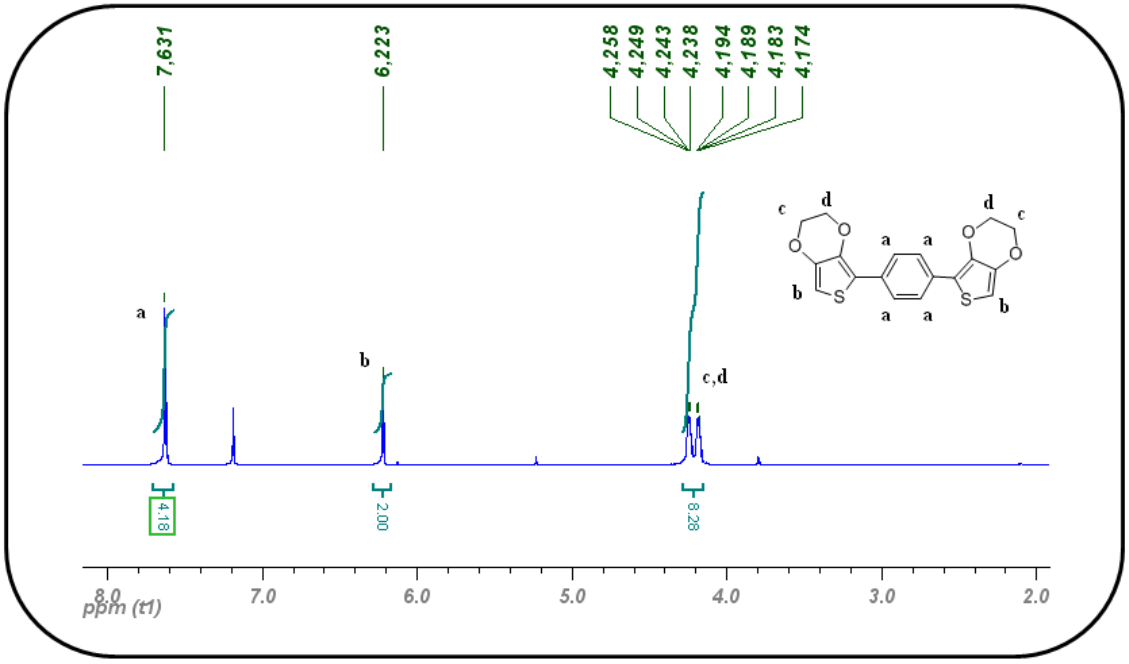


Figure 5.3 ^{1}H-NMR spectrum of BEDOT-B

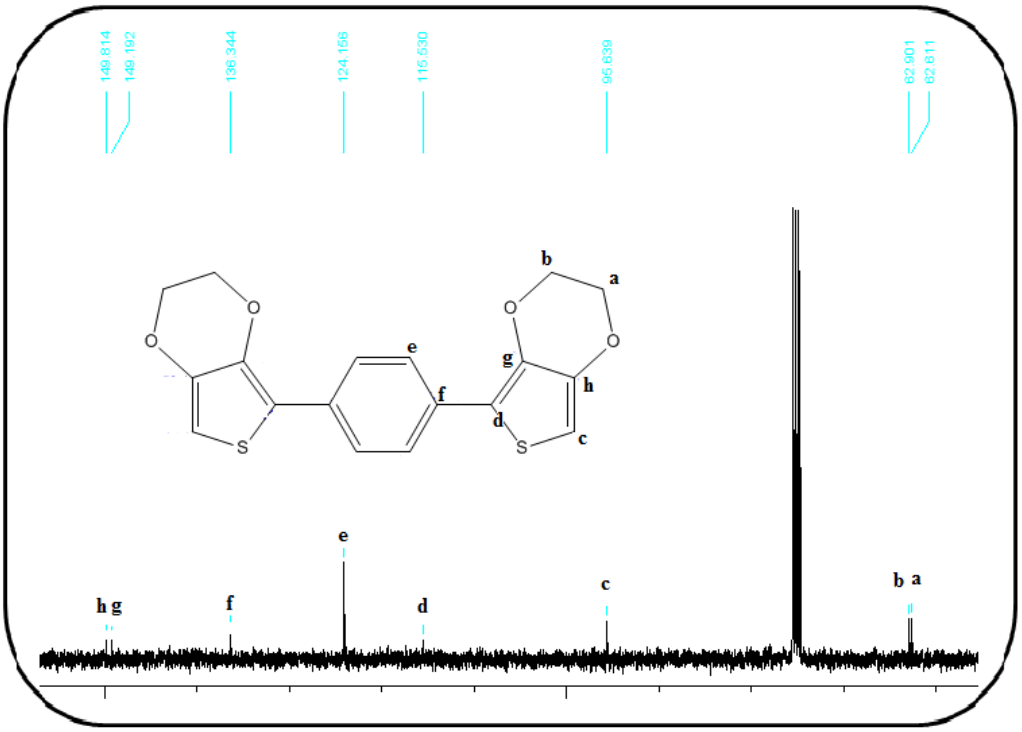


Figure 5.4 ^{13}C-NMR spectrum of BEDOT-B

5.1.3. FT-IR analyses of 4,7-dibromo-2-phenyl-1H-benzo[d]imidazole, 4,7-bis(2,3-dihydrothieno[3,4-b][1,4]dioxin-5-yl)-2-phenyl-1H-benzo[d]imidazole (BImBEd) and 1,4-bis(2,3-dihydrothieno[3,4-b][1,4]dioxin-5-yl)benzene (BEDOT-B)

FT-IR analyses were performed in chloroform in the amine stretching region (between 3250 cm^{-1} and 3350 cm^{-1}) to prove the H-bonding between the hydrogen of the benzimidazole unit and oxygen of the EDOT unit. In order to make comparison, IR spectrum of 4,7-dibromo-2-phenyl-1H-benzo[d]imidazole, BImBEd and BEDOT-B were recorded (Figure 5.5). As BEDOT-B does not contain any amine hydrogen, no peak was raised in the amine stretching region, as expected. The peak at 3445 cm^{-1} for both 4,7-dibromo-2-phenyl-1H-benzo[d]imidazole and BImBEd clearly corresponds to the free secondary amine stretching. An additional peak at 3384 cm^{-1} appeared in the spectra of BImBEd. Plass et al. states that this peak is specific to the C7 intramolecular hydrogen bonded amine stretching [51, 52].

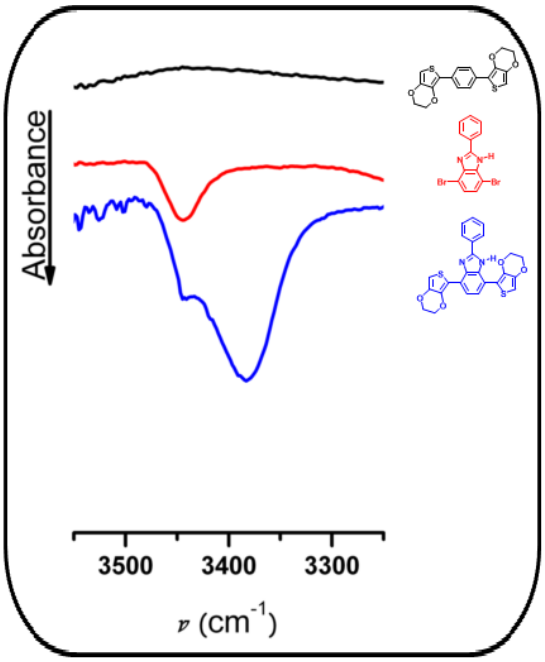


Figure 5.5 FT-IR spectrum of BEDOT-B (up), 4,7-dibromo-2-phenyl-1H-benzo[d]imidazole (middle) and BImBEd (down) scanned in the amine stretching region in $CHCl_3$ solution

5.2. Electrochemical and Electrochromic Properties of 4,7-bis(2,3-dihydrothieno[3,4-b][1,4]dioxin-5-yl)-2-phenyl-1H-benzo[d]imidazole (BImBEd) and 1,4-bis(2,3-dihydrothieno[3,4-b][1,4]dioxin-5-yl)benzene (BEDOT-B)

5.2.1. Electrochemistry of 4,7-bis(2,3-dihydrothieno[3,4-b][1,4]dioxin-5-yl)-2-phenyl-1H-benzo[d]imidazole (BImBEd)

Electrochemical polymerization of BImBEd (1 x 10^{-2} M) was performed in 0.1 M $TBAPF_6$ containing DCM:ACN (5:95, v:v) solution, by sweeping the potential between 0.0 V and 1.2 V versus Ag wire pseudo reference electrode for 10 cycles with 100 mV/s scan rate. In order to investigate the effect of

intramolecular H-bonding, different amounts of acid (TFA) and base (NaOH) were added to the polymerization media. Electrochemical polymerizations in these solutions were performed with the same scanning parameters. CV of all polymerizations can be seen in Figure 5.6. Resulting polymers are named as PBImBEd01a, PBImBEd02a, PBImBEd03a, PBImBEd04a and PBImBEd01b, PBImBEd02b, PBImBEd03b, PBImBEd04b with the addition of 0.1 mL, 0.2 mL, 0.3 mL, 0.4 mL acid and 0.1 mL, 0.2 mL, 0.3 mL, 0.4 mL base to the 2.0 mL of polymerization solution, respectively.

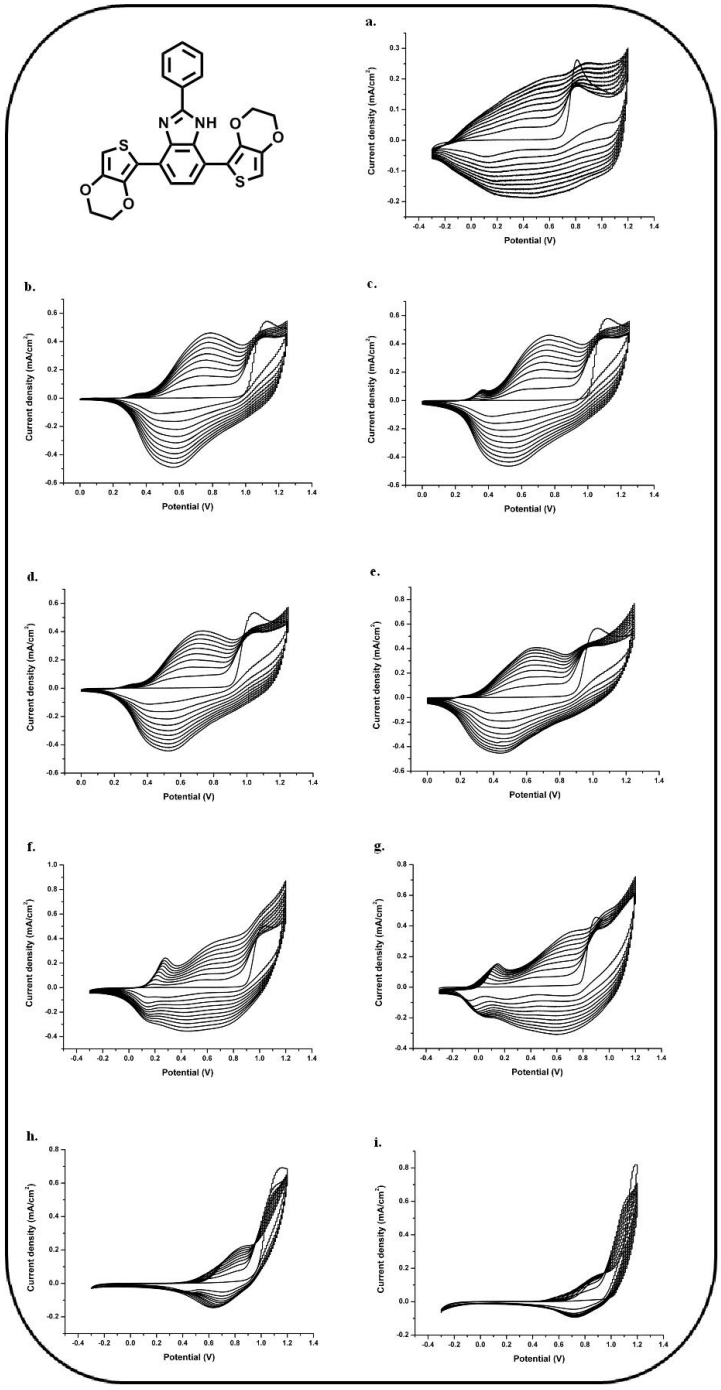


Figure 5.6 Repeated potential scan of electrochemical polymerizations of **(a)** BImBEd, **(b)** BImBEd01a, **(c)** BImBEd02a, **(d)** BImBEd03a, **(e)** BImBEd04a, **(f)** BImBEd01b, **(g)** BImBEd02b, **(h)** BImBEd03b and **(i)** BImBEd04b in 0.1 M $TBAPF_6$, DCM:ACN (5:95, v:v) with 100 mV/s scan rate

It was seen that addition of acid increases the monomer oxidation potential when oxidation potentials of BImBEd and BImBEd01a (Table 5.1). This may have two probable reasons. First, H-bonding causes EDOT to share the electron density with BIm unit thus decreases the donor property. The second and more effective reason is that a positive charge occurs in the imidazole unit as the nitrogen is protonated. As the monomer already possess a positive charge, simply it gets harder to insert another one. Comparing the oxidation potentials of BImBEd01a with BImBEd02a, BImBEd03a and BImBEd04a, it is seen that the monomer oxidation is reduced with increasing amount of acid. This decrease in monomer oxidation can be attributed to the direct effect of acid to the polymerization mechanism. The same trend is also observed for the polymer redox potentials.

On the other hand, addition of base did not result in a certain trend as the base acts as a quencher in the polymerization process. This effect can be seen in the CVs, as the polymer oxidation and reduction of the polymers do not grow with increasing scan number, especially for PBImBEd03b and PBImBEd04b. On the other hand, CVs of PBImBEd01b and PBImBEd02b show increase in the chain length with increasing scan number. It can be deduced that deprotonation of the imine in BIm unit dominates over the quencher effect [53].

Table 5.1 Results of the electrochemical properties of polymers with changing the amounts of acid/base during successive polymerizations of BImBEd.

Polymer	E_m^{ox} (V)	E_p^{ox} (V)	E_p^{red} (V)
PBImBEd	0.80	0.33	0.13
PBImBEd01a	1.10	0.66	0.58
PBImBEd02a	1.08	0.61	0.46
PBImBEd03a	1.03	0.58	0.45
PBImBEd04a	0.99	0.57	0.44
PBImBEd01b	1.02	0.56	0.40
PBImBEd02b	0.89	0.42	0.27
PBImBEd03b	1.08	0.77	0.70
PBImBEd04b	1.11	0.82	0.72

5.2.2. X-ray photoelectron spectroscopy (XPS) studies for PBImBEd, PBImBEd02a and PBImBEd02b

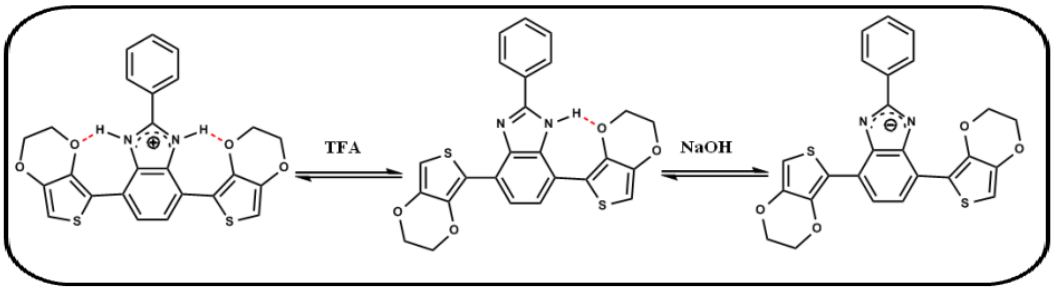


Figure 5.7 Structures of BImBEd derivatives with acid and base addition

The structure of BImBEd with addition of acid and base is given in Figure 5.7. To prove that these predictions are correct XPS analyses were performed for PBImBEd, PBImBEd02b and PBImBEd02a. XPS- N1s spectra of PBImBEd, PBImBEd02b and PBImBEd02a contains the same peak at 398.9 eV which can be attributed to –N= in the imidazole ring of the polymers [54]. The peaks at 400.7 eV belong to -NH- of nitrogen atoms [55]. The positively charged nitrogen ($–N^+$) results in peaks at higher energies precisely 402.3 and 403.0 eV, in this case [56, 57, 58]. The peak at 402.3 eV belonging to the positively charged nitrogen on the imidazole ring disappears in the case of PBImBEd02b (Figure 5.8B) and occurs slightly in the case of PBImBEd (Figure 5.8A) as there exists a partial positive charge caused by the intramolecular hydrogen bonding. This peak is much more intense in the spectrum of PBImBEd02a (Figure 5.8C) proving the protonation of the imine, as expected.

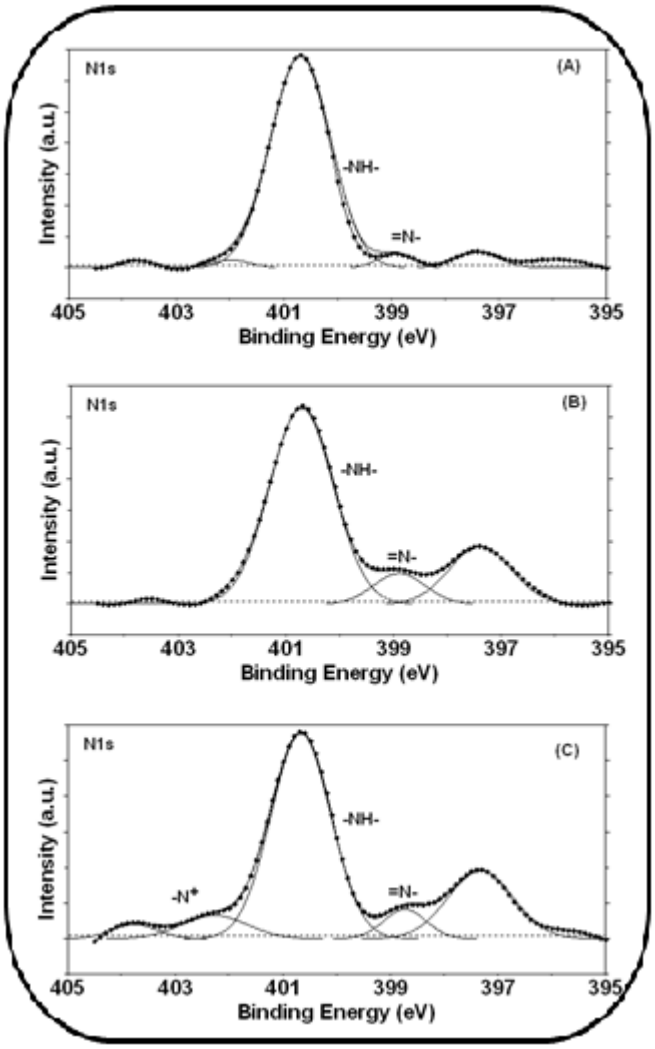


Figure 5.8 N1s XPS data for (A) PBImBEd, (B) PBImBEd02b, and (C) PBImBEd02a

5.2.3. Electrochemistry of 1,4-bis(2,3-dihydrothieno[3,4-b][1,4]dioxin-5-yl)benzene (BEDOT-B)

Electrochemical polymerization of BEDOT-B (1 x 10^{-2} M) was performed in 0.1 M $TBAPF_6$ containing DCM:ACN (5:95, v:v) solution, by sweeping the potential between 0.0 V and 1.45 V versus Ag wire pseudo reference electrode for 5 cycles with 100 mV/s scan rate. In order to investigate the effect of addition of acid in the absence of a side chain open to protonation, BEDOT-B was also polymerized by adding different amounts of acid to the electrolyte solution, by sweeping the potential between -0.4 V and 1.2 V. The resulting polymers were named as PBEDOT-B01a, PBEDOT-B02a, PBEDOT-B03a and PBEDOT-B04a with addition of 0.1 mL, 0.2 mL, 0.3 mL and 0.4 mL acid to the 2.0 mL of polymerization solution, respectively. The CVs of all polymerizations are shown in Figure 5.9.

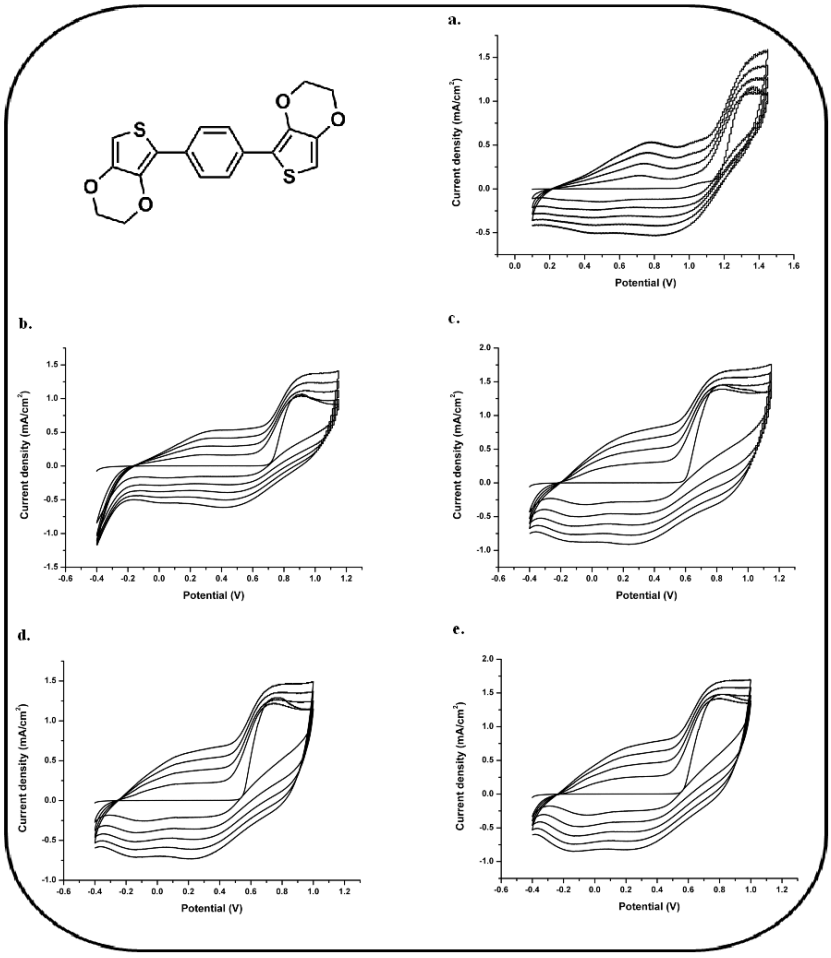


Figure 5.9 Repeated potential scan of electrochemical polymerizations of **(a)** BEDOT-B, **(b)** BEDOT-B01a, **(c)** BEDOT-B02a, **(d)** BEDOT-B03a, **(e)** BEDOT-B04a in 0.1 M $TBAPF_6$, DCM:ACN (5:95, v:v) with 100 mV/s scan rate

Table 5.2 Results of the electrochemical properties of polymers with changing the amounts of acid during successive polymerizations of BEDOT-B.

Polymer	E_m^{ox} (V)	E_p^{ox} (V)	E_p^{red} (V)
PBEDOT-B	1.33	0.71	0.47
PBEDOT-B01a	0.90	0.28	0.06
PBEDOT-B02a	0.80	0.16	-0.11
PBEDOT-B03a	0.71	0.08	-0.14
PBEDOT-B04a	0.77	0.11	-0.12

Addition of acid eases the electrochemical polymerization, thus reduces the monomer oxidation potential in case of BEDOT-B (Table 5.2) except for addition of 0.4 mL acid. This exception is most probably caused by excessive amount. The ease of electrochemical polymerization by addition of acid is caused by the stabilization of intermediate with the strong protic acid (TFA).

It was seen that the addition of even small amount of base prevents polymer formation. This quenching effect can also be explained by the electrochemical polymerization mechanism (Figure 5.10). The intermediate is a radical cation which can be quenched by the hydroxyl ion. This result proves the fact that deprotonation in the polymerization of BImBEd dominated over the quencher effect of base and allows polymer formation.

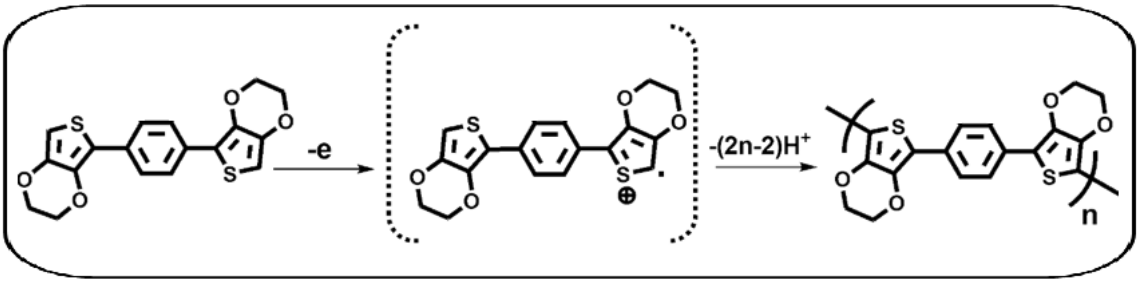


Figure 5.10 Electrochemical polymerization mechanism of BEDOT-B

5.2.4. Spectroelectrochemistry of poly(4,7-bis(2,3-dihydrothieno[3,4-b][1,4]dioxin-5-yl)-2-phenyl-1H-benzo[d]imidazole) (PBImBEd) and poly(1,4-bis(2,3-dihydrothieno[3,4-b][1,4]dioxin-5-yl)benzene) (PBEDOT-B)

Spectral changes of the polymers upon applied potential were investigated using UV-vis-NIR spectrophotometer in a monomer free, 0.1 M $TBAPF_6$ ACN solution. Absorption spectra of the polymers were recorded for reduced and fully oxidized states (Figure 5.11).

Comparing the absorption spectra of all PBImBEd derivatives in their undoped states, it is seen that increasing concentration of acid, decreases the intensity of the absorption at longer wavelength in NIR region. That absorption at higher wavelength is well known to belong to the oxidized polymer. Thus, the reduction in the intensity of this absorption indicates that the polymer can be reduced easier. On the other hand, addition of base increases the intensity of the absorption at higher wavelength even in the most reduced state of the polymer. This means that new electronic states tend to form without applying any external force which can be attributed to the side chain ionization [59]. Addition of base contributes to the side chain by forming negative charge which hardens the reduction which is consistent with the absorption spectra. Addition of acid contributes to the side chain by forming positive charge which eases the reduction, in a similar manner.

The absorbance spectra of PBEDOT-B, PBEDOT-B01a, PBEDOT-B02a, PBEDOT-B03a and PBEDOT-B04a (Figure 5.12) are almost the same for both their reduced and oxidized states. This proves that the change in the NIR absorption in the reduced state of the polymers is caused by the protonation or deprotonation of the imidazole ring, as claimed.

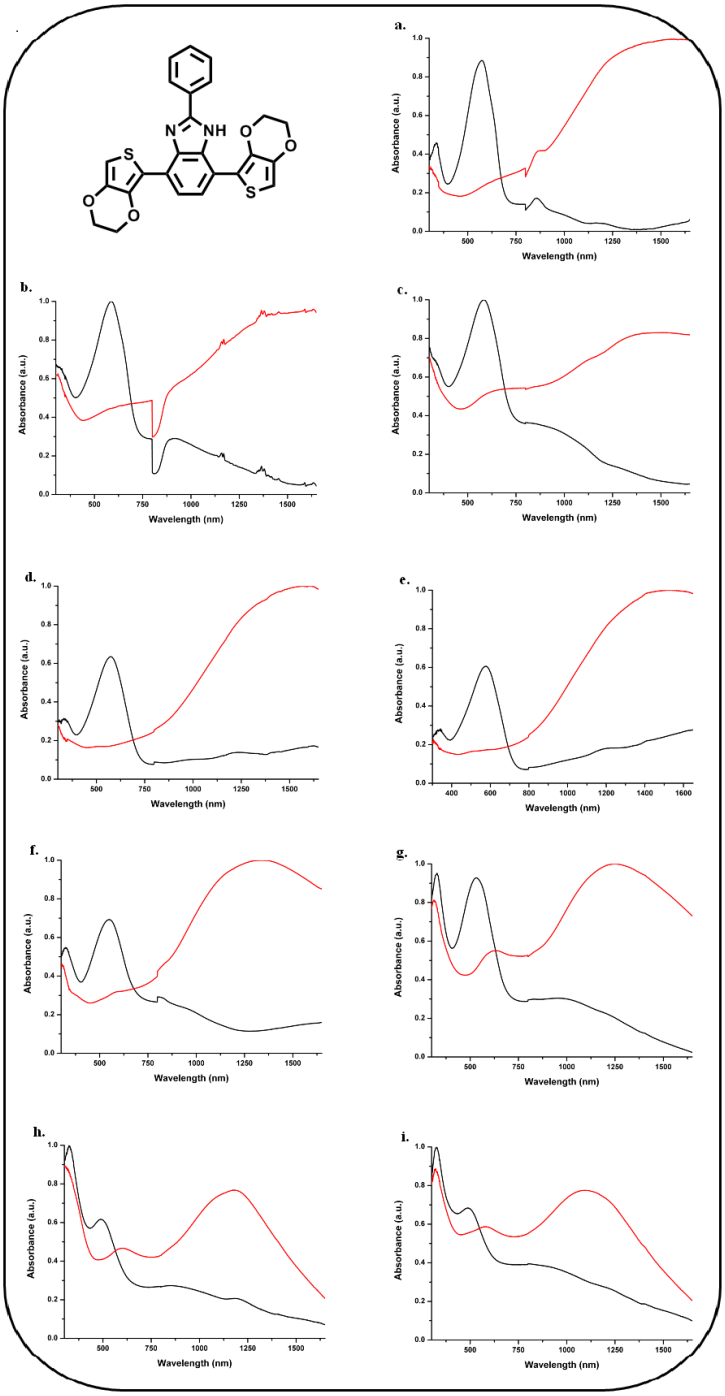


Figure 5.11 Reduced (black lines) and oxidized (red lines) absorption spectra of (a) PBImBEd, (b)PBImBEd01a, (c) PBImBEd02a, (d) PBImBEd03a, (e) PBImBEd04a, (f) PBImBEd01b, (g)PBImBEd02b, (h) PBImBEd03b and (i) PBImBEd04b

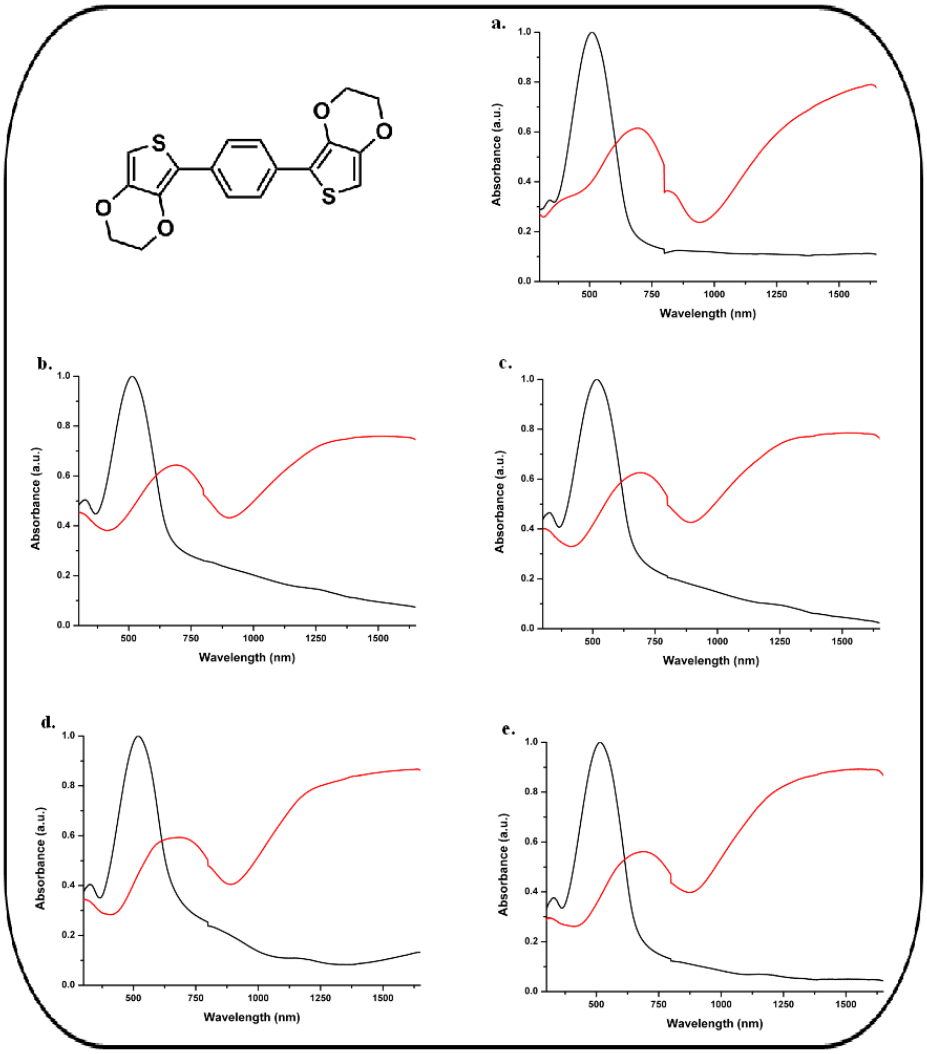


Figure 5.12 Reduced (black lines) and oxidized (red lines) absorption spectra of (a) PBEDOT-B, (b) PBEDOT-B01a, (c) PBEDOT-B02a, (d) PBEDOT-B03a, (e) PBEDOT-B04a

Comparing the normalized visible spectra of PBImBEd derivatives (Figure 5.13), it is seen that addition of acid causes π-π^* absorption to shift to the higher wavelength which corresponds to decrease in the energy. This can be attributed to the higher effective conjugation length as addition of acid increases the amount of H-bonding and prevents the bended conformation [60]. In the same vein, addition of base shifts the π-π^* absorption to higher energy as blocking the H-bonding reproduces twisted conformation. The shifts in case of addition of base are more significant than that of acid which is most probably because of the contribution of quencher effect of the base. As the quencher effect of base causes decrease in the polymer chain length, it also results in higher energy.

To make sure that these shifts in absorption results from the protonation/deprotonation of the imidazole ring, same comparison was done for PBEDOT-B derivatives (Figure 3.14) and no considerable change was seen in the visible spectrum.

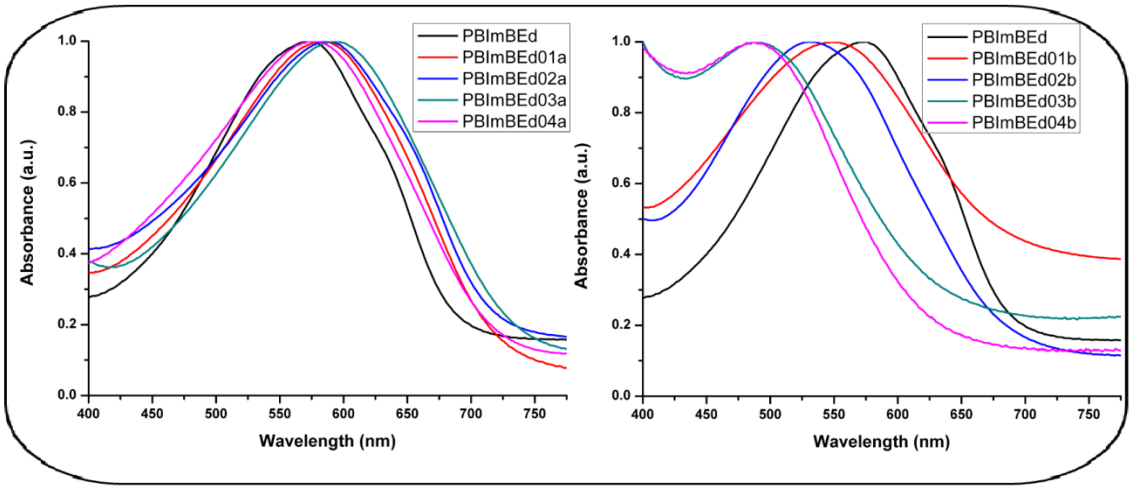


Figure 5.13 Normalized vis spectra of PBImBEd, PBImBEd01a, PBImBEd02a, PBImBEd03a, PBImBEd04a (left) and PBImBEd, PBImBEd01b, PBImBEd02b, PBImBEd03b, PBImBEd04b (right) in their reduced states

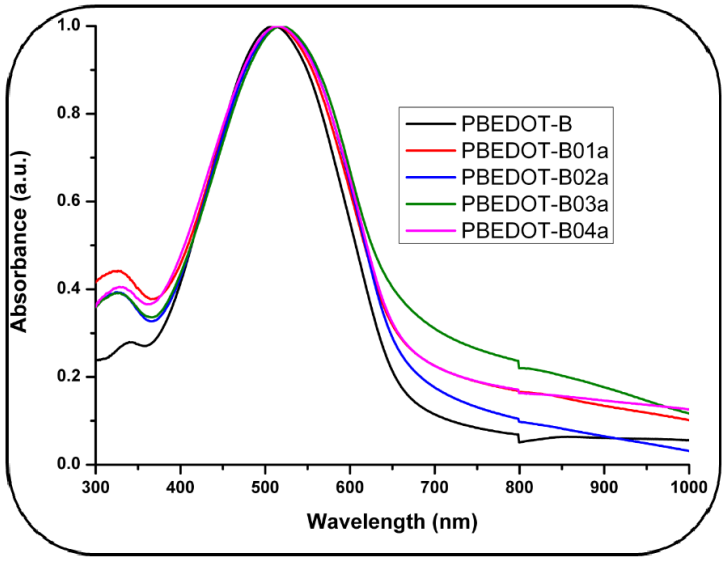


Figure 5.14 Normalized vis spectra of PBEDOT-B, PBEDOT-B01a, PBEDOT-B02a, PBEDOT-B 03a, PBEDOT-B04a in their reduced states

Band gap values of all PBImBEd derivative polymers were calculated using the onset of their π-π^* transitions and recorded in Table 5.3. The band gap values differ between 1.6 eV and 1.8 eV which is a small variation compared to the variations in absorption maxima values. This denotes that even the ratio of the protonated/deprotonated molecules differ with the addition of acid/base, there exists a different distribution of both neutral and protonated/deprotonated structure in the polymer chains.

Table 5.3 Optical band gap values of the polymers with changing the amounts of acid/base during successive polymerizations of BImBEd.

Polymer	E_g (eV)
PBImBEd	1.8
PBImBEd01a	1.7
PBImBEd02a	1.6
PBImBEd03a	1.6
PBImBEd04a	1.7
PBImBEd01b	1.6
PBImBEd02b	1.6
PBImBEd03b	1.7
PBImBEd04b	1.6

Consistent with the absorbance spectra, the color of the polymer films are the same for PBEDOT-B and derivatives while changes for PBImBEd and its derivatives as seen in Figure 5.15.

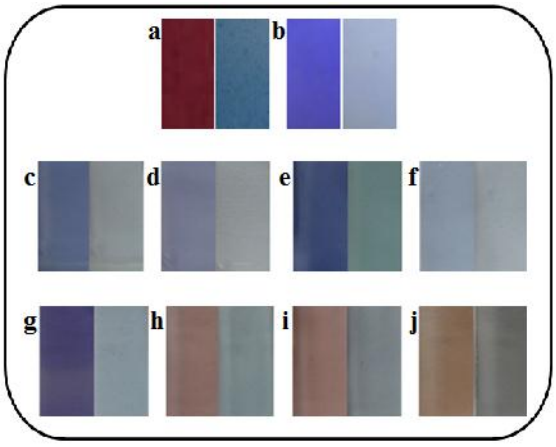


Figure 5.15 Colors of the polymer films in their reduced (left) and oxidized (right) states for a) PBEDOT-B, b) PBImBEd, c) PBImBEd01a, d) PBImBEd02a, e) PBImBEd03a, f) PBImBEd04a, g) PBImBEd01b, h) PBImBEd02b, i) PBImBEd03b and j) PBImBEd04b

The colors of the polymer films are described in CIE color space in Table 5.4, with L, a, b values.

Table 5.4 List of L, a, b values of all the polymer films

Polymer	Reduced state			Oxidized state		
	L	a	B	L	a	b
PBImBEd	30.579	-3.440	-2.316	31.311	4.997	0.870
PBImBEd01a	29.766	-3.593	-0.386	31.937	-5.045	1.317
PBImBEd02a	24.434	-2.554	-2.224	31.937	-4.720	1.253
PBImBEd03a	15.937	-2.236	1.004	16.852	-2.409	1.483
PBImBEd04a	15.875	-1.967	1.170	18.655	-2.481	1.608
PBImBEd01b	14.663	-0.521	0.883	16.186	-2.606	0.993
PBImBEd02b	13.153	-0.608	0.330	16.613	-3.136	0.691
PBImBEd03b	17.349	-1.816	2.097	16.793	-2.522	1.942
PBImBEd04b	17.748	-2.118	2.234	16.813	-2.316	2.062
PBEDOT-B	11.853	8.236	1.757	18.152	-4.407	-3.081
PBEDOT-B01a	17.059	5.527	1.699	20.712	-3.955	-1.357
PBEDOT-B02a	15.083	5.439	0.945	18.317	-3.180	-1.987
PBEDOT-B03a	13.730	4.220	0.704	18.480	-3.759	-2.304
PBEDOT-B04a	15.700	3.415	0.819	19.975	-3.557	-1.948

5.2.5. Kinetic Properties of poly(4,7-bis(2,3-dihydrothieno[3,4-b][1,4]dioxin-5-yl)-2-phenyl-1H-benzo[d]imidazole) (PBImBEd) and poly(1,4-bis(2,3-dihydrothieno[3,4-b][1,4]dioxin-5-yl)benzene) (PBEDOT-B)

Optical contrast values of the polymer films were determined using UV-vis-NIR spectrophotometer in a monomer free, 0.1 M $TBAPF_6$ ACN solution by switching the polymers between their neutral and fully oxidized states with 5 second stepping intervals. The spectra were taken at maximum absorption wavelengths of the polymer films in visible and NIR regions. Percent transmittance differences for PBImBEd, PBImBEd01a, PBImBEd02a, PBImBEd03a, PBImBEd04a, PBImBEd01b, PBImBEd02b,

PBImBEd03b and PBImBEd04b are shown in Figure 5.16 and for BEDOT-B, BEDOT-B01a, BEDOT-B02a, BEDOT03a and BEDOT-B04a in Figure 5.17.

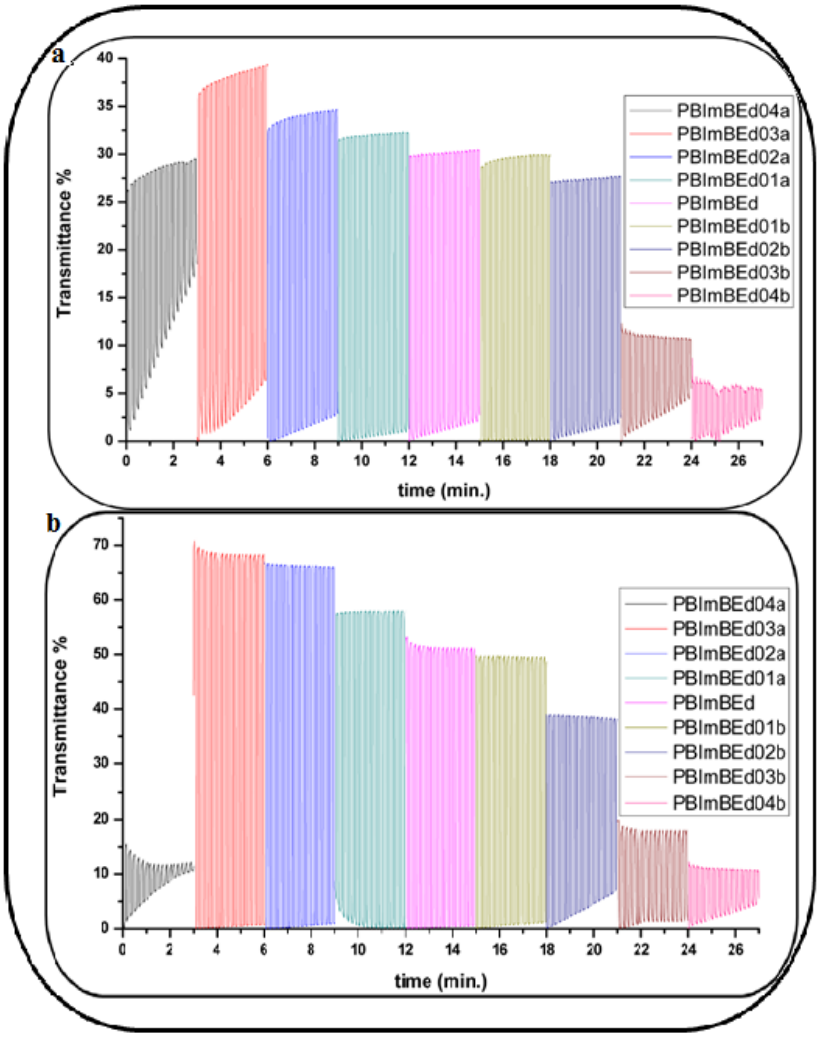


Figure 5.16 Percent transmittance differences for PBImBEd, PBImBEd01a, PBImBEd02a, PBImBEd03a, PBImBEd04a, PBImBEd01b, PBImBEd02b, PBImBEd03b and PBImBEd04b at maximum absorption wavelengths in a) visible region, b) NIR region

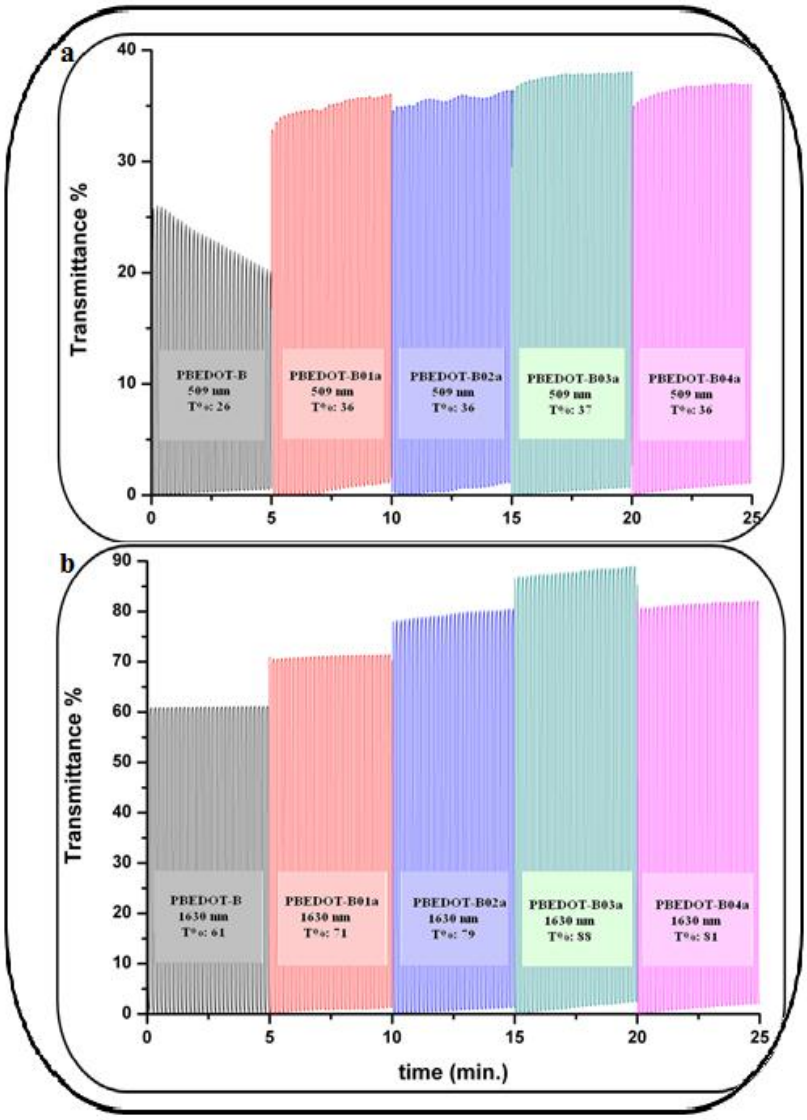


Figure 5.17 Percent transmittance differences for BEDOT-B, BEDOT-B01a, BEDOT-B02a, BEDOT03a and BEDOT-B04a at their maximum absorption wavelengths in a) visible region, b) NIR region

It is seen that the optical contrast of PBImBEd increases with the increasing ratio of H-bonding in the polymer chain from 30 % (PBImBEd) to 38 % (PBImBEd03a) in vis region and from 52 % (PBImBEd) to 68 % (PBImBEd03a) in NIR region. In the same manner, addition of base decreases the optical contrast as recorded in Table 5.5. These results are consistent with the charge loaded on the polymer chain which can be seen in the CVs. Addition of 0.4 mL of acid to the polymerization media significantly disturbs the trend in the optical contrast. This is most probably because this amount of TFA is excess and does not contribute to the H-bond formation.

This trend is also available for the optical contrast values of PBEDOT-B derivatives. As stated before, in the absence of H-bonding formation, addition of a strong aprotic acid stabilizes the intermediate in the

electrochemical polymerization, hence increases the chain length. This increase in the conjugation length increases the loaded charge, thus the optical contrast.

Table 5.5 Optical contrast values of the polymers at their maximum absorption wavelengths in vis and NIR region.

polymer	λ_{max}	ΔT%
PBImBEd	573	30
	1500	52
PBImBEd01a	585	32
	1500	58
PBImBEd02a	587	34
	1535	66
PBImBEd03a	593	38
	1545	68
PBImBEd04a	578	28
	1435	15
PBImBEd01b	550	29
	1320	50
PBImBEd02b	532	27
	1262	39
PBImBEd03b	493	11
	1175	18
PBImBEd04b	486	6
	1100	11
PBEDOT-B	509	26
	1630	61
PBEDOT-B01a	509	36
	1630	71
PBEDOT-B02a	509	36
	1630	79
PBEDOT-B03a	509	37
	1630	88
PBEDOT-B04a	509	36
	1630	81

CHAPTER 6

CONCLUSION

In the first part of this study, the DAD type monomers; BImTh and BImEd were synthesized via bromination, reduction, stannylation and the Stille coupling reactions. The resulting monomers were characterized by NMR and MS analyses. Successfully synthesized monomers were electrochemically polymerized to obtain PBImTh and PBImEd. Cyclic voltammetry experiments, spectroelectrochemistry and kinetic studies were performed to investigate the optoelectronic properties of the polymers. Both polymers showed multichromic properties which makes both polymers reasonable candidates for electrochromic applications. As the acceptor unit was kept same and the donor unit was altered, the donor unit effect was determined comparing the thiophene and EDOT bearing polymers. The results of spectroelectrochemical analyses showed that EDOT causes absorption shift to longer wavelength compared to thiophene, consistent with the electronic structure of EDOT. However BImEd revealed higher oxidation potential than BImTh, which once more proved that the consideration of only electronic structures and individual properties of the donor/acceptor units is not enough. This conclusion led the second part of the study.

In the second part, two DAD type monomers; BImBEd and BEDOT-B were synthesized and characterized by NMR analyses. The H-bonding between the acceptor and donor moieties of BImBEd was further proved via FT-IR and XPS analyses. BImBEd was electrochemically polymerized in the presence of different amounts of acid and base to control the quantity of H-bond. BEDOT-B was treated the same, to be used as a control material. Addition of acid resulted in C7 intramolecular H-bonding in the polymer chain and hindered the rotation of the bond between the donor and the acceptor unit. In the same vain, addition of base eased the aforementioned rotation. These changes enabled to discuss the effect of intramolecular interactions (H-bonding) and planarity on the optoelectronic properties of conducting polymers. Also it was seen that addition of acid eases the extension of the π-conjugation length of the polymers, base behaves as a quencher on polymerization process. Thus the effect of the conjugation length was also studied. The results of the spectroelectrochemistry studies proved that the ionization of the sub-chain affects the optical properties of the polymer significantly. As the properties of the resulting polymers are considerably different from each other, this method can also be used as a way to alter the characteristics of heteroatom containing conducting polymers. The most important outcome of this study was the discovery of a new way of tuning the optical and electrochemical properties of electrochromic polymers applicable even to the insoluble ones.

REFERENCES

1. H. Shirakawa, E.J. Louis, A.G. MacDiarmid, C.K. Chiang, A.J. Heeger, J. Chem. Soc. Chem. Commun. (1977) 578.
2. C.K. Chiang, C.R. Fischer, Y.W. Park, A.J. Heeger, H. Shirakawa, E.J. Louis, S.C. Gau, A.G. MacDiarmid, Phys. Rev. Letters, 39 (1977) 1098.
3. A. Gandini, M. N. Belgancem, Prog. Polym. Sci., 22 (1997) 1203.
4. G. Grem, G. Leditzky, B. Ullrich, G. Leising, Adv. Mater., 4 (1992) 36.
5. V. Rumbau, R. Marcilla, E. Ochoteco, J. Pomposo, D. Mecerreyes, Macromolecules, 39 (2006) 8547.
6. K. Fehse, K. Walzer, K. Leo, W. Loevenich, A. Elschner, Adv. Mater., 19 (2007) 441.
7. D. S. K. Mudigondaa, D. L. Meeker, D. C. Loveday, J. M. Osborn, J. P. Ferraris, Polymer, 40 (1999) 3407.
8. D.J. Crouch, P.J. Skabara, J.E. Lohr, J.J.W. McDouall, M. Heeney, I. McCulloch, D. Sparrowe, M. Shkunov, S.J. Coles, P.N. Horton, Chem. Mater., 17 (2005) 6567.
9. S. Tuncagil, S. Kıralp, S. Varıs, L. Toppare, Reac. Func. Poly., 68 (2008) 710.
10. P. Bamfield, M. G. Hutchings, Chromic Phenomena; technological applications of colour chemistry, Royal Society of Chemistry, Cambridge, 2010, 2.
11. K. Wolfgang, C. A. Rigoberto, Functional Polymer Films, Wiley-VCH, 2012, 995.
12. C. G. Granqvist, Handbook of Inorganic Electrochromic Materials, Elsevier, Amsterdam, 1995, reprinted 2002, 267.
13. P. M. S. Monk, R. J. Mortimer, D. R. Rosseinsky, Electrochromism, Wiley-VCH, 2008, 67.
14. S. H. Kim, J. S. Bae, S. H. Hwang, T. S. Gwon, M. K. Doh, Pigments, 33 (1997) 167.
15. A. A. Argun, A. Cirpan, J. R. Reynolds, Adv. Mater., 15 (2003) 1338.
16. S. Dhawan, K. Kumar, M.K. Ram, S. Chandra, D.C. Trievedi, Sens. Actuat. B, 40 (1997) 99.
17. M. Satoh, S. Tanaka, K. Kaeriyama, J. Chem. Soc. Chem. Commun. (1986) 873.
18. M. A. DePaoli, W. A. Gazotti, J. Braz, Chem. Soc., 13 (2002) 410.
19. C. J. DuBois, F. Larmat, D. J. Irvin, J. R. Reynolds, Synth. Met., 119 (2001) 321.
20. J. H. Burroughes, D. D. C. Bradley, A. R. Brown, R. N. Marks, K. MacKay, R. H. Friend, P. L. Burn, A. B. Holmes, Nature, 348 (1990) 347.
21. D. Kumar, R. C. Sharma, Eur. Polym. J., 34 (1998) 1053.
22. N. Basescu, Z. X. Liu, D. Moses, A. J. Heeger, H. Naarmann, N. Theophilou, Nature, 327 (1987) 403.
23. J. Roncali, Macromol. Rapid Commun., 28 (2007) 1761.
24. M. Kertez, R. Hoffmann, Solid State Commun., 47 (1983) 97.
25. Y. H. Wijsboom, A. Patra, S. S. Zade, Y. Sheynin, M. Li, L. J. W. Shimon, M, Bendikov, Angew. Chem. Int. Ed., 48 (2009) 5443.
26. A. J. Heeger, Chem. Soc. Rev., 39 (2010) 2354.
27. A. J. Heeger, S. Kivelson, J. R. Schrieffer, W. P. Su,, Rev. Mod. Phys., 60 (1988) 781.
28. M. Garcia, E. Ramos, P. Guadarrama, S. Fomine, Synth. Met., 159 (2009) 2081.
29. A. Balan, D. Baran, L. Toppare, J. Mater. Chem., 20 (2010) 9861.
30. A. Tanimoto, K. Shiraishi, T. Yamamoto, Bull. Chem. Soc. Jpn., 77 (2004) 597.
31. S. Celebi, A. Balan, B. Epik, D. Baran, L. Toppare, Org. Electron., 10 (2009) 631.
32. P. Blanchard, J. M. Raimundo, J. Roncali, Synth. Met., 119 (2001) 527.
33. G. Heywang, F. Jonas, Adv. Mater., 4 (1992) 116.
34. C. A. Thomas, K. Zong, K. A. Abboud, P. J. Steel, J. R. Reynolds,, J. Am. Chem. Soc., 126 (2004) 16440.

35. A. Cihaner, F. Algı, Adv. Funct. Mater., 18 (2008) 3583.
36. S. Taj, S. Sankarapapavinasam, M. F. Ahmed, Journal of Applied Polymer Science, 77 (2000) 112.
37. A. P. Monkman, L. Palsson, R. W. T. Higgins, C. Wang, M. R. Bryce, A. S. Batsanov, J. A. K. Howard, J. Am. Chem. Soc., 124 (2002) 6049.
38. A. Grobel, M. Plass, J. Mol. Struct., 480 (1998) 417.
39. K. Takagi, K. Sugihara, J. Ohta, Y. Yuki, S. Matsuoka, M. Suzuki, Polym. J., 40 (2008) 614.
40. A. A. Argun, P. H. Aubert, B. C. Thompson, I. Schwendeman, C. L. Gaupp, J. Hwang, N. J. Pinto, D. B. Tanner, A. G. MacDiarmid, J. R. Reynolds, Chem. Mater., 16 (2004) 4401.
41. B. A. D. Neto, A. S. Lopes, G. Ebeling, R. S. Goncalves, V. E. U. Costa, F. H. Quina, J. Dupont, Tetrahedron, 61 (2005) 10975.
42. K. Bahrami, M. M. Khodaci, F. J. Naali, Org. Chem., 73 (2008) 6835.
43. S. S. Zhu, T. M. Swager, J. Am. Chem. Soc., 119 (1997) 12568.
44. A. G. Nurioglu, H. Akpinar, M. Sendur, J. Polym. Sci. Pol. Chem., 50 (2012) 3499.
45. G. Sonmez, I. Schwendeman, P. Schottland, K. Zong, J. R. Reynolds, Macromolecules, 36 (2003) 639.
46. I. Nurulla, A. Tanimoto, K. Shraishi, S. Sasaki, T. Yamamoto, Polymer, 43 (2002) 1287.
47. F. L. Hedberg, C. S. Marvel, J. Polym. Sci.Polym. Chem., 12 (1974) 1823.
48. J. Padilla, T. F. Otero, Bioinsp. Biomim., 3 (2008) 035006.
49. H. Akpınar, A. Balan, D. Baran, E. K. Ünver, L. Toppare, Polymer, 51 (2010) 6123.
50. G. A. Sotzing, J. R. Reynolds, Chem. Mater., 8 (1996) 882.
51. M. Plass, M. Weychert, I. Wawer, B. Piekarska-Bartoszewicz, A. Temeriusz, J. Carbohyd. Chem., 19 (2000) 1059.
52. A. Grobel, M. Plass, J. Mol. Struct., 480 (1998) 417.
53. H. Akpinar, A. G. Nurioglu, L. Toppare, J. Electroanal. Chem., 683 (2012) 62.
54. A.Kokalj, Comp. Mater. Sci., 28(2003) 155.
55. M. Lin, M. S. Cho, W. S. Choe, Y. Lee, Biosens. Bioelectron., 25 (2009) 28.
56. G. Polzonetti, V. Carravetta, G. Iucci, A. Ferri, G. Paolucci, A. Goldoni, P. Parent, C. Laffon, M. V. Russo, Chem. Phys., 296 (2004) 87.
57. S. Hubert, M. C. Pham, L. H. Dao, B. Piro, Q. A. Nguyen, M. Hedayatullah, Synthetic Met., 128, 2002, 67.
58. G. Bhargava, T. A. Ramanarayanan, S. L. Bernasek, Langmuir, 26 (2010) 215.
59. A. Tanimoto, K. Shiraishi, T. Yamamoto, Bull. Chem. Soc. Jpn., 77 (2004) 597.
60. K. Takagi, K. Sugihara, J. Ohta, Y. Yuki, S. Matsuoka, M. Suzuki, Polym. J., 40 (2008) 614.